

1 **Alma Mater Studiorum – Università di Bologna**

2
3 ***DOTTORATO DI RICERCA IN***

4
5 **Scienze e Tecnologie Agrarie, Ambientali e Alimentari**

6
7 *Ciclo XXX*

8
9 **Settore Concorsuale: 07/B2 – SCIENZE E TECNOLOGIE DEI SISTEMI ARBOREI E FORESTALI**

10 **Settore Scientifico Disciplinare: ASSESTAMENTO FORESTALE E SELVICOLTURA**

11
12 *TITOLO TESI*

13
14 Disentangling the effects of age and global change on *Pseudotsuga menziesii* (Mirb.) Franco growth and
15 water use efficiency

16
17
18 *Presentata da: Dott. Dario Ravaioli*

19
20
21 **Coordinatore Dottorato**

22 Prof. Giovanni Dinelli

Supervisore

Prof. Federico Magnani

Co-Supervisore

Dott. Fabrizio Ferretti

23
24
25
26
27
28 *Esame finale anno 2018*

30 Abstract

31 The recent alterations in forests growth could be the result of a combination of different climatic
32 and non-climatic factors, as rising atmospheric [CO₂], temperature fluctuations, atmospheric
33 nitrogen deposition and drought stress. This study tests the potential effects of global change on
34 trees, assessing the relative importance and functional relationships between environmental drivers
35 and long-term growth trend, as well as physiological response. To investigate such effects, we
36 applied Generalized additive models (GAMs) technique, decoupling the non-linear age related
37 effect from co-occurring environmental effects on basal area increments (BAI) series and isotope
38 proxies (¹³C and ¹⁸O). Two Douglas fir (*Pseudotsuga menziesii* (Mirb.) Franco) chronosequence
39 were considered; the first one, comprises four different age classes (age 65-, 80-, 95- and 120-) and
40 is a even-aged stands plantation located in Italy, while the second one is an old-growth Californian
41 stand, with three age classes (age 100, 200, 300). Results show a 22.9% decrease of the general BAI
42 growth trend over last decades for the Italian Douglas-fir chronosequence, when the age-size non-
43 linear effect was removed. A related trend in water use efficiency (iWUE=A_{max}/g_s, the ratio between
44 photosynthetic assimilation and stomatal conductance) was observed in the same period. Thus,
45 through the application of the so called dual isotope approach, was possible to attribute to a
46 reduction in A_{max} the cause of such a trend, probably driven by a reduction in N deposition. On
47 other hand, BAI trend accounted for the Californian old-growth stand shows an increase of roughly
48 the 60% since the 1960, which was found to be mostly determinate by a strong effect of
49 atmospheric [CO₂]. These findings highlight how this species has been affected by global change
50 impact in both sites and provide important insights on its future behavior, potentially driving
51 management choices.

52 Key words: *Pseudotsuga menziesii*, BAI, iWUE, long-term trends, global change, GAMs, isotope
53 dual approach.

54

55	Summary	
56	Abstract	
57	Chapter I - Disentangling the effects of age and global change on Douglas-fir growth.....	9
58	1. Introduction.....	9
59	2 Materials and methods.....	11
60	2.1 Study area.....	11
61	2.2 Tree-ring data	13
62	2.3 Environmental data	14
63	2.4 Data analysis.....	17
64	3 Results	19
65	3.1 Dendrochronology.....	19
66	3.2 Model output.....	22
67	4. Discussion	26
68	5 Conclusions.....	27
69	6. Acknowledgments	28
70	7. Bibliography.....	29
71	Chapter II - Douglas fir eco-physiological response to global change.....	36
72	1. Introduction.....	36
73	2. Material and Methods.....	38
74	2.1 Study area.....	38
75	2.2 Samples preparation and isotopic analysis	40
76	2.3 $\delta^{13}\text{C}$ theory.....	41
77	2.4 $\delta^{18}\text{O}$ theory	43
78	2.5 Dual isotope conceptual model.....	45
79	2.6 GAM model.....	46
80	3. Results	48
81	3.1 Effects of cellulose extraction.....	48
82	3.2 Carbon isotope and iWUE dynamics	49
83	3.3 Oxygen isotope dynamics.....	56
84	3.4 Dual isotope approach.....	61
85	4. Discussion	62
86	4.1 Age-related effects	62
87	4.2.Environmental and biogeochemical effects	63
88	5.Conclusions.....	67
89	6.Bibliography.....	68

90	Chapter III - Old-growth stand trees reaction to global change, an explorative study	75
91	1. Introduction	75
92	2 Material and methods	78
93	2.1 Study area	78
94	2.2 Sampling strategy	79
95	2.3 Tree-ring data	81
96	2.4 Climate data.....	83
97	2.2 Geochemical data	85
98	2.3 GAMs	86
99	3. Results and discussion	87
100	4. Conclusions	95
101	5. Bibliography.....	97
102		
103		

104 General introduction

105

106 The ongoing global changes are intimately linked to the increase in the concentration of greenhouse
107 gases in the atmosphere, due to anthropogenic emission. The lower degree of infrared solar
108 radiation that can be dissipated out of the earth system results in an increase in global average
109 temperatures, attended to reach levels included between 2°C up to 4.5°C degrees by the end of this
110 century, as well as an alteration of extent and distribution of precipitation (IPCC 2014). The main
111 greenhouse gas, CO₂, has reached today a concentration of 406 μmol mol⁻¹, the highest in the last
112 650000 years. Over the past 250 years, atmospheric CO₂ has been increased globally by the 30%
113 from the concentration of 285 ppm in the pre-industrial era, with an exponential progression. The
114 human carbon source, resulting by fossil fuel combustion and land use change, is estimated in 8.8
115 Gt C y⁻¹. The main sinks, which absorb actively carbon from atmosphere, are oceans and terrestrial
116 ecosystems, able to remove roughly 2 Gt C each one every year. The extent of the terrestrial sink,
117 mainly represented by forest ecosystems, is directly and indirectly influenced by global change. The
118 temperature variations can increase (enlarging the vegetative period)(Menzel and Fabian, 1999) or
119 decrease (water stress due to excessive evapo-transpiration)(Allen et al. 2010) plants'
120 photosynthetic assimilation. On the other hand, the greater amount of CO₂ available to plants
121 photosynthesis could acts positively on the growth capacity of trees, amplifying their mitigating
122 effect (Ainsworth and Long 2005). For what concern the northern hemisphere and temperate forests
123 in particular was observed, both through satellite direct measurement of NDVI (Normalized
124 Difference Vegetation Index) and ground-based data, an increase in net primary productivity (NPP,
125 gross primary productivity minus autotrophic respiration, GPP-R_a) of 20% in the last decades of
126 the 20th century (Boisvenue and Running 2006). The causes were attributed for a 50% to direct
127 effects of forest management, for 33% to the direct and indirect effects caused by global change and
128 for 8-17% to historical effects related to age stands dynamics (Vetter et al. 2005). Contrarily, more
129 recent observations seem to highlight an inversion of this trend. The NPP in the first decade of the

130 new millennium suffers a global decrease, probably due to the drought events induced by higher
131 temperatures (Zhao & Running, 2010). A better understanding of how [CO₂] acts on forests both
132 directly and through the improvement of positive or negative feedbacks, as which one involved
133 temperature and water stress process or trees growth enhancement, is of crucial importance. Indeed,
134 it determine the capacity of realize predictive reliable models on the future global change entity.

135 Another key factor determining these anomaly in forest growth has been identified in the potential
136 fertilizing effect of atmospheric nitrogen depositions (Hyvönen et al., 2007), caused by atmospheric
137 pollution of nitrogen oxidized (NO_y deriving from combustion) and of reduced form (NH_x deriving
138 from agricultural fertilization). Discounted the age-related effect, a quasi-linear relationship
139 between N depositions and net ecosystem productivity (NEP, difference between gross primary
140 productivity and total ecosystem respiration, GPP-R) has been hypothesized (Magnani et al. 2007),
141 caused by the direct nitrogen canopy uptake which can bypass bacterial competition in the soil and
142 the relative increase in heterotrophic respiration (R_h, source of C). It would increase C sequestered
143 by plants in temperate forest ecosystems (typically N-limited) increasing their sink effect.
144 Furthermore, when long-term analysis on trees growth is performed, it should be taken into
145 consideration also that forests normally display a progressive reduction in productivity as stand age
146 increase. For example, Aboveground Productivity (P_a, one of the components of NPP) is influenced
147 by age-size related dynamics in the leaf area index (LAI, defined as the relationship between the
148 photosynthetically active leaf surface and the surface of the soil on which the leaves are projected).
149 After a juvenile phase of expansion, determining an increase in time of P_a, LAI reaches a
150 culmination at stand canopy closure, exceeded which the increase in inter-tree competition for
151 light, water and nutrients progressively reduces P_a (Ryan and Yoder, 1997). Another component of
152 this age-effect is explained by the hydraulic limitation hypothesis (HLH) which relates productivity
153 decrease and tree dimension. The gradual increase in hydraulic resistance with the increase of the
154 height of the stem, the length of the branches and the thickness of the roots, would cause an
155 enhancement in the internal water potential difference between roots and shoots, if hydraulic leaf

156 conductance (k) is maintained constant. Instead, a k reduction is observed with trees ageing, caused
157 by a decrease of stomatal conductance (g_s). This link between hydraulic resistances and the degree
158 of stomatal closure affect net photosynthesis rates, decreasing the amount of CO_2 which could be
159 assimilated in relation to LAI (Gower *et al.* 1996). The maintenance of a almost constant leaf
160 potential, obtained through the reduction of stomatal conductance is a compromise between the
161 photosynthesis, water transport at greater heights (which would be more effective at more negative
162 leaf water potential) and cavitations avoidance (embolisms caused by the vascular system water
163 chain brake) which would be suffered by the xylem if extremely negative water potentials would be
164 reached (Tyree and Sperry, 1988; Magnani *et al.* 2000).

165 Separate these age-size related effects from the co-occurring environmental changes effects
166 affecting trees growth, is virtually impossible if a single age-class is considered because both of
167 them are time correlated (Bowman *et al.*, 2013). Indeed, exogenous effects, as climate-related
168 covariates or biogeochemical pollutants impact, varying along calendar year while age-size effects
169 (endogenous), varying along cambial age. To overcome such inter-correlation issues is possible to
170 apply a sampling strategy aimed on the collection of a wide range of age-classes from a multi-age
171 stand or from different even-aged stands growing in comparable environmental condition, but
172 established in different dates. This chronosequence-based approach *sensu* Walker *et al.* (2010)
173 allow to assess the effects of changing environmental conditions affecting tree growth (i.e, rising
174 $[\text{CO}_2]$, temperature or water availability) trough the deviation from the attended age-related mean
175 trend. Based on this eco-physiological and environmental background, the first objective of this
176 PhD thesis is to evaluate the possible impact of global change affecting two Douglas fir
177 (*Pseudotsuga menziesii* (Mirb.) Franco) chronosequences, separating age-related growth changes
178 from environmentally-driven long-term growth trends superimposed on them. The second aim is to
179 test the possibility to disentangling among singular environmental factors which one have mostly
180 determined long-term growth and eco-physiological response trend variations, with the idea of

181 highlight potential vulnerability or strength points exhibited by this species, also in a future
182 adaptation prospective of this species to the Italian environment.

183

184 Bibliography

185 Ainsworth, Elizabeth A., and Stephen P. Long. 2005. "What Have We Learned from 15 Years of Free-Air CO₂
186 Enrichment (FACE)? A Meta-Analytic Review of the Responses of Photosynthesis, Canopy Properties
187 and Plant Production to Rising CO₂." *New Phytologist* 165 (2): 351–71. doi:10.1111/j.1469-
188 8137.2004.01224.x.

189 Allen, Craig D., Alison K. Macalady, Haroun Chenchouni, Dominique Bachelet, Nate McDowell, Michel
190 Vennetier, Thomas Kitzberger, et al. 2010. "A Global Overview of Drought and Heat-Induced Tree
191 Mortality Reveals Emerging Climate Change Risks for Forests." *Forest Ecology and Management* 259
192 (4): 660–84. doi:10.1016/j.foreco.2009.09.001.

193 Bowman, David M.J.S., Roel J.W. Brienen, Emanuel Gloor, Oliver L. Phillips, and Lynda D. Prior. 2013.
194 "Detecting Trends in Tree Growth: Not so Simple." *Trends in Plant Science* 18 (1). Elsevier Ltd: 11–17.
195 doi:10.1016/j.tplants.2012.08.005.

196 Gower ST, McMurtrie RE, Murty D (1996) Aboveground net primary production decline with stand age:
197 potential causes. *Trends Ecol Evol Res* 11: 378-382.

198 Hyvönen, Riitta, Göran I Agren, Sune Linder, Tryggve Persson, M Francesca Cotrufo, Alf Ekblad, Michael
199 Freeman, et al. 2007. "The Likely Impact of Elevated [CO₂], Nitrogen Deposition, Increased
200 Temperature and Management on Carbon Sequestration in Temperate and Boreal Forest Ecosystems:
201 A Literature Review." *The New Phytologist* 173 (3): 463–80. doi:10.1111/j.1469-8137.2007.01967.x.

202 IPCC. 2014. *Summary for Policymakers. Climate Change 2014: Synthesis Report. Contribution of Working*
203 *Groups I, II and III to the Fifth Assessment Report of the Intergovernmental Panel on Climate Change.*
204 doi:10.1017/CBO9781107415324.

205 Magnani, F., M. Mencuccini, and J. Grace. 2000. "Age-Related Decline in Stand Productivity: The Role of
206 Structural Acclimation under Hydraulic Constraints." *Plant, Cell and Environment* 23 (3): 251–63.
207 doi:10.1046/j.1365-3040.2000.00537.x.

208 Magnani, Federico, Maurizio Mencuccini, Marco Borghetti, Paul Berbigier, Frank Berninger, Sylvain Delzon,
209 Achim Grelle, et al. 2007. "The Human Footprint in the Carbon Cycle of Temperate and Boreal
210 Forests." *Nature* 447 (7146): 848–50. doi:10.1038/nature05847.

211 Menzel, Annette, and Peter Fabian. 1999. "Growing Season Extended in Europe." *Nature* 397 (6721): 659–
212 659. doi:10.1038/17709.

213 Ryan, Michael G., and Barbara J. Yoder. 1997. "Hydraulic Limits to Tree Height and Tree Growth."
214 *BioScience* 47 (4): 235–42. doi:10.2307/1313077.

215 Tyree, M T, and J S Sperry. 1988. "Do Woody-Plants Operate Near the Point of Catastrophic Xylem
216 Dysfunction Caused By Dynamic Water-Stress - Answers From A Model." *Plant Physiology* 88 (3): 574–
217 80. doi:10.1104/pp.88.3.574.

218 Vetter, Mona, Christian Wirth, Hannes Böttcher, Galina Churkina, Ernst Detlef Schulze, Thomas Wutzler,
219 and Georg Weber. 2005. "Partitioning Direct and Indirect Human-Induced Effects on Carbon

- 220 Sequestration of Managed Coniferous Forests Using Model Simulations and Forest Inventories.”
221 *Global Change Biology* 11 (5): 810–27. doi:10.1111/j.1365-2486.2005.00932.x.
- 222 Walker, Lawrence R., David a. Wardle, Richard D. Bardgett, and Bruce D. Clarkson. 2010. “The Use of
223 Chronosequences in Studies of Ecological Succession and Soil Development.” *Journal of Ecology* 98 (4):
224 725–36. doi:10.1111/j.1365-2745.2010.01664.x.

225

226 **Chapter I - Disentangling the effects of age** 227 **and global change on Douglas-fir growth**

228 Submitted for publication on the journal iForest (ISSN: 1971-7458; IF 1.623)'

229

230 **1. Introduction**

231 Over recent decades, significant changes in forest growth have been observed, particularly in
232 Europe, which have been interpreted as a result of the ongoing global change (Boisvenue and
233 Running 2006; Zhao and Running 2010) . However, the main drivers and functional basis of this
234 have not been ascertained. The potential effect of atmospheric CO₂ fertilisation during the
235 Anthropocene is one of the most widely discussed explanations, based on the expected stimulation
236 in photosynthetic rates at plant and ecosystem scale, with a positive effect on net primary
237 productivity (NPP). Only a few experiments have gathered evidence to test this hypothesis
238 (Ainsworth and Long 2005), the majority of which did not find a clear relationship between CO₂
239 and growth enhancement (Lévesque et al. 2014). Other studies have reported such an increase,
240 although stressing the importance of concomitant related factors, for example disturbance history or
241 an increasing vegetative period (McMahon et al. 2010). Indeed, interactions with other
242 environmental variables such as atmospheric nitrogen deposition (Magnani et al. 2007) are expected
243 to play a determinant role especially in resource-limited environments. Moreover, a parallel
244 increase in transpiration rates as a result of increasing temperatures could negate this positive effect,
245 in particular in drought-prone areas (Gómez-Guerrero et al. 2013)There is therefore a pressing need
246 to understand which key drivers have been affecting forest growth rates, and quantify the magnitude

247 of their effects. Even in the absence of controlled experiments, the analysis of long-term trends in
248 tree growth can help elucidate the relationship with environmental factors, as variations in the
249 growth pattern of a tree are the result of changing conditions, as well as ontogenetic processes
250 (Babst et al. 2014). Tree-ring widths are a direct measure of stem growth, hence the inspection of
251 this time series provides a reliable and datable source of data that can be used to investigate high
252 and low-frequency variability in forest growth trends. In order to highlight the environmental-
253 related signals enclosed in the tree-ring series, however, the superimposed age-related signal must
254 be first removed. An age-related decline in ring widths is generally observed with increasing age, as
255 a result of biological processes as well as geometrical constraints; basal area increments, on the
256 contrary, generally display an increase with age, followed by a gradual stabilization. Canonical
257 procedures applied in dendrochronological studies remove this age-related biological trend through
258 the application of de-trending techniques, such as spline or negative exponential fitting (Peters et al.
259 2015). However, a consequence of this is the depletion of low-frequency signals associated to tree-
260 ring series (Cook et al. 1995). Preserving low-frequency variations is of fundamental importance if
261 the objective of the analysis is to investigate long-term trends (Esper et al. 2002). In this study,
262 Generalised Additive Models (GAMs) were used as a tool to detect and separate the effect of
263 different variables, both biological (i.e. age) and environmental, and to determine tree-rings series
264 trends on a Douglas-fir (*Pseudotsuga menziesii* (Mirb.) Franco) chronosequence. This non-linear
265 regression technique is a *ceteris paribus* form of analysis, looking at the effect of a single factor
266 while keeping remaining factors constant (Rita et al. 2016). Hence, it is possible to take into
267 account tree age effects as a simple additive variable and look at the parallel effects of other
268 environmental covariates (Federal et al. 2015). Therefore, such a model can provide an alternative
269 to the traditional de-trending procedures, with the advantage to retain low frequency variability in
270 the series. In addition, it deals with the non-linearity of the relationship between the response and
271 the explanatory variables.

272 The aim of the present study is:

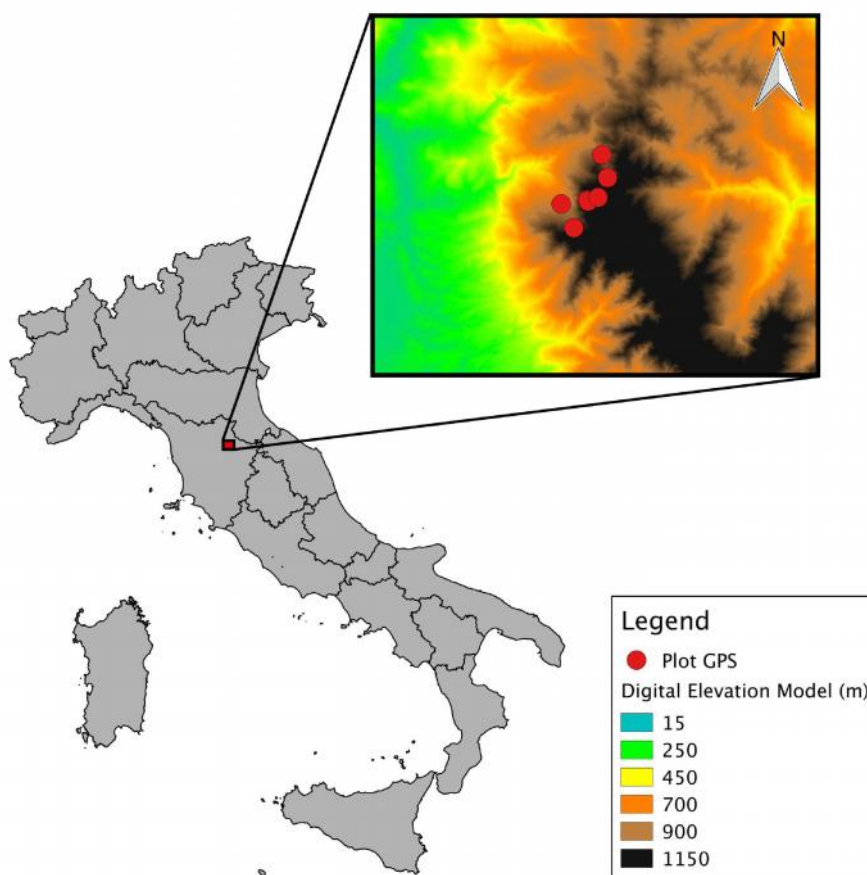
273 (i) to evaluate the possibility of separating age/size effects from environmentally-induced long-term
274 growth trends, avoiding the use of common de-trending methods and

275 (ii) to understand if Douglas-fir is affected by the changing environmental pressure in a long-term
276 perspective, looking at which variable or combination of variables drives the observed change in
277 growth rates.

278 2 Materials and methods

279

280 2.1 Study area



281

282 **Fig.1 Map** shows the location of the seven plots sampled (red dots). Different colors are related to different
283 elevations (m, a.s.l).

284

285 This study was performed in a Douglas-fir plantation located in the Vallombrosa Forest, in the
286 Apennine mountain range near Florence, Italy (43°43'59.6"N 11°33'16.9"E). The region has a
287 Mediterranean climate without significant summer droughts, and the mean annual precipitation is

288 approximately 1400 mm, of which less than 10% occurs in the summer months (72.48 mm). The
289 mean annual temperature is 9.8°C. The soils, derived from the Macigno del Chianti sandstone
290 series, vary between Humic Dystrudept and Typic Humudept (USDA Soil Survey Staff, 1999) in the
291 younger and older stands, respectively, indicating similar soil conditions at the sites. Douglas-fir is a
292 non-indigenous evergreen species and was imported from the Pacific Coast of the United States
293 during the last decades of the 19th century. It was chosen for the present study because of its high
294 economic importance. The sampled areas are part of the experimental permanent plot network
295 managed by CREA Research Centre for Forestry and Wood, and include the oldest experimental
296 plots established in Italy at the beginning of the 20th century (Pavari 1916).

297 A chronosequence of plots was selected for the study; a chronosequence is here defined as a set of
298 even-aged stands growing under the same environmental conditions and differing only for their age
299 (Walker et al. 2010). The chronosequence comprises four different age classes (65, 85, 100 and 120
300 years), covering the longest temporal extension that is possible to achieve in Italy for this species.
301 The summary characteristics of the four age classes are summarized in Table 1. Seven plots were
302 sampled that were consistent for management, aspect and elevation. Two plots were selected for
303 each age class, in order to ensure replication; however this was not possible for the oldest class, as
304 only one of this age was present in the area. In all sites, only dominant trees were chosen for the
305 analysis. Data from repeated forest inventories at the sites ensured the permanence of their
306 dominant status, thus partially avoiding potential sampling biases which occur when the currently
307 largest-diameter trees are wrongly considered to have always been in the dominant class (Cherubini
308 et al. 1998). However, the growth of shade intolerant trees is very much dependent by stand density,
309 especially in even-aged stands. Even if the trees sampled have been maintaining the dominant status
310 and thus should be considered exempt by growth suppression deriving to competition effect, is not
311 possible to exclude the presence of positive influence of thinning (i.e release effect) (Fernández-de-
312 Una et al. 2016).

313

Tab. 1| Mean characteristics of the Douglas fir chronosequence plots.

	Age-class						
	120	100		85		65	
Plot (code)	1	2	3	4	5	6	7
Max age (yrs)	126	101	102	86	86	69	69
Elevation (a.s.l.)	900	1100	1009	1095	1280	1113	1113
Eposition	N	N	SW	NE	NE	SW	SW
Dominant diameter (cm)	--	60.8	67.5	58.2	61,5	50.3	43.3
Dominant high (m)	--	47.2	54.4	49.9	44.3	39.9	39.8
Stand density (n°ha-1)	30*	375	380	360	280	600	550
Trees sampled (n°)	5	5	5	5	5	5	5

315 *for the oldest plot only 30 plants are left standing

316 2.2 Tree-ring data

317 In the spring and fall of 2013, 35 trees were sampled, five from each of the aforementioned plots.
318 One single core was extracted at breast height from each tree with a 5.1 mm Pressler borer (Haglöf,
319 Sweden). The extracted cores were then air-dried and polished with progressively finer sandpaper
320 (60- to 300-grit), so as to distinguish annual ring boundaries. Ring width series were measured on
321 pictures taken with a long-focal high definition camera (Canon, Japan) with the COORECORDER
322 image software analyser (Cybis Elektronik and Data AB) with 0.01 mm precision. Samples were
323 visually cross-dated against a reference curve, between and within the series using a correlation
324 coefficient, Gleichläufigkeit values and Student's t-test as indices. The closest tree ring chronology
325 available in the International Tree Rings Data Base (ITRDB) was used as a reference for pointer
326 year detection; the selected dataset (Schweingruber, F.H. - Mount Falterona - ABAL - ITAL008)
327 refers to an *Abies alba* chronology from Mount Falterona (23 km from Vallombrosa). As a further
328 check, a reference curve was developed using the Douglas-fir dataset itself by the 'leave-one-out'
329 methodology, starting from samples with a high correlation with the previous reference curve used.
330 Therefore, the quality of cross-dating was checked and cross-correlation analysis was performed
331 using the CDENDRO software (Cybis Elektronik and Data AB) and the R dplR package (Bunn
332 2008). Where the extracted core did not reach the pith of the tree, the length to the centre was

333 estimated using the curvature of the last complete ring, and the number of missing rings was
334 calculated by dividing this distance by the last five-year ring width average (Applequist et al. 1958).
335 These values were then checked against the year of plantation establishment, according to the forest
336 management plan.

337 Subsequently, the raw-ring widths recorded were converted into basal area increment (BAI), as the
338 latter allows to compensate for the age effect associated with the geometry of stems, especially at
339 young age, while preserving low-frequency variability (Biondi 1999). Moreover, BAI is considered
340 a better proxy of growth compared with radial increments. It was calculated as:

$$341 \quad \text{BAI} = (r_t^2 - r_{t-1}^2) \quad (1)$$

342 where r_t is the stem radius in a given year and r_{t-1} is the value corresponding to the previous year.

343 **2.3 Environmental data**

344 Daily records of mean, maximum and minimum temperatures and precipitation were obtained from
345 the Regional Hydrological Service of the Tuscany Region (SIR). Measurements for the 1922-2013
346 period were derived from the closest weather station, located at less than 3 km from sampled plots,
347 and integrated with the dataset obtained by Gandolfo-Sulli (1990) for the 1897-1922 period.

348 Mean annual data of air CO₂ concentration were obtained from the NOAA Earth System Research
349 Laboratory, as recorded at the Mauna Loa observatory in Hawaii from 1959 to present day, and
350 from McCarroll and Loader (2004) for the 1890-1958 period.

351 Average annual values of oxide (NO_y) and ammonium (NH_x) atmospheric deposition (both dry and
352 wet deposition) for the period from 1850 to 2014 were extracted from the NCAR global data set
353 managed by the IGAC-SPARC CCMi (Chemistry-Climate Model Initiative; available for download
354 at <http://blogs.reading.ac.uk/ccmi/>)(Figure 2). These N depositions data were generated with the
355 NCAR atmospheric transport model (National Center for Atmospheric Research), which provides
356 gridded (resolution of 2.0°x 2.25°, longitude x latitude) temporal simulations of the chemical
357 composition of the atmosphere.

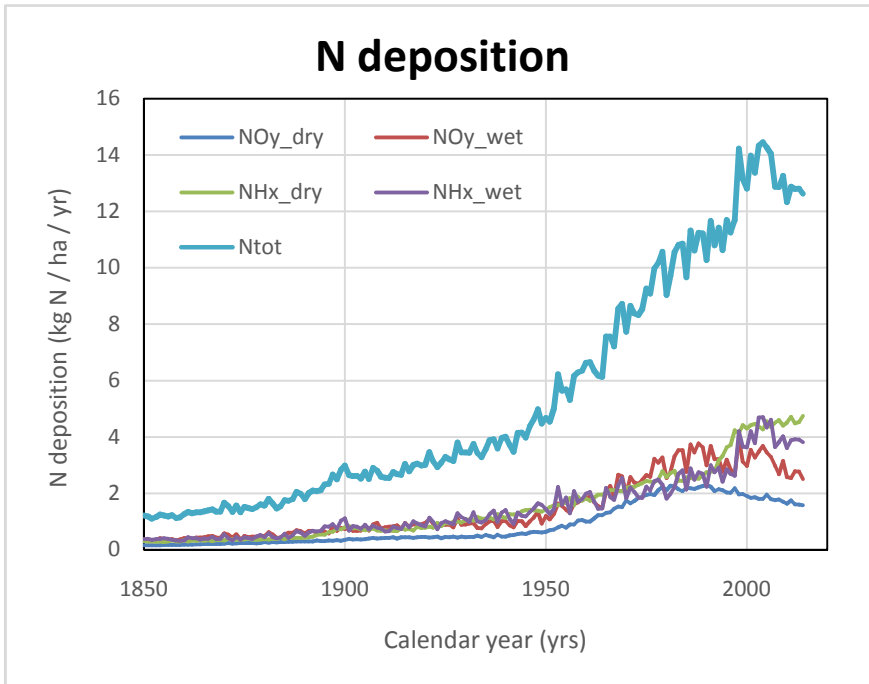
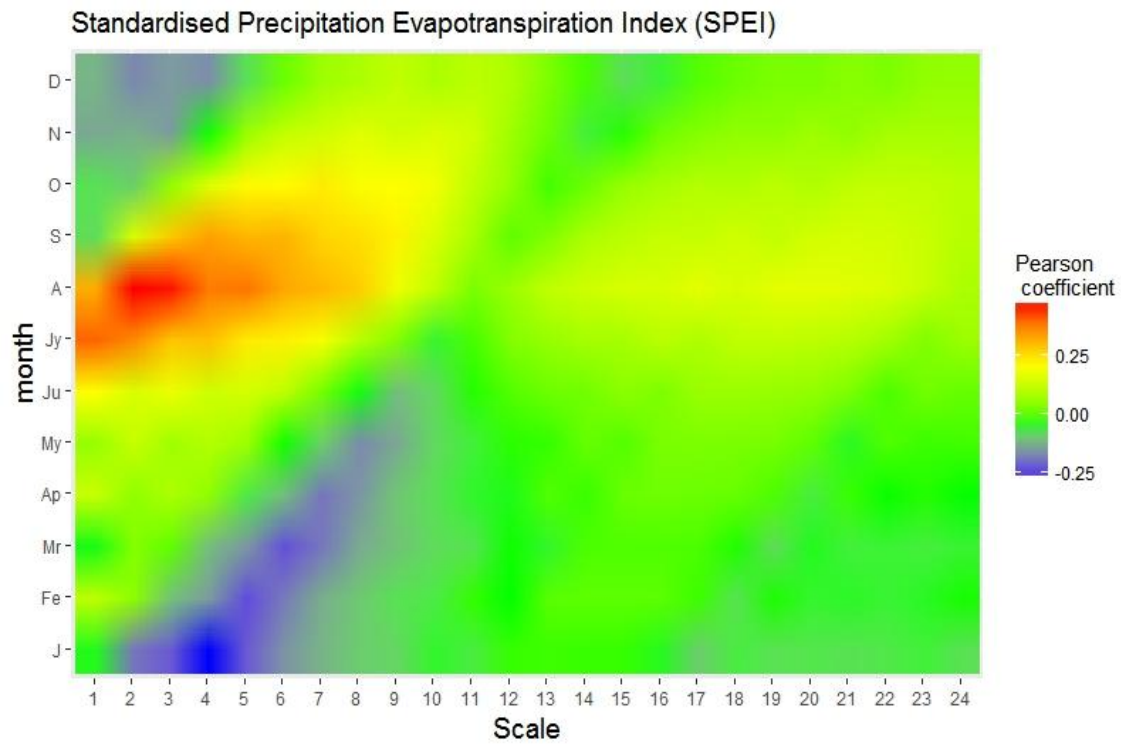


Fig 2. N deposition. Nitrogen deposition trends at Vallombrosa site as modeled by NCAR. Different colors represent the different species (oxide or ammonium) and different form of deposition (wet or dry) plus the total. On the x-axis calendar year (yrs), on the y-axis amount of deposition (kg N/ha/yr).

358

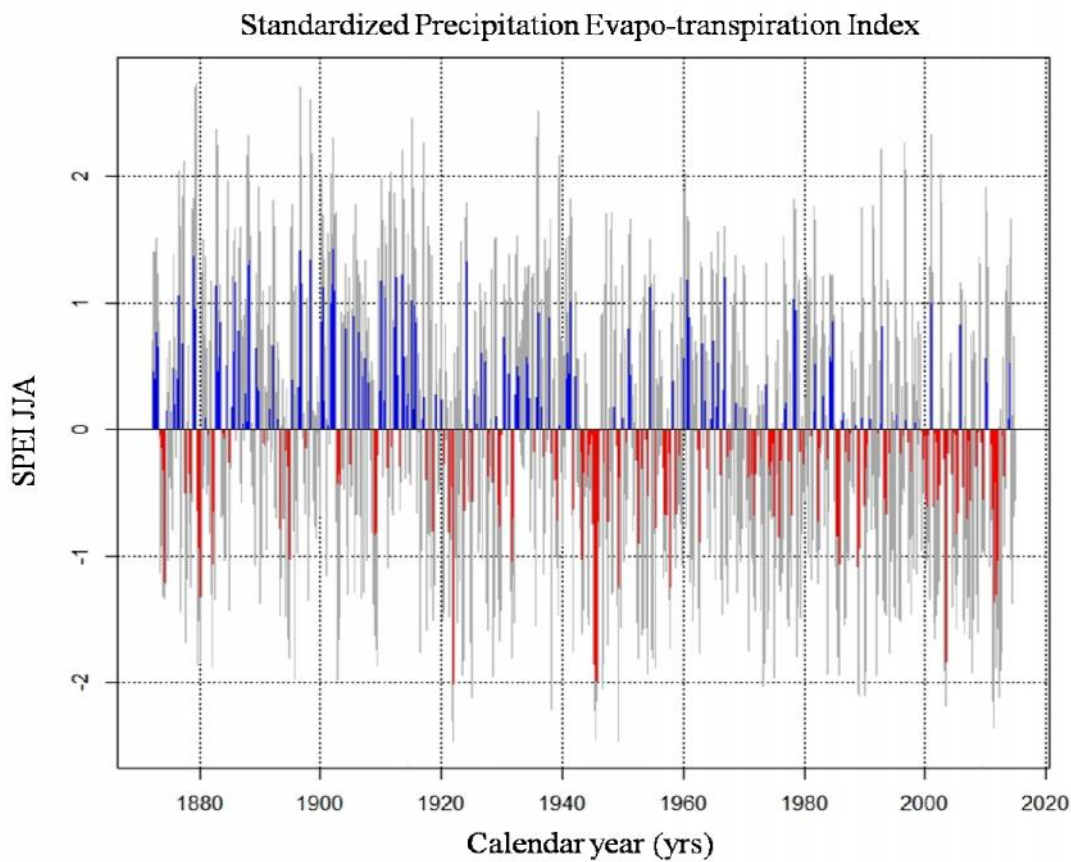
359

360 In order to evaluate the potential effects of drought stress, the Standardized Precipitation
 361 Evapotranspiration Index (SPEI; Vicente-Serrano et al., 2010) was included in the analysis. SPEI
 362 considers the sensitivity to changes in evapotranspiration demand and precipitation (P-PET) at
 363 different timescales, computing the cumulate influence of n previous months on the water
 364 deficit/surplus of the month of interest. Here, P-PET is derived from the Thornthwaite equation
 365 (Thornthwaite, 1948). For further calculations, a representative month at defined timescales was
 366 selected on the basis of the corresponding Pearson correlation coefficient. Correlations were
 367 performed between tree-rings width index series (RWI), de-trended with the negative exponential
 368 curve method (most conservative one), and the 1–24 timescale SPEI values computed for each
 369 month (Vicente-Serrano et al., 2014; Figure 3-4).



370

371 **Fig.3 SPEI correlation RWI heatmap.** Correlations (Pearson coefficient) between the Standardized
 372 Precipitation Evapotranspiration Index (SPEI) at 1- to 24 month scales, and de-trended tree-rings index
 373 (RWI), with on the *x*-axis temporal scale of SPEI and on the *y*-axis related months.



374

375 **Fig.4 SPEI JJA.** Trend of August SPEI at 3 month scales (June, July, August), which displays the highest
 376 with RWI, with on the *x*-calendar year (yrs) and on the *y*-axis SPEI values centered around 0. Red bar
 377 represent water deficit, while blue bars represent water surplus.

379 **2.4 Data analysis**

380 As tree growth exhibits strong non-linear patterns caused by both biological (i.e. age and size) and
 381 environmental (i.e. changes in CO₂, temperature, precipitation...) drivers, generalized additive
 382 models (GAMs; Hastie and Tibshirani 1990) were applied to identify the shape of the inherent
 383 relationships existing between BAI and predictor variables. GAMs are non-linear regression models
 384 that specify the value of the dependent variable as the sum of smooth functions of independent
 385 variables in a non-parametric fashion. Such a model relaxes any *a priori* assumptions of the
 386 functional relationship between response and predictors, therefore resulting in a more flexible range
 387 of application. It can be expressed as:

$$388 \quad y_i = \mu + f_1(x_{i1}) + \dots + f_n(x_{in}) + \epsilon_i \quad \text{for } \epsilon_i \sim N(0, \sigma^2) \quad (2)$$

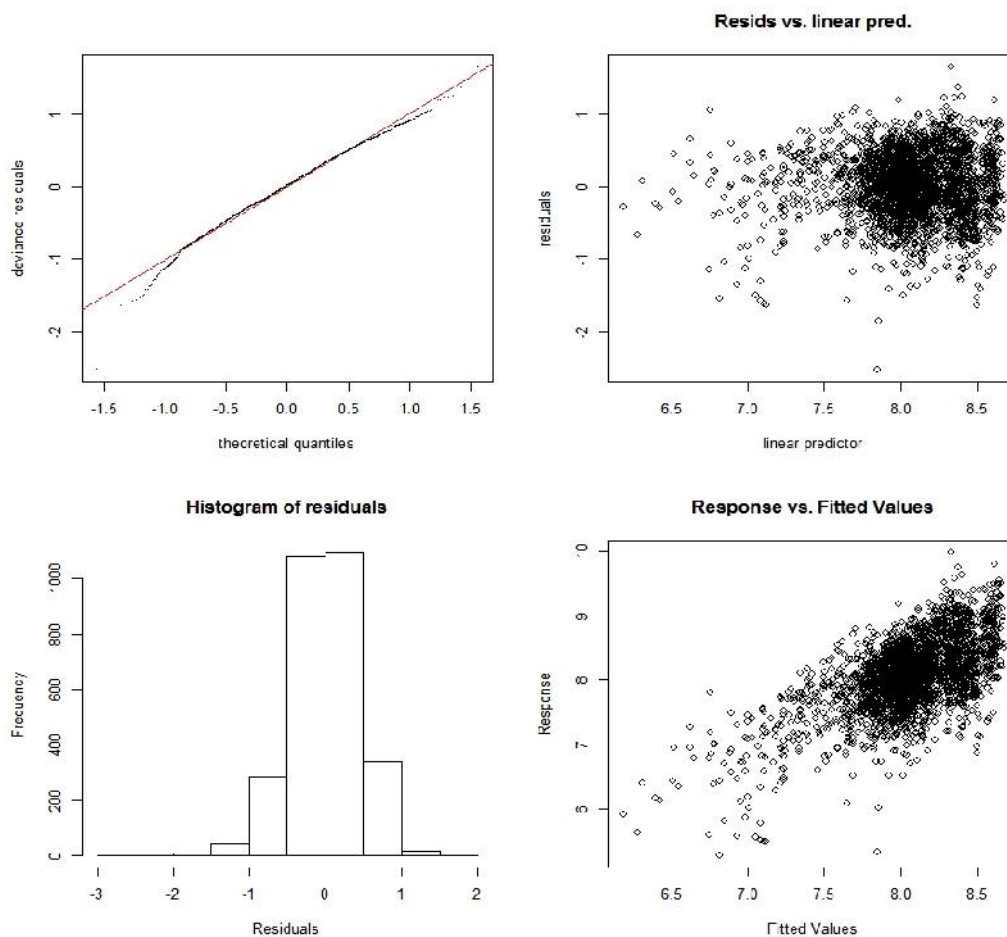
389 where y_i is the response variable, μ is the unknown intercept of fixed parameters, x_1, \dots, x_n are
 390 independent variables, f_1, \dots, f_n are smooth functions and ϵ_i are residuals with normal (Gaussian)
 391 distribution and constant variance. The GAM model was applied to log-transformed BAI data, so
 392 as to correct for heteroscedasticity. A cubic penalized spline was used as smooth function. This is
 393 the result of the simultaneous fitting of basis functions (i.e. natural cubic spline) penalized to
 394 achieve the optimal degree of smoothness, avoiding data over-fitting. The amount of penalizations
 395 was automatically computed by the maximum likelihood estimation (ML) (Wood, 2017). The
 396 selection of covariates was performed by a stepwise backward process. Tree age, atmospheric
 397 [CO₂], total atmospheric N deposition or its NH_x and NO_y components, mean (T_m) or maximum
 398 (T_{max}) and minimum (T_{min}) annual temperatures, annual precipitation (P) and the SPEI value of the
 399 current and previous year (SPEI_{t-1}) were considered as possible covariates. Candidates for removal
 400 were identified based on their lower approximate p-values and the model resulting after the
 401 subtraction of such variables was compared with the previous one based on Bayesian information
 402 criterion (BIC). This index was used instead of the Akaike information criterion (AIC) because it is

403 less conservative and more useful to assess the ‘true’ model in confirmatory analysis; in model
404 selection, the BIC provides a better opportunity to understand which pool of variables represent the
405 simpler model (Aho et al. 2014). All of the GAMs analyses were performed with the mgcv package
406 (Wood, 2006) of the R statistical suite (R Core Team, 2017). No pre-whitening processes (i.e.
407 addition of an autocorrelation structure of residuals) were applied to the radial increments time
408 series, with the aim to preserve long-term trends. The concurvity level (i.e. the generalization of co-
409 linearity in non-linear models) was also checked to assess a potential correlation among variables
410 (Tab.2). Concurvity could be an issue in models including a time-dependent smooth function with
411 other time-varying covariates, making model estimation unstable (Wood 2006), although GAMs are
412 able to deal with some degree of concurvity (Wood 2008). Finally, model results were tested to
413 ensure that the assumptions of normal distribution of observations and absence of heteroscedasticity
414 of residuals were respected (Fig. 5).

415 **Tab. 2**| Concurvity (collinearity for non-linear regression techniques) between GAM covariates. Values equal to 1
416 represent complete concurvity among covariates. Values under the threshold of 0.5 are deemed acceptable.

Covariate	parameters	Age	CO2	NOy dep	SPEI JJA	SPEI JJA t-1
parameters		1.50E-31	4.62E-32	7.28E-32	1.05E-31	8.60E-33
Age	1.44E-28		1.64E-01	7.88E-02	1.52E-02	1.56E-02
CO2	1.76E-29	1.74E-01		4.61E-01	8.21E-02	8.38E-02
NOy dep	4.88E-30	1.25E-01	5.34E-01		7.17E-02	1.05E-01
SPEI JJA	1.13E-29	1.73E-02	1.03E-01	7.04E-02		6.68E-02
SPEI JJA t-1	3.67E-31	1.84E-02	1.05E-01	1.03E-01	7.20E-02	

417



418

419 **Fig.5 Test of GAMs results for BAI as a function of age and time.** Residual distribution of the whole
 420 model and against linear predictor. Response against fitted values for the whole model.

421 **3 Results**

422 **3.1 Dendrochronology**

423

424 All of the trees used in this study were satisfactorily cross-dated and no missing rings were
 425 detected. The basal area increments of the different age classes are presented in Fig. 6 and Fig. 7,
 426 along calendar year and along cambial age respectively. The general statistics of the tree-ring
 427 chronologies are summarized in Table 3. The mean series inter-correlation (SI) that represents the
 428 strength of the common signal shared by all series is about 0.5, while the expressed population
 429 signal is above the conventional threshold ($ESP > 0.85$) used to define the acceptability of the
 430 chronology. This index confirms the goodness of cross-dating and the possibility to use this dataset
 431 for further analysis. Furthermore, mean sensitivity (MS), which is an index of year-to-year
 432 variability related to climate and/or disturbances, was also checked; a value ranking about 0.2

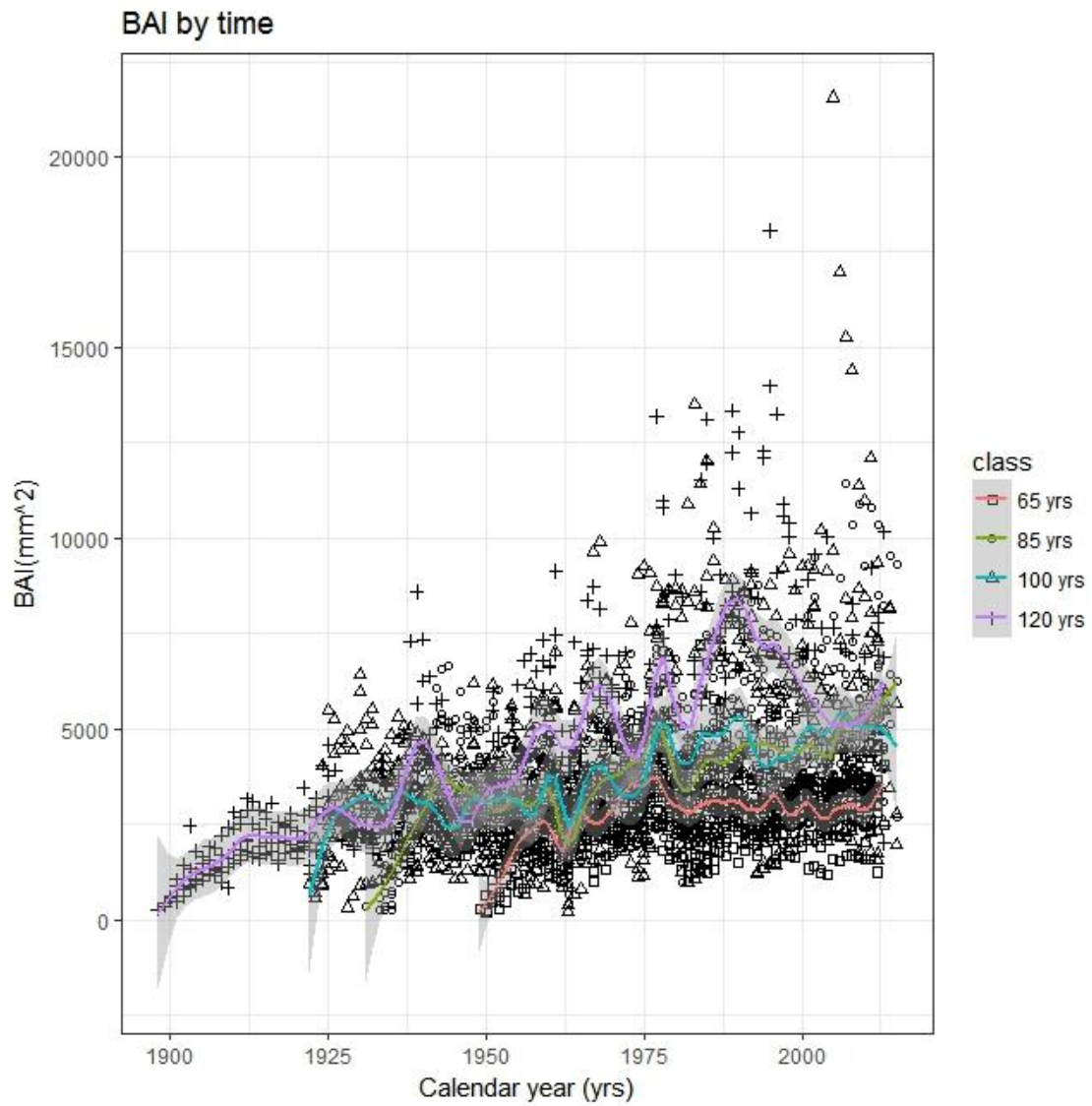
433 shows an adequate sensitive series, normally useful for climatic correlation analysis.

434

Tab.3] Descriptive statistics for raw (TRW) and ring width index (RWI) chronologies of the 4 different age-classes. *MW* is mean ring width, *SD* is standard deviation, *MS* is mean sensitivity, *ARI* the first order autocorrelation, *ESP* the expressed population signal, *SI* the series inter-correlation

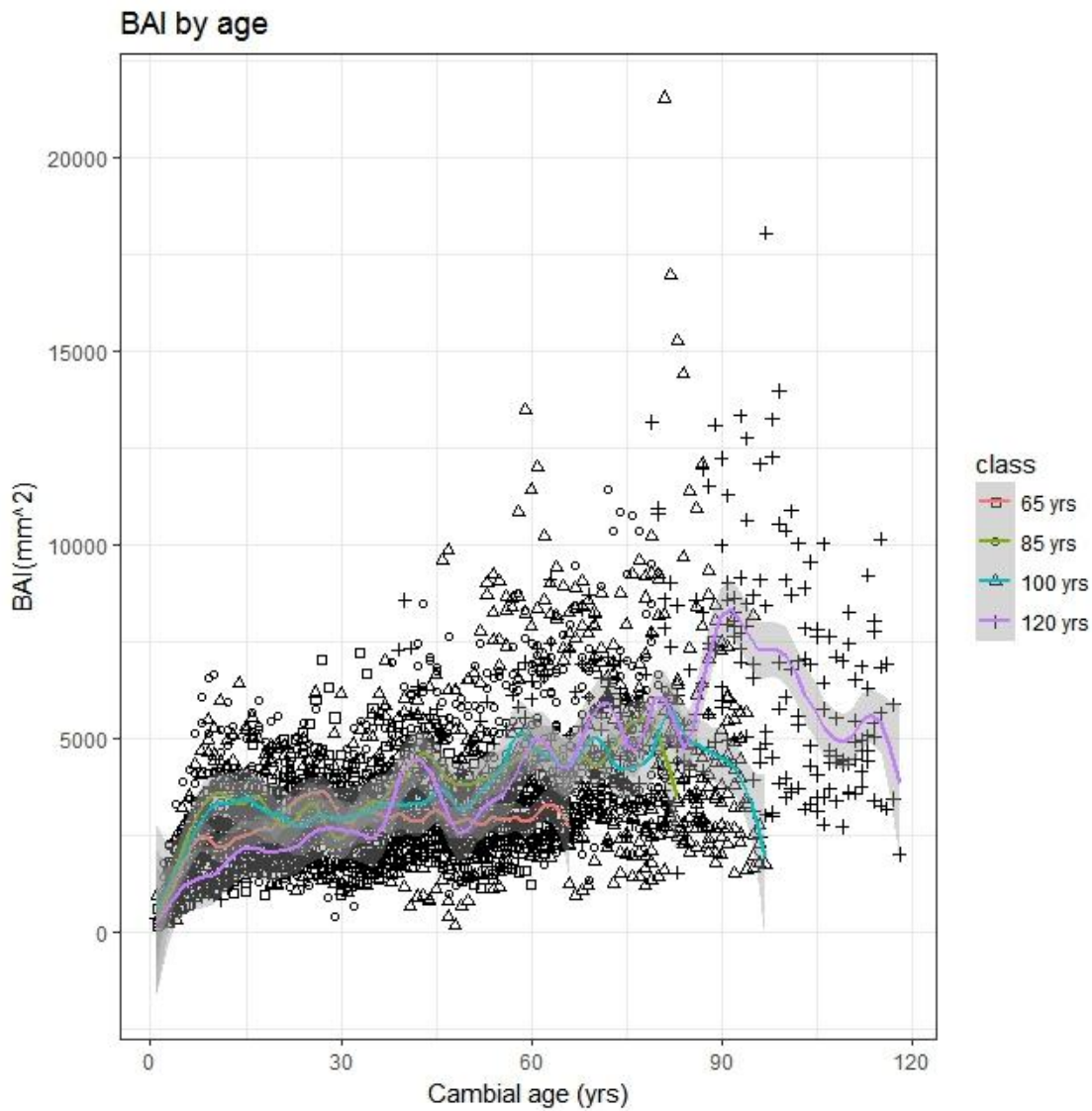
Age-class	TRW				RWI	
	<i>MW</i>	<i>SD</i>	<i>MS</i>	<i>ARI</i>	<i>ESP</i>	<i>SI</i>
70	3.5484	1.6647	0.1488	0.8506		
85	3.4193	2.0175	0.1871	0.855		
100	3.605	1.7718	0.198	0.7519		
120	3.3214	1.2572	0.2004	0.7088		
total	3.495257	1.737886	0.181171	0.8034	0.855	0.50

435



436

437 **Fig. 6 Time-related dynamics of basal area increments in different age-classes.** Time series of basal area
 438 increments (BAI), grouped by age-class and fitted with a cubic spline. The shaded areas indicate the
 439 95% prediction interval of the function



440

441 **Fig. 7 Diachronic analysis of age effects on basal area increments in different age-classes.** Time
 442 series of basal area increments (BAI), grouped by age-classes and fitted with a cubic spline. The shaded
 443 areas indicate the 95% prediction interval of the spline function

444

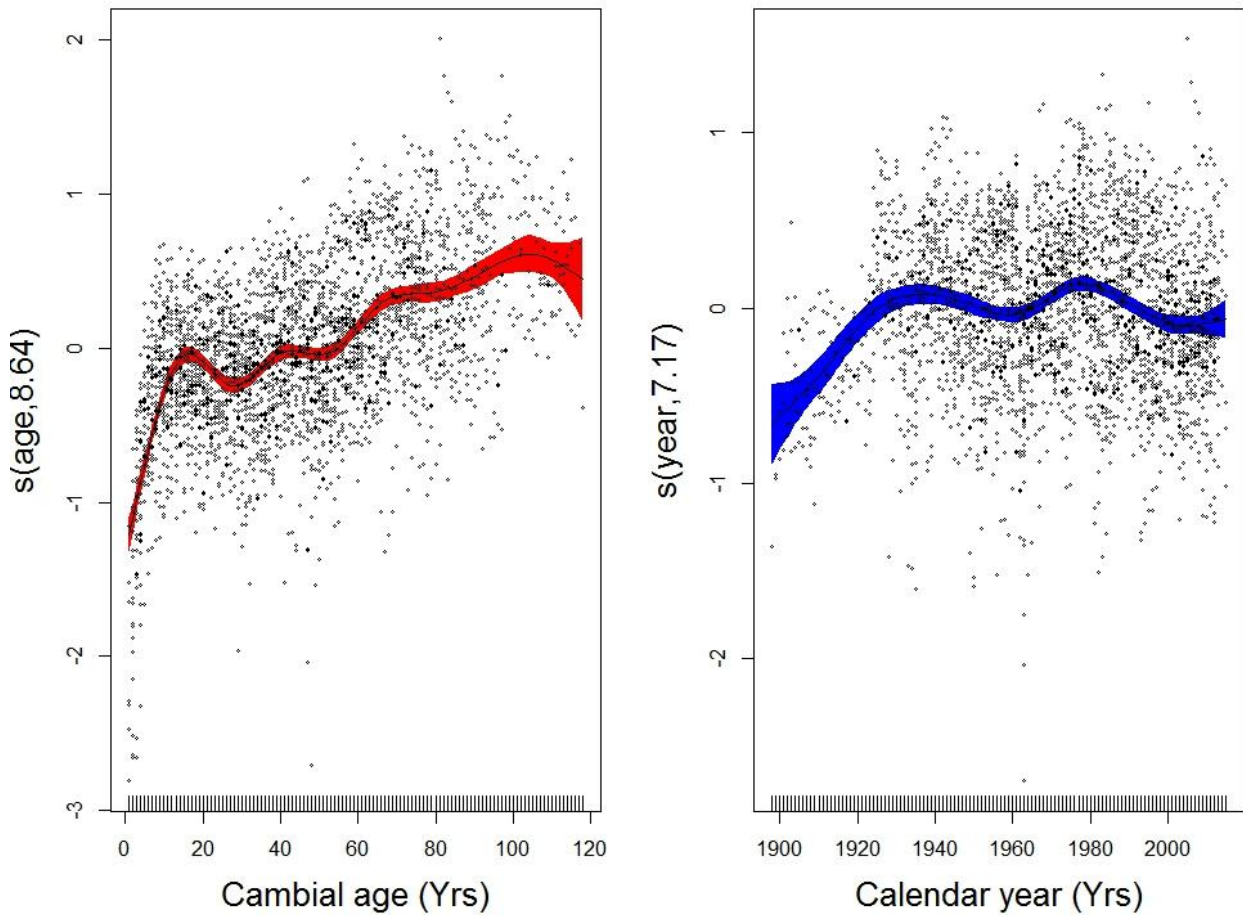
445 3.2 Model output

446 In order to assess possible changes of growth rates over time, independent of the co-occurring
 447 effects of ontogenetic factors, tree basal area increments (BAI) were modeled as:

$$448 \quad \ln(\text{BAI}) = f(\text{AGE}) + f(\text{TIME}) + \epsilon_i \quad (3)$$

449 where $f(\text{AGE})$ is the cambial age effect and $f(\text{TIME})$ represents all of the environmental effects
 450 cumulated into a single global variable, varying over time. The BAI global long-term trend (Fig.
 451 8b), after the subtraction of the age-related signal (Fig. 8a), shows an initial increase, two

452 culminations around the '30s and the '80s of the last century, a lower growth in between and a
 453 subsequent decrease until the first decade of this century. The age-related effect displays the
 454 expected shape, with a steep increase at early age in the first part of the curve, followed by a less
 455 pronounced growth, and an apparent culmination at an age of 100.



456

457 **Fig. 8 GAM analysis of the independent effects on BAI of age and time.**

- 458 **a.** Trend of basal area increments (BAI) as a function of age , after correcting for time-related effects. On
 459 x -axis age (years), and on y -axis the function of age $f(\text{Age})$, dimensionless and centered around 0.
 460 **b.** Global trend of BAI as a function of time , after correcting for age-related effects. On y -axis the
 461 function of time $s(\text{TIME})$, dimensionless and centered around 0. Points represent partial residuals from
 462 the fitted function and the shaded areas indicate the 95% prediction interval of fitted adaptive splines.
 463 The GAM model was applied to log-transformed BAI data, so as to correct for heteroscedasticity.

464

465 Successively, in order to partition to individual drivers the effect so far attributed to global change,
 466 seasonal climatic and geochemical variables were added to the model instead the time variable, and
 467 after the backward stepwise variable selection, it was specified as follow:

468
$$\ln(\text{BAI}) = f(\text{Age}) + f(\text{CO}_2) + f(\text{NO}_{y \text{ dep}}) + f(\text{SPEI JJA}) + f(\text{SPEI JJA t-1}) + \epsilon_i$$

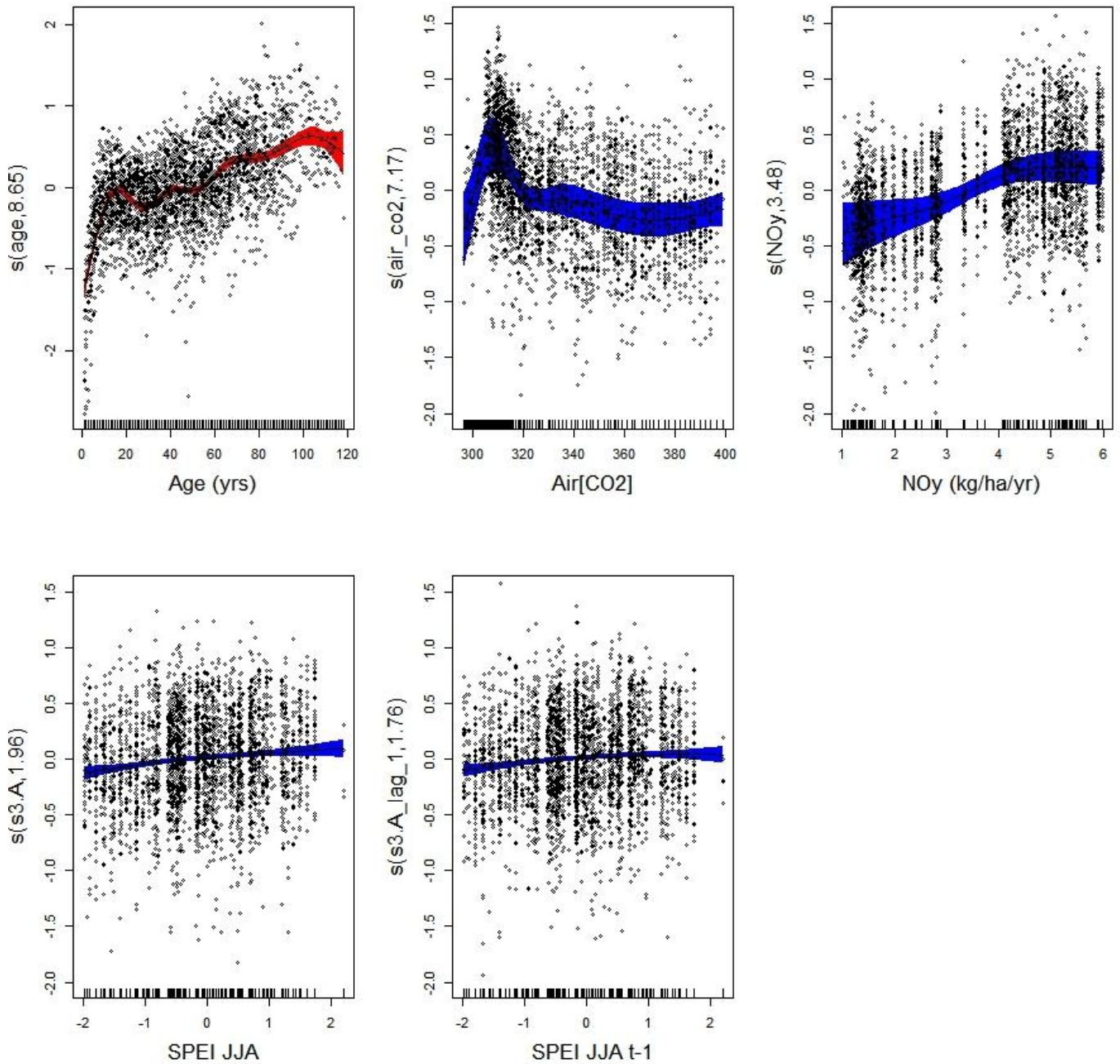
469 Age is the age/size effect associated with variations in cambial age, CO₂ is the annual level of
 470 atmospheric [CO₂], NO_{y dep} is the annual sum of dry and wet deposition of oxide N (NO_y) species,
 471 SPEI JJA and SPEI JJA t-1 represent the summer SPEI (Standardized Precipitation-
 472 Evapotranspiration Index; Vicente-Serrano et al. 2010) values in the ongoing and previous summer,
 473 respectively. All variables exhibit a significant p-value at 0.001 level (Tab. 4), with a global
 474 adjusted R² for the whole model of 0.371.

475

Tab. 4| Generalized additive model (GAM) results. Climatic and biological factors relationships with BAI series (as a dependent variable) in *Pseudotsuga menziesii*. *e.d.f.* are effective degrees of freedom, *F* is the F-test for variance explained, *P* is the p-values and *R²(adj)* is the adjusted regression coefficient of the entire model.

Factor	<i>e.d.f.</i>	<i>F</i>	<i>P</i>	<i>R²(adj)</i>
Age	8.652	83.872	< 2e-16	
CO2	7.172	14.951	< 2e-16	
Noy dep	3.485	1.614	0.000705	
SPEI JJA	1.961	3.513	4.80E-09	
SPEI JJA t-1	1.757	2.16	5.25E-06	
Whole model				0.371

476



477

478

479

480

481

482

483

484

485

486

487

488

Fig. 9. GAM analysis of increment response to individual drivers. Generalized additive models (GAMs) results show the relationship between basal area increments (BAI) and environmental and biological factors remaining after the backward selection procedure: cambial age, atmospheric [CO₂] and Standardized Precipitation Evapotranspiration Index computed over June, July and August of the current year (SPEI JJA) and of the previous year (SPEI JJA_{t-1}). Values on the y-axis indicate the independent effect of each covariate on basal area increments, as predicted by the model (continuous line) dimensionless and centered around 0, plus the estimated degree of freedom (edf). Points represent partial residuals from the fitted function and the shaded areas indicate the 95% prediction interval. The GAM model was applied to log-transformed BAI data, so as to correct for heteroscedasticity.

489 4. Discussion

490 The primary purpose of this study was to assess if any changes in growth rates have occurred over
491 time in Douglas-fir in the northern Apennines, once correcting for age-related patterns. The global
492 long-term trend illustrates a decrease in the productivity of this species in the last four decades,
493 amounting to about 22.9%. These findings appear to be consistent with several other studies that
494 looked at forest growth changes in central Apennines (Piovesan et al. 2008), in the Mediterranean
495 region by and large (Linares et al., 2010) and in other European areas (Vitas and Žeimavičius 2006).
496 All of these studies found that the increase in summer drought had a negative effect on growth, in
497 association with co-varying factors, such as stand dynamics, competition and/or pests. These could
498 exacerbate the role of the imbalance in water availability and overcome the potentially positive
499 effects of atmospheric nitrogen deposition, of the increase in the length of the growing season, and
500 of the rise in atmosphere [CO₂]. The general trend recorded in this study can be partially explained
501 by examining the shape of the relationship between significant environmental factors and BAI. The
502 response to atmospheric [CO₂] (Fig. 9b) presents a strong positive pattern at the low end of the
503 concentration range, with a culmination at around 310 ppm, followed by a decline and an apparent
504 lack of effect at higher concentrations. Although the lack of evidence of a clear fertilization effect
505 of CO₂ is in agreement with previous studies (Peñuelas et al. 2011; Lévesque et al. 2014), it could
506 lead to different conclusions, depending on the processes involved. In a biological perspective, for
507 example, both long-term photosynthetic acclimation (Medlyn et al. 1999) and a shift in allocation
508 of assimilated C to faster-turnover pools such as fine roots or canopy foliage (Korner et al., 2005)
509 are possible explanations. Moreover, this lack of response could be the result of an interaction
510 between CO₂ and nutrient availability effects, which cannot be accounted by a simple additive
511 model. Finally, such an apparent saturation effect of CO₂ could be the result of the lack of significant
512 variables, not included in the model, as for example inter-tree competition. Indeed the radial
513 growth of shade intolerant trees is very much dependent on forest management practices, especially
514 in even-aged stands. Moreover, the extent of drought events could have been insufficiently

515 represented by the rather crude approach applied in the study. Summer water availability (Figure
516 9d), which is related to the transpiration demand, is the second most important variable affecting the
517 behavior of this species in the long-term, conditioning its growth performance (Beedlow et al.
518 2013) and distribution (Rehfeldt et al. 2014). Air dryness, which is also known to affect Douglas fir,
519 was not included as a potential driver due to a lack of suitable information. Furthermore, the
520 influence of the previous growing seasons' summer water balance (Figure 9e) also affects the
521 growth trend, as early-wood width is related to the amount of carbon storage reserves built-up in the
522 preceding year, which are subject to remobilisation in the first phase of vegetative growth (Lee et al.
523 2016). At last, our findings suggest a positive relationship between growth and N deposition
524 (Figure 9c), which potentially reflects the beneficial effect of N increase on photosynthetic rates due
525 to the resulting increase in photosynthetic pigments as well as Rubisco foliar content. The possible
526 stabilization observed at the higher rate of N deposition, if significant, could be interpreted as a
527 saturation of the nitrogen effect on the system. Although N-mineralisation rates at the site are not
528 known, such a saturation above a deposition a N deposition rate of 4.5 kg /ha/yr, however, seems
529 unlikely since Douglas-fir soils at the site display rather high C:N ratios, with an average value of
530 27 (Di Biase et al. 2015), although N mineralisation data are not available to support such the
531 hypothesis of substantial N limitations. Besides, N uptake by Douglas-fir was found to increase
532 asymptotically, until at least 35 kg N ha⁻¹ yr⁻¹ of net nitrogen available (Perakis and Sinkhorn 2011)
533 in US Pacific Coast environments. A possible influence caused by concurrency with other factors,
534 namely CO₂ concentration, should be also taken into consideration. Indeed, when non-stationary
535 forcing factors (i.e., atmospheric [CO₂] and nitrogen deposition) co-vary, it is difficult to
536 disentangle their individual effects on long-term tree growth, and this complication increases with
537 the complexity of the model (Carrer and Urbinati 2006).

538 **5 Conclusions**

539 Given the importance of Douglas-fir as a timber species, the ongoing decrease in growth
540 performance illustrated by this study for the northern Apennines could have relevant implications

541 from a management perspective. For this reason, understanding which factors have been
542 determining such a trend is particularly important. Our model, despite the rather low amount of
543 variance explained and the simplicity of the model structure (only few variables considered), as
544 well as its additive nature, allows us to draw some conclusions. The impact of summer water
545 availability, which is projected to decrease in the Mediterranean region (IPCC, 2014), could be
546 responsible to a considerable extent for the observed decrease in growth rates in recent decades, due
547 to the increase in magnitude and frequency of drought events. A parallel positive effect ascribable
548 to N deposition, which should have promoted the stem growth in the past, may no longer be able to
549 counterbalance the summer drought stress effect, due to the stabilization in NO_y emission and an
550 apparent saturation of the N response. Especially in the absence of a positive effect of fertilization
551 by rising atmospheric [CO₂], the observed trend can be expected to be exacerbated in the next
552 future.

553 Finally, GAMs appear to have a promising potential to disentangle non-linear biological and
554 environmental effects affecting tree growth, resulting in long-term trend preservation, which is
555 fundamental if a better understanding of past environmental effects is to be used to understand the
556 future behavior of forests in a changing world.

557 **6. Acknowledgments**

558 We thank NOAA (ITRDB and ESRL) and the Regional Hydrological Service of the Tuscany
559 Region (SIR), for providing the data used in this study; also the “Reparto Carabinieri per la
560 biodiversità di Vallombrosa” which kindly provided sampling permission.

561 This work was carried out within the framework of the Convention between the Department of
562 Agricultural Sciences of the University of Bologna and the Council for Agricultural Research and
563 Economics.



564

565 7. Bibliography

566 ABER, JOHN D., CHRISTINE L. GOODALE, SCOTT V. OLLINGER, MARIE-LOUISE
567 SMITH, ALISON H. MAGILL, MARY E. MARTIN, RICHARD A. HALLETT, and JOHN
568 L. STODDARD. 2003. "Is Nitrogen Deposition Altering the Nitrogen Status of Northeastern
569 Forests?" *BioScience* 53 (4): 375. doi:10.1641/0006-3568(2003)053[0375:INDATN]2.0.CO;2.

570 Aho, Ken, DeWayne Derryberry, and Teri Peterson. 2014. "Model Selection for Ecologists: The
571 Worldview of AIC and BIC." *Ecology* 95 (March): 631–36. doi:10.1890/13-1452.1.

- 572 Ainsworth, Elizabeth A., and Stephen P. Long. 2005. "What Have We Learned from 15 Years of
573 Free-Air CO₂ Enrichment (FACE)? A Meta-Analytic Review of the Responses of
574 Photosynthesis, Canopy Properties and Plant Production to Rising CO₂." *New Phytologist* 165
575 (2): 351–71. doi:10.1111/j.1469-8137.2004.01224.x.
- 576 Babst, Flurin, M. Ross Alexander, Paul Szejner, Olivier Bouriaud, Stefan Klesse, John Roden,
577 Philippe Ciais, et al. 2014. "A Tree-Ring Perspective on the Terrestrial Carbon Cycle."
578 *Oecologia* 176 (2): 307–22. doi:10.1007/s00442-014-3031-6.
- 579 Beedlow, Peter A., E. Henry Lee, David T. Tingey, Ronald S. Waschmann, and Connie A. Burdick.
580 2013. "The Importance of Seasonal Temperature and Moisture Patterns on Growth of Douglas-
581 Fir in Western Oregon, USA." *Agricultural and Forest Meteorology* 169. Elsevier B.V.: 174–
582 85. doi:10.1016/j.agrformet.2012.10.010.
- 583 Biondi, Franco. 1999. "Comparing Tree-Ring Chronologies and Repeated timber Inventories as
584 Forest Monitoring Tools." *Ecological Applications* 9 (1): 216–27. doi:10.1890/1051-
585 0761(1999)009[0216:CTRCAR]2.0.CO;2.
- 586 Boettger, Tatjana, Marika Haupt, Kay Knöller, Stephan M. Weise, John S. Waterhouse, Katja T.
587 Rinne, Neil J. Loader, et al. 2007. "Wood Cellulose Preparation Methods and Mass
588 Spectrometric Analyses of ¹³C, ¹⁸O, and Nonexchangeable ²H Values in Cellulose,
589 Sugar, and Starch: An Interlaboratory Comparison." *Analytical Chemistry* 79 (12): 4603–12.
590 doi:10.1021/ac0700023.
- 591 Boisvenue, Céline, and Steven W. Running. 2006. "Impacts of Climate Change on Natural Forest
592 Productivity - Evidence since the Middle of the 20th Century." *Global Change Biology* 12 (5):
593 862–82. doi:10.1111/j.1365-2486.2006.01134.x.
- 594 Brienen, R J W, E Gloor, S Clerici, R Newton, L Arppe, A Boom, S Bottrell, et al. n.d. "Isotopes."
595 *Nature Communications*. Springer US, 1–10. doi:10.1038/s41467-017-00225-z.
- 596 Brunel, J.P., G.R. Walker, C.D. Walker, J.C. Dighton, and A. Kennett-Smith. 1991. "Using Stable
597 Isotopes of Water to Trace Plant Water Uptake." *International Symposium on the Use of Stable*
598 *Isotopes in Plant Nutrition, Soil Fertility and Environmental Studies*, 543–551.
599 doi:10.2144/000114133.
- 600 Bunn, Andrew G. 2008. "A Dendrochronology Program Library in R (dplR)." *Dendrochronologia*
601 26 (2): 115–24. doi:10.1016/j.dendro.2008.01.002.
- 602 Camarero, J. Julio, Antonio Gazol, Jacques C. Tardif, and France Conciatori. 2015. "Attributing
603 Forest Responses to Global-Change Drivers: Limited Evidence of a CO₂-Fertilization Effect in
604 Iberian Pine Growth." *Journal of Biogeography* 42 (11): 2220–33. doi:10.1111/jbi.12590.
- 605 Carrer, Marco, and C Urbinati. 2006. "Long-Term Change in the Sensitivity of Tree ring Growth
606 to Climate Forcing in *Larix Decidua*." *New Phytologist* 170 (iv): 861–72.
- 607 Cook, Edward R., Keith R. Briffa, David M Meko, Donald A Graybill, and Gary Funkhouser. 1995.
608 "The 'segment Length Curse' in Long Tree-Ring Chronology Development for Palaeoclimatic
609 Studies." *The Holocene* 5 (2): 229–37. doi:10.1177/095968369500500211.
- 610 Dawson, T E. 1998. "Fog in the Californian Redwood Forest: Ecosystem Inputs and Use by
611 Plants." *Oecologia* 117: 476–85.
- 612 Dawson, Todd E., Stefania Mambelli, Agneta H. Plamboeck, Pamela H. Templer, and Kevin P. Tu.

- 613 2002. "Stable Isotopes in Plant Ecology." *Annual Review of Ecology and Systematics* 33 (1):
614 507–59. doi:10.1146/annurev.ecolsys.33.020602.095451.
- 615 Dawson, Todd E., and John S Pate. 1996. "Seasonal Water Uptake and Movement in Root Systems
616 of Australian Phraeatophytic Plants of Dimorphic Root Morphology: A Stable Isotope
617 Investigation." *Oecologia* 107 (1): 13–20. doi:10.1007/BF00582230.
- 618 Di Biase, Giampaolo, Gloria Falsone, Anna Graziani, Gilmo Vianello, and Livia Vittori Antisari.
619 2015. "Carbon Sequestration in Soils Affected By Douglas Fir Reforestation in Apennines
620 (Northern Italy)." *Eqa-International Journal of Environmental Quality* 17: 1–11.
621 doi:10.6092/issn.2281-4485/5208.
- 622 Dongmann, G, and H W Nürnberg. 1974. "On the Enrichment of H²18O in the Leaves of
623 Transpiring Plants I T L Q E" 52: 1–2.
- 624 Esper, Jan, Edward R Cook, and Fritz H Schweingruber. 2002. "Low-Frequency Signals in Long
625 Tree-Ring Chronologies for Reconstructing Past Temperature Variability." *Science (New York,
626 N.Y.)* 295 (5563). American Association for the Advancement of Science: 2250–53.
627 doi:10.1126/science.1066208.
- 628 Esper, Jan, David C. Frank, Giovanna Battipaglia, Ulf Büntgen, Christopher Holert, Kerstin
629 Treydte, Rolf Siegwolf, and Matthias Saurer. 2010a. "Low-Frequency Noise in ¹³C and
630 ¹⁸O Tree Ring Data: A Case Study of Pinus Uncinata in the Spanish Pyrenees." *Global
631 Biogeochemical Cycles* 24 (4): 1–11. doi:10.1029/2010GB003772.
- 632 Esper, Jan, David C Frank, Giovanna Battipaglia, Ulf Büntgen, Christopher Holert, Kerstin Treydte,
633 Rolf Siegwolf, and Matthias Saurer. 2010b. "Low Frequency Noise in D ¹³ C and D ¹⁸ O
634 Tree Ring Data : A Case Study of Pinus Uncinata in the Spanish Pyrenees" 24 (2): 1–11.
635 doi:10.1029/2010GB003772.
- 636 Farquhar, G. D., L. A. Cernusak, and B. Barnes. 2006. "Heavy Water Fractionation during
637 Transpiration." *Plant Physiology* 143 (1): 11–18. doi:10.1104/pp.106.093278.
- 638 Farquhar, G D, J R Ehleringer, and K T Hubick. 1989. "Carbon Isotope Discrimination and
639 Photosynthesis." *Annual Review of Plant Physiology and Plant Molecular Biology*.
640 doi:10.1146/annurev.pp.40.060189.002443.
- 641 Federal, Swiss, Universitat De Barcelona, J. Julio Camarero, Antonio Gazol, Juan Diego Galván,
642 Gabriel Sangüesa-Barreda, and Emilia Gutiérrez. 2015. "Disparate Effects of Global-Change
643 Drivers on Mountain Conifer Forests: Warming-Induced Growth Enhancement in Young Trees
644 vs. CO₂ Fertilization in Old Trees from Wet Sites." *Global Change Biology* 21 (2): 738–49.
645 doi:10.1111/gcb.12787.
- 646 Fenn, Mark E, Jeremy S Fried, Haiganoush K Preisler, Andrzej Bytnerowicz, Susan Schilling,
647 Sarah Jovan, and Olaf Kuegler. 2015. "REMEASURED FIA PLOTS REVEAL TREE-LEVEL
648 DIAMETER GROWTH AND TREE MORTALITY IMPACTS OF NITROGEN
649 DEPOSITION ON CALIFORNIA ' S FORESTS" 2013 (Time 2): 2013–16.
- 650 Francey, R. J., C. E. Allison, D. M. Etheridge, C. M. Trudinger, I. G. Enting, M. Leuenberger, R. L.
651 Langenfelds, E. Michel, and L. P. Steele. 1999. "A 1000-Year High Precision Record of ¹³C
652 in Atmospheric CO₂." *Tellus, Series B: Chemical and Physical Meteorology* 51 (2): 170–93.
653 doi:10.1034/j.1600-0889.1999.t01-1-00005.x.
- 654 Frank, D. C., B. Poulter, M. Saurer, J. Esper, C. Huntingford, G. Helle, K. Treydte, et al. 2015.

- 655 “Water-Use Efficiency and Transpiration across European Forests during the Anthropocene.”
656 *Nature Climate Change*, no. May. doi:10.1038/nclimate2614.
- 657 Giustini, Francesca, Mauro Brilli, and Antonio Patera. 2016. “Mapping Oxygen Stable Isotopes of
658 Precipitation in Italy.” *Journal of Hydrology: Regional Studies* 8. Elsevier B.V.: 162–81.
659 doi:10.1016/j.ejrh.2016.04.001.
- 660 Gómez-Guerrero, Armando, Lucas C.R. R Silva, Miguel Barrera-Reyes, Barbara Kishchuk,
661 Alejandro Velázquez-Martínez, Tomás Martínez-Trinidad, Francisca Ofelia Plascencia-
662 Escalante, and William R. Horwath. 2013. “Growth Decline and Divergent Tree Ring Isotopic
663 Composition (^{13}C and ^{18}O) Contradict Predictions of CO_2 Stimulation in High Altitudinal
664 Forests.” *Global Change Biology* 19 (6): 1748–58. doi:10.1111/gcb.12170.
- 665 Griffin, Daniel, and Kevin J Anchukaitis. 2014. “How Unusual Is the 2012 – 2014 California
666 Drought ?,” 9017–23. doi:10.1002/2014GL062433.1.
- 667 Guerrieri, R, Maurizio Mencuccini, L J Sheppard, M Saurer, M P Perks, P Levy, M a Sutton, Marco
668 Borghetti, and J Grace. 2011. “The Legacy of Enhanced N and S Deposition as Revealed by
669 the Combined Analysis of Delta ^{13}C , Delta ^{18}O and Delta ^{15}N in Tree Rings.” *Global
670 Change Biology* 17 (5): 1946–62. doi:10.1111/j.1365-2486.2010.02362.x.
- 671 Harris, I., P. D. Jones, T. J. Osborn, and D. H. Lister. 2014. “Updated High-Resolution Grids of
672 Monthly Climatic Observations - the CRU TS3.10 Dataset.” *International Journal of
673 Climatology* 34 (3): 623–42. doi:10.1002/joc.3711.
- 674 Hastie, T. J., and R. J. Tibshirani. 1990. “Generalized Additive Models.” *Monographs on Statistics
675 and Applied Probability*. doi:10.1016/j.csda.2010.05.004.
- 676 IPCC. 2014. “Climate Change 2014 Synthesis Report Summary Chapter for Policymakers.” *Ippc*,
677 31. doi:10.1017/CBO9781107415324.
- 678 Keenan, Trevor F, David Y Hollinger, Gil Bohrer, Danilo Dragoni, J William Munger, Hans Peter
679 Schmid, and Andrew D Richardson. 2013. “Increase in Forest Water-Use Efficiency as
680 Atmospheric Carbon Dioxide Concentrations Rise.” *Nature* 499 (7458): 324–27.
681 doi:10.1038/nature12291.
- 682 Korner, C. 2005. “Carbon Flux and Growth in Mature Deciduous Forest Trees Exposed to Elevated
683 CO_2 .” *Science* 309 (5739): 1360–62. doi:10.1126/science.1113977.
- 684 Leavitt, Steven W. 2010. “Tree-Ring C-H-O Isotope Variability and Sampling.” *The Science of the
685 Total Environment* 408 (22): 5244–53. doi:10.1016/j.scitotenv.2010.07.057.
- 686 Lee, E. Henry, Peter A. Beedlow, Ronald S. Waschmann, David T. Tingey, Charlotte Wickham,
687 Steve Cline, Michael Bollman, and Cailie Carlile. 2016. “Douglas-Fir Displays a Range of
688 Growth Responses to Temperature, Water, and Swiss Needle Cast in Western Oregon, USA.”
689 *Agricultural and Forest Meteorology* 221. Elsevier B.V.: 176–88.
690 doi:10.1016/j.agrformet.2016.02.009.
- 691 Leonardi, Stefano, Tiziana Gentilesca, Rossella Guerrieri, Francesco Ripullone, Federico Magnani,
692 Maurizio Mencuccini, Twan V. Noije, and Marco Borghetti. 2012. “Assessing the Effects of
693 Nitrogen Deposition and Climate on Carbon Isotope Discrimination and Intrinsic Water-Use
694 Efficiency of Angiosperm and Conifer Trees under Rising CO_2 Conditions.” *Global Change
695 Biology* 18 (9): 2925–44. doi:10.1111/j.1365-2486.2012.02757.x.

- 696 L vesque, Mathieu, Rolf Siegwolf, Matthias Saurer, Britta Eilmann, and Andreas Rigling. 2014.
697 "Increased Water-Use Efficiency Does Not Lead to Enhanced Tree Growth under Xeric and
698 Mesic Conditions." *New Phytologist* 203 (1): 94–109. doi:10.1111/nph.12772.
- 699 Linares, Juan Carlos, Jes s Julio Camarero, and Jos  Antonio Carreira. 2010. "Competition
700 Modulates the Adaptation Capacity of Forests to Climatic Stress: Insights from Recent Growth
701 Decline and Death in Relict Stands of the Mediterranean Fir *Abies Pinsapo*." *Journal of
702 Ecology* 98 (3): 592–603. doi:10.1111/j.1365-2745.2010.01645.x.
- 703 Magnani, Federico, Maurizio Mencuccini, Marco Borghetti, Paul Berbigier, Frank Berninger,
704 Sylvain Delzon, Achim Grelle, et al. 2007. "The Human Footprint in the Carbon Cycle of
705 Temperate and Boreal Forests." *Nature* 447 (7146): 848–50. doi:10.1038/nature05847.
- 706 Marshall, D D, and R O Curtis. 2002. "Levels-of-Growing-Stock Cooperative Study in Douglas-
707 Fir: Report No. 15 - Hoskins: 1963-1998." *Research Paper Pacific Northwest Research
708 Station, USDA Forest Service*, no. PNW-RP-537: 80.
- 709 McCarroll, Danny, and Neil J. Loader. 2004. "Stable Isotopes in Tree Rings." *Quaternary Science
710 Reviews* 23 (7–8): 771–801. doi:10.1016/j.quascirev.2003.06.017.
- 711 McMahon, Sean M, Geoffrey G Parker, and Dawn R Miller. 2010. "Evidence for a Recent Increase
712 in Forest Growth." *Proceedings of the National Academy of Sciences of the United States of
713 America* 107 (8): 3611–15. doi:10.1073/pnas.0912376107.
- 714 Medlyn, B. E., F. -W. Badeck, D. G. G. De Pury, C. V. M. Barton, M. Broadmeadow, R.
715 Ceulemans, P. De Angelis, et al. 1999. "Effects of Elevated [CO₂] on Photosynthesis in
716 European Forest Species: A Meta-Analysis of Model Parameters." *Plant, Cell & Environment*
717 22 (12): 1475–1495. doi:10.1046/j.1365-3040.1999.00523.x.
- 718 Nair, Richard K F, Micheal P Perks, Andrew Weatherall, Elizabeth M Baggs, and Maurizio
719 Mencuccini. 2015. "Does Canopy Nitrogen Uptake Enhance Carbon Sequestration by Trees?"
720 *Global Change Biology*, September. doi:10.1111/gcb.13096.
- 721 Nehrbass-Ahles, Christoph, Flurin Babst, Stefan Klesse, Magdalena N tzli, Olivier Bouriaud,
722 Raphael Neukom, Matthias Dobbertin, and David Frank. 2014. "The Influence of Sampling
723 Design on Tree-Ring-Based Quantification of Forest Growth." *Global Change Biology* 20 (9).
724 doi:10.1111/gcb.12599.
- 725 Norby, Richard J, Jeffrey M Warren, Colleen M Iversen, Belinda E Medlyn, and Ross E
726 McMurtrie. 2010. "CO₂ Enhancement of Forest Productivity Constrained by Limited Nitrogen
727 Availability." *Proceedings of the National Academy of Sciences of the United States of
728 America* 107 (45): 19368–73. doi:10.1073/pnas.1006463107.
- 729 Pe uelas, Josep, Josep G. Canadell, and Rom  Ogaya. 2011. "Increased Water-Use Efficiency
730 during the 20th Century Did Not Translate into Enhanced Tree Growth." *Global Ecology and
731 Biogeography* 20 (4): 597–608. doi:10.1111/j.1466-8238.2010.00608.x.
- 732 Perakis, Steven S., and Emily R. Sinkhorn. 2011. "Biogeochemistry of a Temperate Forest Nitrogen
733 Gradient." *Ecology* 92 (7): 1481–91. doi:10.1890/10-1642.1.
- 734 Peters, Richard L., Peter Groenendijk, Mart Vlam, and Pieter a. Zuidema. 2015. "Detecting Long-
735 Term Growth Trends Using Tree Rings: A Critical Evaluation of Methods." *Global Change
736 Biology*, n/a-n/a. doi:10.1111/gcb.12826.

- 737 Phillips, Nathan G., Thomas N. Buckley, and David T. Tissue. 2008. "Capacity of Old Trees to
738 Respond to Environmental Change." *Journal of Integrative Plant Biology* 50 (11): 1355–64.
739 doi:10.1111/j.1744-7909.2008.00746.x.
- 740 Piovesan, Gianluca, Franco Biondi, Aalfredo Di Filippo, Alfredo Alessandrini, and Maurizio
741 Maugeri. 2008. "Drought-Driven Growth Reduction in Old Beech (*Fagus Sylvatica* L.) Forests
742 of the Central Apennines, Italy." *Global Change Biology* 14 (6): 1265–81. doi:10.1111/j.1365-
743 2486.2008.01570.x.
- 744 Poage, Nathan J, and John C Tappeiner, II. 2002. "Long-Term Patterns of Diameter and Basal Area
745 Growth of Old-Growth Douglas-Fir Trees in Western Oregon." *Canadian Journal of Forest
746 Research* 32: 1232–43. doi:10.1139/x02-045.
- 747 Rehfeldt, Gerald E., Barry C. Jaquish, Javier Lòpez-Upton, Cuauhtémocmoc Sáenz-Romero, J.
748 Bradley St Clair, Laura P. Leites, and Dennis G. Joyce. 2014. "Comparative Genetic
749 Responses to Climate for the Varieties of *Pinus Ponderosa* and *Pseudotsuga Menziesii*:
750 Realized Climate Niches." *Forest Ecology and Management* 324. Elsevier B.V.: 126–37.
751 doi:10.1016/j.foreco.2014.02.035.
- 752 Ripullone, Francesco, Marco Lauteri, Giacomo Grassi, Mariana Amato, and Marco Borghetti. 2004.
753 "Variation in Nitrogen Supply Changes Water-Use Efficiency of *Pseudotsuga Menziesii* and
754 *Populus X Euroamericana*; a Comparison of Three Approaches to Determine Water-Use
755 Efficiency." *Tree Physiology* 24 (6): 671–79.
- 756 Rita, Angelo, Marco Borghetti, Luigi Todaro, and Antonio Saracino. 2016. "Interpreting the
757 Climatic Effects on Xylem Functional Traits in Two Mediterranean Oak Species: The Role of
758 Extreme Climatic Events." *Frontiers in Plant Science* 7 (August): 1–11.
759 doi:10.3389/fpls.2016.01126.
- 760 Roden, John, and Rolf Siegwolf. 2012. "Is the Dual-Isotope Conceptual Model Fully Operational?"
761 *Tree Physiology* 32 (10): 1179–82. doi:10.1093/treephys/tps099.
- 762 Rozanski, Kazimierz, Luis Araguas-araguas, and Roberto Gonfiantini. 2016. "Relation Between
763 Long-Term Trends of Oxygen-18 Isotope Composition of Precipitation and Climate Author (S
764): Kazimierz Rozanski , Luis Araguás-Araguás and Roberto Gonfiantini Published by :
765 American Association for the Advancement of Science Stable URL :." 258 (5084): 981–85.
- 766 Ryan, Mg, D Binkley, and Jh Fownes. 1997. "Age-Related Decline in Forest Productivity: Pattern
767 and Process." *Advances in Ecological Research*.
- 768 Ryan, Michael G., Nathan Phillips, and Barbara J. Bond. 2006. "The Hydraulic Limitation
769 Hypothesis Revisited." *Plant, Cell and Environment* 29 (3): 367–81. doi:10.1111/j.1365-
770 3040.2005.01478.x.
- 771 Ryan, Michael G., and Barbara J. Yoder. 1997. "Hydraulic Limits to Tree Height and Tree
772 Growth." *BioScience* 47 (4): 235–42. doi:10.2307/1313077.
- 773 Saurer, Matthias, Rolf T. W. Siegwolf, and Fritz H. Schweingruber. 2004. "Carbon Isotope
774 Discrimination Indicates Improving Water-Use Efficiency of Trees in Northern Eurasia over
775 the Last 100 Years." *Global Change Biology* 10 (12): 2109–20. doi:10.1111/j.1365-
776 2486.2004.00869.x.
- 777 Scheidegger, Y., M. Saurer, M. Bahn, and R. Siegwolf. 2000. "Linking Stable Oxygen and Carbon
778 Isotopes with Stomatal Conductance and Photosynthetic Capacity: A Conceptual Model."

- 779 *Oecologia* 125 (3): 350–57. doi:10.1007/s004420000466.
- 780 Sitch, Stephan, C. Huntingford, N. Gedney, P. E. Levy, M. Lomas, S. L. Piao, R. Betts, et al. 2008.
781 “Evaluation of the Terrestrial Carbon Cycle, Future Plant Geography and Climate-Carbon
782 Cycle Feedbacks Using Five Dynamic Global Vegetation Models (DGVMs).” *Global Change
783 Biology* 14 (9): 2015–39. doi:10.1111/j.1365-2486.2008.01626.x.
- 784 Sternberg, Leonel Da Silveira Lobo O.Reilly. 2009. “Oxygen Stable Isotope Ratios of Tree-Ring
785 Cellulose: The next Phase of Understanding.” *New Phytologist* 181 (3): 553–62.
786 doi:10.1111/j.1469-8137.2008.02661.x.
- 787 Treydte, Kerstin, Sonja Boda, Elisabeth Graf Pannatier, Patrick Fonti, David Frank, Bastian Ullrich,
788 Matthias Saurer, et al. 2014. “Seasonal Transfer of Oxygen Isotopes from Precipitation and
789 Soil to the Tree Ring : Source Water versus Needle Water Enrichment.”
- 790 Vicente-Serrano, Sergio M., Santiago Beguería, and Juan I. López-Moreno. 2010. “A Multiscalar
791 Drought Index Sensitive to Global Warming: The Standardized Precipitation
792 Evapotranspiration Index.” *Journal of Climate* 23 (7): 1696–1718.
793 doi:10.1175/2009JCLI2909.1.
- 794 Vicente-Serrano, Sergio M., J. Julio Camarero, and Cesar Azorin-Molina. 2014. “Diverse
795 Responses of Forest Growth to Drought Time-Scales in the Northern Hemisphere.” *Global
796 Ecology and Biogeography* 23 (9): 1019–30. doi:10.1111/geb.12183.
- 797 Vitas, A., and K. Žeimavi ius. 2006. “Trends of Decline of Douglas Fir in Lithuania :
798 Dendroclimatological Approach.” *Baltic Forestry* 12 (2): 200–208.
- 799 Walker, Lawrence R., David a. Wardle, Richard D. Bardgett, and Bruce D. Clarkson. 2010. “The
800 Use of Chronosequences in Studies of Ecological Succession and Soil Development.” *Journal
801 of Ecology* 98 (4): 725–36. doi:10.1111/j.1365-2745.2010.01664.x.
- 802 Warren, Cr, Jf McGrath, and Ma Adams. 2001. “Water Availability and Carbon Isotope
803 Discrimination in Conifers.” *Oecologia* 127 (4): 476–86. doi:10.1007/s004420000609.
- 804 Williams, David G., R. David Evans, Jason B. West, and James R. Ehleringer. 2007. *Stable
805 Isotopes as Indicators of Ecological Change. Terrestrial Ecology*. Vol. 1. doi:10.1016/S1936-
806 7961(07)01024-X.
- 807 Wood, Simon N. “Package ‘ Mgcv ’.” doi:10.1186/1471-2105-11-11.Bioconductor.
- 808 Wood, Simon N. 2017. “Package ‘ Mgcv .’”
- 809 Wood, Simon N. 2006. *Generalized Additive Models: An Introduction with R*. Chapman and
810 Hall/CRC.
- 811 Wood, Simon N. 2008. “Fast Stable Direct Fitting and Smoothness Selection for Generalized
812 Additive Models.” *Journal of the Royal Statistical Society. Series B: Statistical Methodology*
813 70 (3): 495–518. doi:10.1111/j.1467-9868.2007.00646.x.
- 814 Zhao, Maosheng, and Steven W Running. 2010. “Drought-Induced Reduction in Global Terrestrial
815 Net Primary Production from 2000 Through 2009.” *Science* 329 (5994): 940–43.
816 doi:10.1126/science.1192666.
- 817 Zweifel, Roman, Lukas Zimmermann, Fabienne Zeugin, and David M. Newbery. 2006. “Intra-

820

821 **Chapter II - Douglas fir eco-physiological** 822 **response to global change**

823

824 **1. Introduction**

825

826 Global change has resulted in a significant alteration of forests growth over recent decades, in
827 Europe in particular (Boisvenue and Running 2006; Zhao and Running 2010), but the main drivers
828 and functional basis of this trend still have to be ascertained.

829 State-of-the-art earth system models (e.g. Sitch et al. 2008) predict a stimulation of photosynthetic
830 rates (A_{\max}) as a result of increasing atmospheric $[\text{CO}_2]$ and temperatures, as well as atmospheric N
831 deposition (Magnani et al. 2007), resulting in higher rates of Gross Primary Production (GPP). On
832 the other hand, this positive effect could be negated by parallel changes in stomatal conductance
833 (g_s) and transpiration rates, in particular in dry regions (Gómez-Guerrero et al. 2013). The balance
834 between these two processes reflects in variations in intrinsic water-use efficiency ($i\text{WUE} =$
835 A_{\max}/g_s), which affects the amount of carbon gained by the tree per unit of water lost and is
836 therefore an important functional parameter, in particular in dry climates where water acts as an
837 important limiting factor.

838 At tree level, both manipulative experiments under elevated air $[\text{CO}_2]$ (Ainsworth and Long 2005)
839 and studies on field-growth trees, considering the effects of increasing atmospheric CO_2 in
840 combination with a range of co-limiting factors, demonstrate an increase in $i\text{WUE}$ as a result of
841 global change (Peñuelas et al., 2011; Frank et al. 2015). On the other hand, contrasting results were
842 obtained on the effects of CO_2 enrichment on growth.

843 As a complement to long-term experimentation the stable isotope composition recorded in wood
844 tree rings can be considered as reliable eco-physiological proxies for retrospective analysis on

845 iWUE trends (Farquhar et al.,1989). Plant carbon isotopic composition (^{13}C) is known to be
846 directly related to iWUE and therefore affected by variations in either A or g_s , or both, while
847 oxygen isotopic composition (^{18}O) is mainly affected by evaporative enrichment at the leaf level,
848 linked to g_s , but is independent from A changes. As a result, the combined analysis of both isotope
849 signals, the so called dual isotope approach, can be used to isolate the effects of A and g_s on iWUE
850 long-term trends (Scheidegger et al. 2000).

851 This would eventually make it possible to recognize if the observed trends are driven by a CO₂
852 fertilization effect or by changes in water availability constraints.

853 Both growth and iWUE, however, are potentially affected also by tree age and size, possibly due to
854 a gradual decline in g_s with the progressive increase of hydraulic resistance in taller stems (Ryan
855 and Yoder 1997). The separation of such an (endogenous) age/size signal from the combined
856 (exogenous) environmental signal is therefore a pre-requisite for the correct interpretation of global
857 change impact on forest growth and iWUE.

858 A better understanding of the long-term reaction of forest ecosystems to the combined action of
859 rising [CO₂] and climate covariates is determinant to forecast their future role as a carbon sink or
860 source and the magnitude of their mitigation effect on global change. Furthermore it can provide
861 important insights in the future behavior of economically important timber species such as Douglas
862 fir (*Pseudotsuga menziesii* (Mirb.) Franco), thus affecting management choices.

863 The aim of the present study is therefore

864 (i) to evaluate the impact of age/size and global change effects on isotopic long-term variations in
865 Douglas fir on the Italian Appennines,

866 (ii) to understand the main global change components driving Douglas-fir eco-physiological
867 response and

868 (iii) using the dual isotope approach to disentangle the role of changes in photosynthetic activity or
869 stomatal conductance in recent iWUE trends.

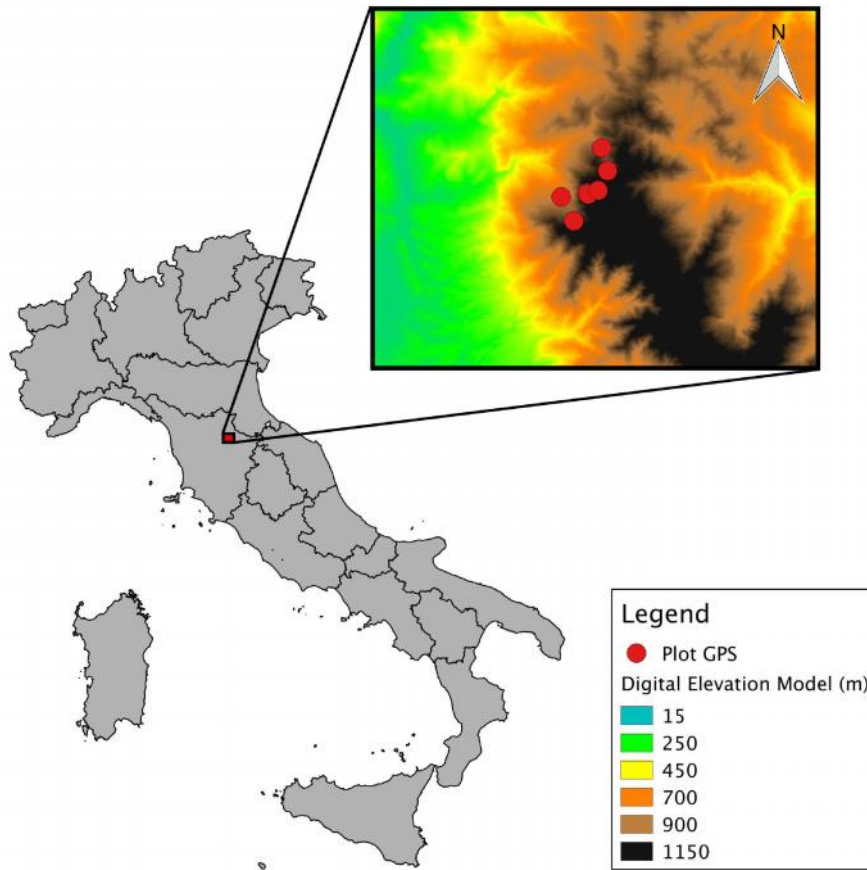
870

871

872 2. Material and Methods

873

874 2.1 Study area



875

876 **Fig.1 Map** shows the location of the seven plots sampled (red dots). Different colors are related to different
877 elevations (m, a.s.l.).

878

879 This study was performed in a Douglas-fir plantation located in the Vallombrosa Forest, in the
880 Apennine mountain range near Florence, Italy (43°43'59.6"N 11°33'16.9"E). The region has a
881 Mediterranean climate without significant summer droughts, and the mean annual precipitation is
882 approximately 1400 mm, of which less than 10% occurs in the summer months (72.48 mm). The
883 mean annual temperature is 9.8°C. The soils, derived from the Macigno del Chianti sandstone
884 series, vary between Humic Dystrudept and Typic Humudept (USDA Soil Survey Staff, 1999) in the
885 younger and older stands, respectively, indicating similar soil conditions at the sites. Douglas-fir is a

886 non-indigenous evergreen species and was imported from the Pacific Coast of the United States
887 during the last decades of the 19th century. It was chosen for the present study because of its high
888 economic importance. The sampled areas are part of the experimental permanent plot network
889 managed by CREA Research Centre for Forestry and Wood, and include the oldest experimental
890 plots established in Italy at the beginning of the 20th century (Pavari 1916).

891 A chronosequence of plots was selected for the study; a chronosequence is here defined as a set of
892 even-aged stands growing under the same environmental conditions and differing only for their age
893 (Walker et al. 2010). The chronosequence comprises four different age classes (with mean age 65,
894 80, 100 and 120 years), covering the longest temporal extension that is possible to achieve in Italy
895 for this species. The summary characteristics of the four age classes are summarized in Table 1.
896 Seven plots were sampled that were consistent for management, aspect and elevation. Two plots
897 were selected for each age class, in order to ensure replication; however this was not possible for
898 the oldest class, as only one of this age was present in the area. In all sites, only dominant trees
899 were chosen for the analysis, in order to avoid competition effects. Data from repeated forest
900 inventories at the sites ensured the permanence of their dominant status, thus partially avoiding
901 potential sampling biases, which occur when the currently largest-diameter trees are wrongly
902 considered to have always been in the dominant class (Cherubini et al. 1998). 3
903

Tab. 1 | Mean characteristics of the Douglas fir chronosequence plots.

	Age-class						
	120		100		80		65
Plot (code)	1	2	3	4	5	6	7
Max age (yrs)	126	101	102	86	86	69	69
Elevation (a.s.l.)	900	1100	1009	1095	1280	1113	1113
Esposition	N	N	SW	NE	NE	SW	SW
Dominant diameter (cm)	--	60.8	67.5	58.2	61,5	50.3	43.3
Dominant high (m)	--	47.2	54.4	49.9	44.3	39.9	39.8
Stand density (n°ha-1)	30*	375	380	360	280	600	550
Trees sampled (n°)	5	5	5	5	5	5	5

904 *for the oldest plot only 30 plants are left standing

905 2.2 Samples preparation and isotopic analysis

906

907 Stable isotopes series were measured for individual trees at 5-years resolution. After cross-dating
908 (following the procedure described in chapter I), cores were subdivided in 5-rings blocks with a
909 scalpel under a stereo-microscope. The blocks were subsequently ground with a ball-mill (MM400,
910 Retsch, Germany) and pooled together. No fixative (glue or adhesive tape) or substance to highlight
911 the rings (dye or chalk) were used during tree-rings analysis, so as to avoid any potential chemical
912 contamination (Williams et al. 2007). All analyses were performed on whole wood rather than -
913 cellulose samples; however, since lignin or other mobile compounds (i.e. resins, oils and hemi-
914 cellulose) could be deposited after the year of ring formation, so leading to biological
915 misinterpretation, the isotopic composition of both whole wood and -cellulose was measured on a
916 representative sub-set of samples (n=35, coming from 7 different trees, one for each plot). The
917 calibration equation derived from the comparison of the two groups was used to correct all
918 measurements for a constant offset as discussed in Warren (2001; Fig.1 and 2). The -cellulose
919 extraction method adopted was the one proposed by Boettger (2007); 10 mg of fine-powdered
920 wood samples were weighted and sealed in Teflon bags. In a first step, samples were incubated
921 twice for 2 hours at 60 °C in a 5% NaOH solution to remove fats, oils, resins, tannins and some
922 hemi-cellulose. Afterward, samples were washed three times with boiling deionizer water to stop
923 the reaction. In a second step, lignin was removed with a 7 % NaClO₂ solution, with the addition of
924 8-16 ml of acetic acid (CH₃OOH) per liter, until the solution achieved a pH level between 4-5. The
925 reaction was run for 36 h at 60°C, changing the solution every 10 hours. Finally, samples were
926 washed three times in boiling deionizer water and dried at 50 °C. For each sample, an amount of
927 0.250 mg ±0.02 and 0.55 ±0.03 was weighted into tin or silver cups for carbon (C) or oxygen (O)
928 analysis, respectively. A total of 1222 (n=611 for both C and O) whole-wood samples were
929 measured, in addition to the 70 tested for pairwise comparison of -cellulose against whole wood
930 measurements. Carbon stable isotope analysis were performed in continuous flow-isotope ratio
931 mass spectrometry (CF-IRMS), with an isotopic mass spectrometer (DELTA Plus, Thermofisher)

932 interfaced to an elemental analyzer. Oxygen stable isotopes were measured in an elemental analyzer
933 (EA-1108, Carlo Erba Thermoquest, Milan, Italy), after decomposition into CO of the material with
934 thermal pyrolysis at 1080°C and analyzed with a isotope ratio mass spectrometer (Delta Plus XP,
935 Thermo Finnigan) also in continuous flow. The precision of the analyses was $\pm 0.1\%$ for carbon and
936 $\pm 0.2\%$ for oxygen, and raw data were expressed as relative deviation from the international
937 standards V-PDB (Vienna Pee Dee Belemnite for $^{13}\text{C}/^{12}\text{C}$) and V-SMOW (Vienna Standard Mean
938 Ocean Water for $^{18}\text{O}/^{16}\text{O}$).

939

940 2.3 $\delta^{13}\text{C}$ theory

941

942 Carbon isotopic composition (^{13}C) in tree rings provides an integrative measurement of the whole
943 tree photosynthetic and gas exchange activity throughout the period the wood was synthesized
944 (Todd E. Dawson et al. 2002). In fact, plants tend to discriminate against $^{13}\text{CO}_2$, therefore the
945 resulting organic matter is enriched in the lighter isotope, ^{12}C , compared to atmosphere. The level of
946 this enrichment is mediated by environmental conditions, such as temperature and water
947 availability, which influence the conductance (g_s), but also by biogeochemical factors affecting
948 photosynthesis (A_{max}), such as atmospheric CO_2 concentration or N deposition. Thus, the analysis
949 of carbon isotope discrimination recorded in tree rings can provide a dated source of information
950 useful to reconstruct tree long-term physiological activity. Sample isotopic composition is
951 expressed as the relative abundance $^{13}\text{C}/^{12}\text{C}$ of the sample (R_{sample}) compared to the V-PDB standard
952 (R_{standard})

953

$$954 \quad \delta^{13}\text{C} = [(R_{\text{sample}}/R_{\text{standard}}) - 1] \times 1000 \quad (1)$$

955

956 To remove the effect of the atmospheric decline in ^{13}C caused by anthropogenic emissions
957 (typically depleted in $^{13}\text{CO}_2$), the so called “Suess effect” (Francey et al. 1999), the ^{13}C
958 composition was expressed in terms of discrimination against ^{13}C by the equation:

959

960

$$^{13}\text{C} = (^{13}\text{C}_a - ^{13}\text{C}_p)/(1+ ^{13}\text{C}_p) \quad (2)$$

961

962 where $^{13}\text{C}_a$ and $^{13}\text{C}_p$ are the isotopic composition of carbon of atmospheric CO_2 and plant
963 material, respectively. The stable isotope discrimination of plants tissue was related to c_i/c_a through
964 the linear model developed by Farquhar (1989) as:

965

966

$$^{13}\text{C} = a + (b-a) c_i/c_a \quad (3)$$

967

968 where a is the isotopic fractionation during photosynthetic gas exchange caused by the slower
969 diffusion of $^{13}\text{CO}_2$ through stomata (4.4‰), b is the net fractionation associated with RuBP
970 carboxylase activity (27‰), and c_a and c_i are the atmospheric and intercellular $[\text{CO}_2]$. On the other
971 hand, the c_i/c_a ratio can also be linked to changes in intrinsic water-use efficiency (iWUE), defined
972 as the ratio between maximum photosynthetic capacity (A_{max}) and stomatal conductance (g_s):

973

974

$$\text{iWUE} = A_{\text{max}} / g_s = (c_a - c_i) / 1.6 \quad (4)$$

975

976 As a result, it is possible to infer iWUE changes from ^{13}C as:

977

978

$$\text{iWUE} = 0.625 c_a [1 - (^{13}\text{C} - a) / (b - a)] \quad (5)$$

979

980 Mean annual $^{13}\text{C}_a$ values used in the present study were obtained from the NOAA Earth System
981 Research Laboratory, recorded at the Mauna Loa observatory in Hawaii from 1959 to present,
982 integrated with those published by McCarroll and Loader (2004) for previous years.

983

984 2.4 $\delta^{18}\text{O}$ theory

985 Tree-ring oxygen isotope composition depends on the one hand on the ^{18}O signal of the water
986 source used by the tree, on the other hand on evaporative enrichment, which occurs at leaf level as a
987 result of transpiration (Sternberg 2009). The primary source of water for forest trees is typically
988 meteoric, but its ^{18}O signature can vary in space and time. Temporal variations at an inter-annual
989 scale are related to climatic factors; for example warmer years are characterized by an enrichment
990 in the composition of meteoric water due to higher proportion of H_2^{18}O molecules evaporated from
991 oceans (Rozanski et al., 1992). Moreover, intra-annual variations in plants' main source of water
992 (precipitation, ground water, fog or snow), as well as seasonal isotopic changes of these sources
993 themselves, due to temperature dependent fractionation, can determine an additional shift in the
994 input signal (Todd E. Dawson and Pate 1996). The spatial variation in precipitation ^{18}O is
995 influenced by both distance from the sea and elevation (Giustini et al., 2016): as air moves from a
996 lower to a higher region, the temperature differential produces an isotope vertical gradient. This
997 altitude-dependent fractionation is determined by the progressive depletion from the rain of the
998 H_2^{18}O , which tends to condensate faster relative to H_2^{16}O . Once in the soil, water tends to
999 become gradually enriched in the heavier isotope (H_2^{18}O) close to the surface (0.1-0.5 m). This
1000 process is caused by the preferential depletion in H_2^{16}O due to evaporative effect and it is enhanced
1001 by the residence time of water in the ground. Deeper moisture remains unaffected, mirroring the
1002 system water source composition (Brunel et al. 1991). As a result, the depth at which root systems
1003 are tapping water can determine the input isotopic signal and it could change over the life of the tree
1004 as the root system grows deeper. This is one of the possible causes proposed to explain a possible
1005 age-related ^{18}O decreasing trend observed in trees (Esper et al. 2010). No additional isotopic
1006 fractionation is expected when water enters into roots and during its transport through the xylem to
1007 the leaves (Dawson and Ehleringer, 1991).

1008 Secondly, a process of evaporative enrichment relative to the source of water takes place at the leaf
1009 level (Dongmann and Nürnberg 1974). The mechanistic model proposed by Craig and Gordon

1010 (1965) to explain the degree of enrichment at the evaporation sites ($^{18}\text{O}_e$) above the xylem water
1011 predicts that:

1012

$$1013 \quad {}^{18}\text{O}_e = \alpha + \beta ({}^{18}\text{O}_v - \alpha) \frac{e_a}{e_i} \quad (6)$$

1014

1015 where α is the (temperature dependent) equilibrium fractionation between liquid water and water
1016 vapour, β is the kinetic fractionation during water diffusion through stomata and the leaf boundary
1017 layer, ${}^{18}\text{O}_v$ is the water vapour isotope composition in the air relative to the source of water (= ${}^{18}\text{O}_v - {}^{18}\text{O}_s$) and e_a and e_i are the ambient and intercellular vapour pressure, respectively. This
1018 equation highlights the inverse relationship which exists between air relative humidity (RH), which
1019 influences e_a/e_i , and ${}^{18}\text{O}$ in leaf water. The degree of leaf water enrichment is expected to be
1020 directly related to transpiration (E) rates, if this variation is mainly driven by evaporative demand
1021 (Farquhar et al., 2006). However, this model was found to overestimate the degree of enrichment
1022 due to the failure to consider the mixing of ${}^{18}\text{O}$ of enriched water at evaporation sites with un-
1023 enriched water from the xylem, known as Péclet effect (Farquhar and Lloyd 1993). This tends to be
1024 higher at high transpiration rates (greater xylematic flow), so decreasing the evaporative enrichment
1025 at leaf level. In this way the Péclet effect increases the importance of ${}^{18}\text{O}_s$ in determining the
1026 ${}^{18}\text{O}_{\text{cel}}$, as described by Barbour and Farquhar (2000):

1028

$$1029 \quad {}^{18}\text{O}_{\text{cel}} = {}^{18}\text{O}_s (P_{\text{ex}} * P_x) + {}^{18}\text{O}_l (1 - P_{\text{ex}} * P_x) + \alpha_{\text{wc}} \quad (7)$$

1030

1031 where α_{wc} is the equilibrium fractionation between water and carbonyl groups, P_{ex} is the proportion
1032 of exchangeable oxygen in cellulose and P_x is the proportion of xylem water in the meristematic
1033 tissue where cellulose is synthesized, whereas ${}^{18}\text{O}_l$ is the leaf water isotopic composition. This

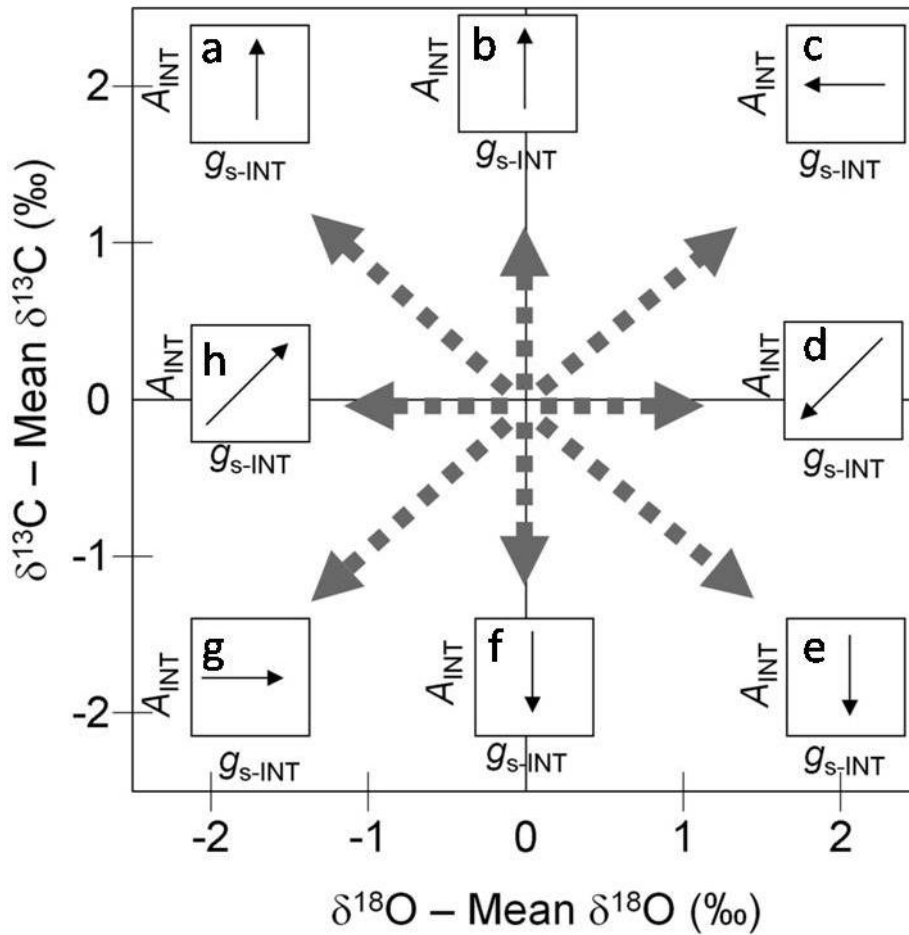
1034 equation highlights the inverse relationship between $^{18}\text{O}_{\text{cel}}$ and stomatal conductance (Grams et al.
1035 2007).

1036 Assuming that the relative strength of evaporative enrichment at the leaf level is preserved and
1037 overshadows the source ^{18}O signal (meteoric), this information could be used to infer the response
1038 of tree stomatal conductance to environmental factors.

1039

1040 **2.5 Dual isotope conceptual model**

1041 The limit in the application of iWUE as a proxy of tree eco-physiological response to environmental
1042 or biochemical forcing is that its variations cannot be attributed unambiguously to changes in either
1043 A_{max} or g_s . For example, a reduction in the ^{13}C values observed in organic matter can be ascribed
1044 to a rise in c_i level and therefore to a reduction in iWUE. This reduction can be ascribed either (i) to
1045 a decrease in photosynthetic activity (at constant g_s) or (ii) to an enhancement in stomatal
1046 conductance (at constant A_{max}). This limitation can be overcome through the application of the
1047 qualitative model proposed by Scheidegger et al. (2000), so as to try to disentangle which factor is
1048 driving the observed iWUE trend. The model enables the deduction of changes in g_s and A_{max} in
1049 subsequent time intervals from different C and O isotope composition patterns. The eight possible
1050 combinations are depicted in the central part of the scheme presented in Fig. 1, representing the
1051 observed patterns, while the arrows in the external boxes highlight the most likely interpretation of
1052 these scenarios. Due to the temporal changes in atmospheric $^{13}\text{C}_a$ (Suess effect) a correction was
1053 preliminarily performed by adding to each $^{13}\text{C}_p$ value a factor corresponding to the deviation of the
1054 corresponding annual $^{13}\text{C}_a$ value from the pre-industrial reference value of -6.4% (McCarroll et al.,
1055 2004). Furthermore, each isotopic series was normalized in respect to its mean to remove infra-
1056 series variability and the possible effect of different water sources among plots for ^{18}O (Barnard et
1057 al.2012).



1058

1059 **Fig.1 Dual isotope conceptual model scheme.** Scheidegger model for relationship interpretation
 1060 between ^{13}C and ^{18}O (here expressed as deviation from the mean). The central part of the pictures
 1061 summarize the 8 possible directions in which temporal variations can move (between time periods).
 1062 Each arrow points on the "most likely case", explaining the behavior of A_{INT} (A_{max} integrated on the
 1063 considered period) and $g_{\text{s-INT}}$ (g_{s} integrated on the considered period). From Barnard et al 2012

1064

1065

1066

1067 **2.6 GAM model**

1068 Since iWUE can potentially show non-linear patterns in response to both biological (i.e. age/size
 1069 and juvenile effect) and environmental (i.e. temperature and precipitation, geochemical variables)
 1070 drivers, Generalized Additive Models (GAMs; (Hastie and Tibshirani 1990) were applied to
 1071 conveniently capture the shape of the inherent relationships existing between iWUE and predictor
 1072 variables, and the superposition of their effects. GAMs are non-linear regression models that

1073 specify the value of the dependent variables as the sum of smooth functions of a number of
1074 independent variables in a non-parametric fashion. Such a model relaxes the *a priori* assumption
1075 of a linear functional relationship between response and predictors that is central to multiple linear
1076 regression models, therefore resulting in a more flexible range of the application. The relationship is
1077 expressed as:

1078

$$1079 \quad y_i = X_i \beta + s_1(x_{i1}) + \dots + s_n(x_{in}) + \epsilon_i \quad \text{where } \epsilon_i \sim N(0, \sigma^2) \quad (8)$$

1080

1081 where y_i is the i -th value of the response variable, β is a vector of fixed parameters, X_i is the fixed i
1082 rows of the model matrix, x_1, \dots, x_n are independent variables, s_1, \dots, s_n are smooth functions of the
1083 independent variables and ϵ_i are residuals with Gaussian normal distribution and constant variance.
1084 A cubic penalized spline was used as a smooth function. This is the result of the simultaneous
1085 fitting of basis functions (i.e. natural cubic spline) penalized to achieve the optimal degree of
1086 smoothness, avoiding data over-fitting. The amount of penalization was automatically computed by
1087 the maximum likelihood estimation (ML; Wood and Wood 2013). The covariate selection was
1088 performed by a stepwise backward process. Tree age, atmospheric $[\text{CO}_2]$, total atmospheric N
1089 deposition or its NH_x and NO_y components, mean (T_m) or maximum (T_{\max}) and minimum (T_{\min})
1090 annual temperatures, annual precipitation (P) and the SPEI value of the current and previous year
1091 (SPEI_{t-1}) were considered as possible covariates. Candidates for removal were identified through
1092 their lower approximate p-values, and the model resulting from the subtraction of such variable was
1093 compared with the previous one in terms of their Bayesian information criterion (BIC). This index
1094 was used instead of the Akaike's information criterion (AIC) because it is less conservative and
1095 more useful to assess the 'true' model in confirmatory analysis; indeed in model selection, the BIC
1096 provides a better opportunity to understand which pool of variables generated the real data (Aho,
1097 Derryberry, and Peterson 2014). The GAMs analysis was performed with the *mgcv* package (Wood

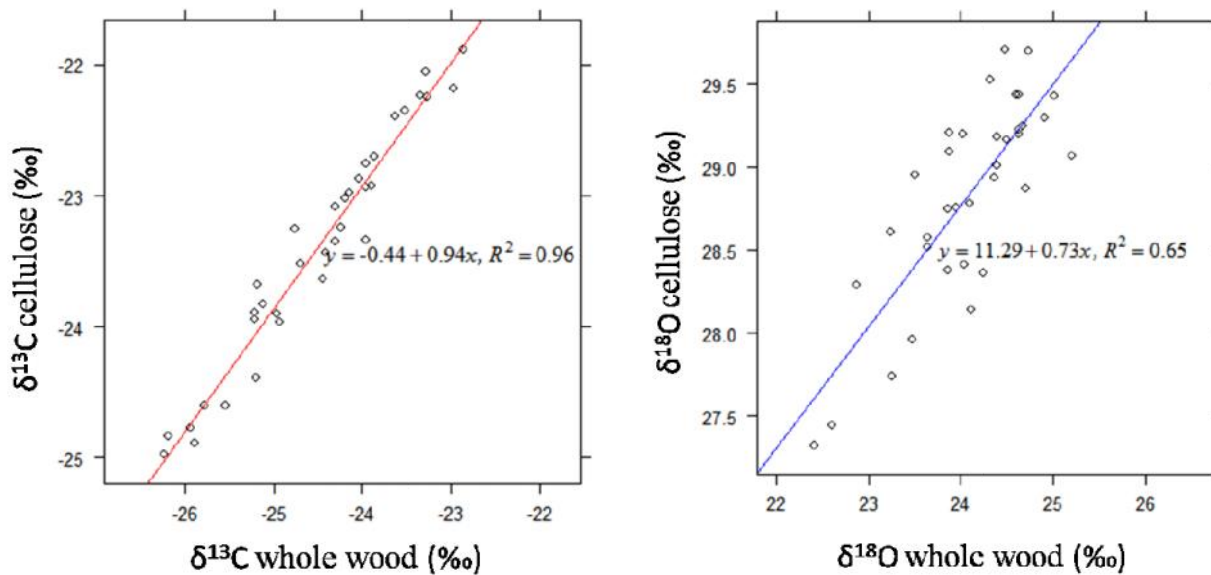
1098 2006) using the R statistical suite (R Core Team, 2017). No pre-whitening processes (i.e addition of
1099 an AR1 model for the correction of residuals autocorrelation) were applied to the iWUE and ^{18}O
1100 time series, with the aim to preserve the true long-term trend. The concurvity level (i.e. the
1101 generalization of non-linear models' co-linearity) was also checked to assess a potential correlation
1102 among independent variables. It could be an issue in models including a time-dependent smooth
1103 function with other time-varying covariates, making model estimation unstable (Wood, 2006).
1104 Nevertheless, GAMs are able to deal with some degree of concurvity (Wood, 2008). Finally, the
1105 model was validated to ensure that the assumption of normal distribution of observations and the
1106 absence of heteroscedasticity of residuals were respected.

1107

1108 **3. Results**

1109 **3.1 Effects of cellulose extraction**

1110 Our preliminary comparison of C and O isotope composition on paired whole-wood or -cellulose
1111 samples (Fig. 2) confirms the possibility of obtaining unbiased results from untreated material,
1112 when interested in temporal dynamics rather than absolute values. A very tight relationship between
1113 extracted and unextracted samples was observed in the case of ^{13}C (Fig. 2a; $R^2 = 0.96$), although
1114 with a slope significantly different from unity. The relationship could be therefore used to estimate
1115 the cellulose isotopic value from whole-wood measurements, using this value for the estimation of
1116 iWUE. A worse relationship was observed in the case of ^{18}O (Fig. 1b; $R^2 = 0.65$), although a
1117 consistent relationship was observed within each wood core, demonstrating the possibility to
1118 reconstruct the pattern of long-term tree dynamics from unextracted samples.



1119

1120

1121

1122

1123

1124

1125

Fig.2 a, b isotope composition on extracted against un-extracted. Relationship between ^{13}C

(red) and ^{18}O (blue) in cellulose (%), on y-axis, and in whole wood (%), on x-axis, of the test's

sub-set ($n=35$). The equations were used to correct the offsets in whole wood values on the

main data-sets.

3.2 Carbon isotope and iWUE dynamics

1126

1127

1128

1129

1130

1131

Trees were grouped into four age classes, based on their age at the time of sampling (approximately 65, 85, 100 and 120 years). The attributes (iWUE, $\delta^{13}\text{C}$, $\delta^{18}\text{O}$) and relative statistics of each Douglas-fir cohort are summarized in Table 1. Across the entire dataset, estimated iWUE ranged between 70.09 and 138.44, as a result of inter-individual differences as well as time dynamics; the associated range in $\delta^{13}\text{C}$ was between -21.87 and -26.58, while $\delta^{18}\text{O}$ varied between 22.10 and 26.44 in the oldest age class.

1132

1133

1134

1135

The iWUE raw time series (Fig. 3) show rather coherent trends between all the different age-classes, confirming the reliability of the measurements. When considering the time pattern of the variable (values aligned by calendar year), iWUE shows an increasing trend during the period from 1960 to 1980 for all age-classes (coloured lines, representing a spline curve fitted on all the data of

1136 each cohort), followed by a less pronounced growth in recent decades (Fig.3). Higher iWUE values
 1137 were achieved by the older class, even if only in a slightly significant way, but no clear separation
 1138 among age-classes is apparent, making it difficult to attribute the pattern to either age or variable
 1139 environmental conditions over time.

1140 Taking a diachronic view (values aligned by cambial age), the younger classes exhibit remarkably
 1141 higher values at any given age, in comparison with the older ones (Fig.4), underling a possible effect
 1142 due to changing environmental condition over time.

1143

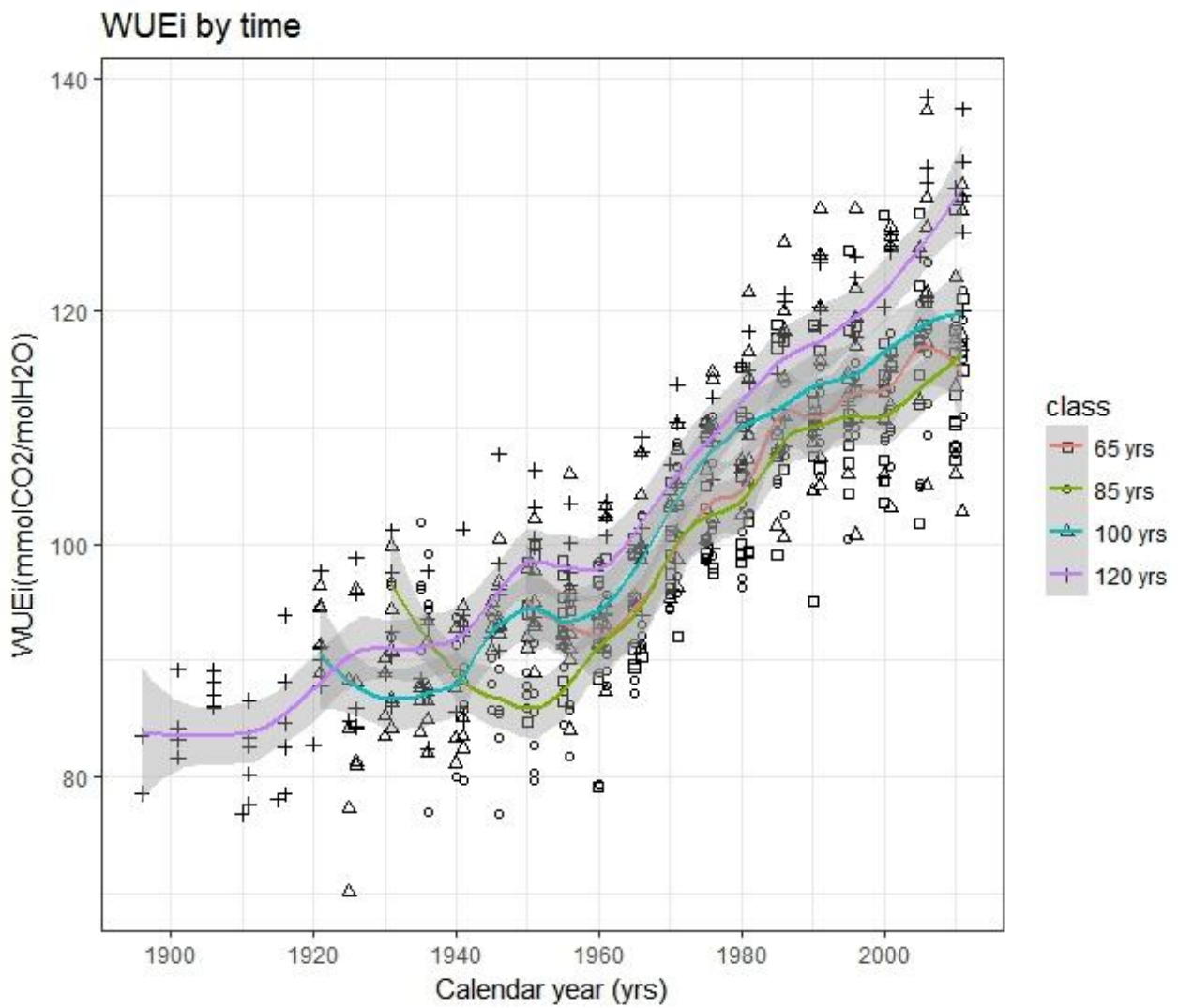
1144

1145 **Tab.1** | Descriptive statistics for water use efficiency (iWUE), oxygen composition (^{18}O) and carbon
 1146 composition (^{13}C) chronologies of the four age-classes in which trees were grouped.

<i>Var</i>	Age-class	<i>N</i>	<i>Mean</i>	<i>SD</i>	<i>Median</i>	<i>Min</i>	<i>Max</i>
iWUE	65	63	107.44	11.27	107.89	89.34	128.77
	85	172	100.95	11.23	101.19	76.82	124.22
	100	210	102.10	12.76	100.52	70.09	137.31
	120	166	101.37	14.52	99.69	76.76	138.44
^{18}O	65	63	24.24	0.70	24.29	22.42	25.66
	85	172	23.92	0.80	23.98	22.10	25.60
	100	210	24.33	0.56	24.27	22.92	25.78
	120	166	24.99	0.80	25.15	22.98	26.44
^{13}C	65	63	-23.89	0.66	-23.95	-25.43	-22.72
	85	172	-24.24	0.72	-24.21	-25.97	-22.41
	100	210	-23.93	0.85	-23.89	-26.58	-22.09
	120	166	-23.74	0.78	-23.00	-24.97	-21.87

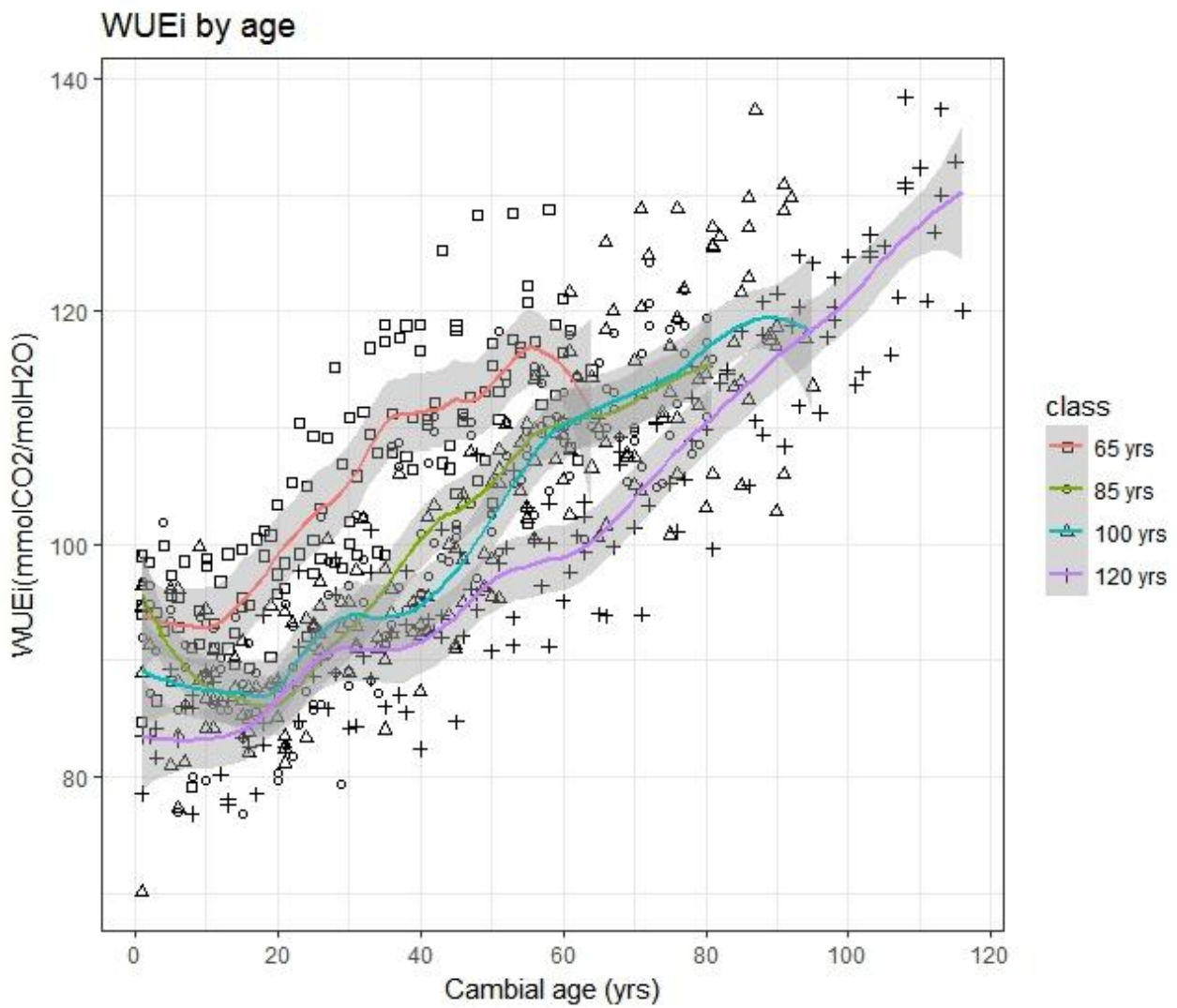
1147 *n* is the number of 5-yr ring blocks for each age-class, *Mean* is the mean value, *SD* is standard deviation, *Median* is the
 1148 median value, *Min* is minimum value, *Max* is the maximum value, *Var* is the variable considered.

1149



1150

1151 **Fig.3 Time-related dynamics of iWUE in different age-classes.** Lines represent splines fitted to
 1152 different age classes. The shaded areas indicate the 95% prediction interval of the spline function



1153

1154 **Fig.4 Diachronic analysis of age effects on iWUE in different age-classes.** Lines represent
 1155 splines fitted to differnt age classes. The shaded areas indicate the 95% prediction interval of the
 1156 spline function..

1157

1158 Subsequently, in order to quantify the strength of this possible environmntal forcing, a GAM model
 1159 was applied to the data. In a first step, to assess the possible change of water use efficiency over
 1160 time, decoupled from the influence of age, iWUE was modeled as:

1161

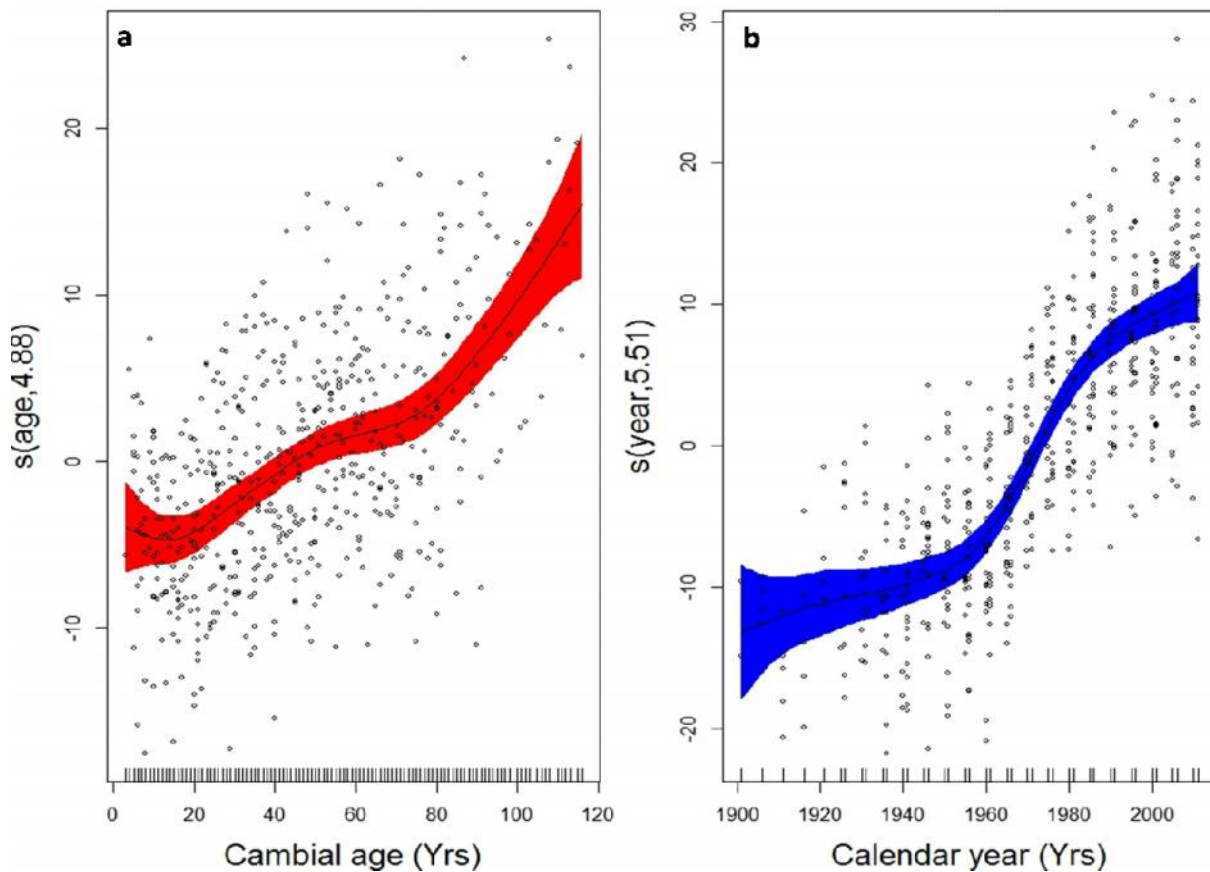
$$1162 \quad iWUE = s(\text{Age}) + s(\text{TIME}) + \epsilon_i \quad (9)$$

1163

1164 where $s(\text{AGE})$ is the cambial age effect and $s(\text{TIME})$ represents all of the environmental and
 1165 geochemical effects cumulated into a single global variable, varying along time (as in chapter I).

1166 The variation of iWUE as a function of time alone, i.e. removing the co-occurring effects of age,
 1167 shows an increase of the 17.3 % in the period included between 1960-1980, with a near stabilization
 1168 afterwards (Fig. 5b). On the other hand the age-smoother displays a brief initial decreasing trend,
 1169 followed by a quasi-constant increase with increasing age (Fig. 5a).

1170



1171

1172 **Fig.5 GAM analysis of the independent effects on iWUE of age and time .**

1173 **a.** Global trend of iWUE in time decupled by age-related effects. On x -axis time (Yrs), and on y -axis the
 1174 function of time $s(\text{TIME})$, dimensionless and centered around 0. The shaded areas indicate the 95%
 1175 confidence interval.

1176 **b.** Trend of iWUE along age decupled by time-related effects. On x -axis age (Yrs), and on y -axis the
 1177 function of age $f(\text{AGE})$, dimensionless and centered around 0. The shaded areas indicate the 95%
 1178 confidence interval

1179

1180

1181 As a final step, in order to attribute the global change effect to changes in individual environmental
 1182 variables, a number of candidate annual climatic and geochemical variables were added to the

1183 model instead of the time variable; after a backward stepwise selection, the selected model could
 1184 be eventually specified as follows (Fig. 6):

1185

$$1186 \quad iWUE = s(CO_2) + s(Age) + s(SPEI \text{ JJA } t-1) + s(NO_{y \text{ dep}}) + i \quad (10)$$

1187

1188 where CO_2 is the annual level of atmospheric $[CO_2]$, Age is the age/size effect associated with
 1189 variations in cambial age, "SPEI JJA t-1" represents the August SPEI (Standardized Precipitation-
 1190 Evapotranspiration Index; Vicente-Serrano et al. 2010) values in the previous summer, cumulated
 1191 over the preceding 3-months period and $NO_{y \text{ dep}}$ is the annual sum of dry and wet deposition of
 1192 oxide N (NO_y) species. All variables exhibit a significant p-value at 0.001 level, with the exception
 1193 of the SPEI factor, which is significant at the 0.005 level (Tab. 2). The global adjusted R^2 for the
 1194 whole model is 0.795. The most relevant biological factor that explains the long-term trend in the
 1195 Douglas-fir iWUE is the Age covariate (F-test= 12.970), followed by the CO_2 atmospheric
 1196 concentration, the nitrogen deposition and finally by the drought index of the previous summer.
 1197 Model goodness-of-fit and respect of the model assumptions were also evaluated (Fig.7).

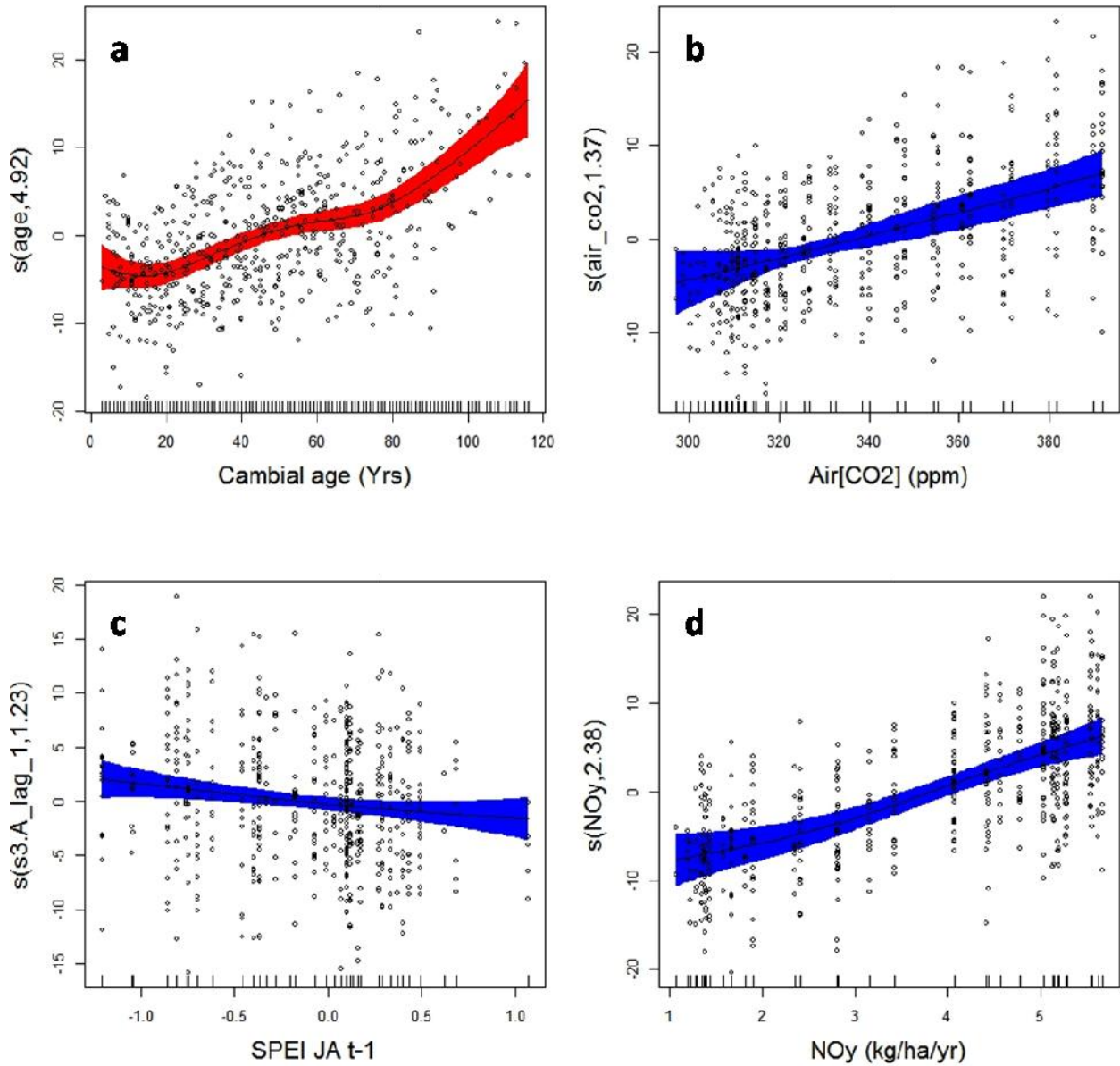
1198

Tab. 2 Generalized additive model results. Environmental and biological covariates' relationships with iWUE series (as dependent variable) in *Pseudotsuga menziesii*.

Factor	<i>e.d.f.</i>	<i>F</i>	<i>P</i>	$R^2(\text{adj})$
CO ₂	1.672	4.628	7.28E-12	
Age	5.395	12.97	< 2e-16	
SPEI JJA t-1	1.278	0.998	0.00127	
NO _{y dep}	2.34	3.411	8.71E-13	
				0.795

1199 *e.d.f.* are effective degree of freedom, *F* is the F-test for variance explained, *P* is the p-values and $R^2(\text{adj})$ is the adjusted
 1200 regression coefficient of the model.

1201



1202

1203

1204

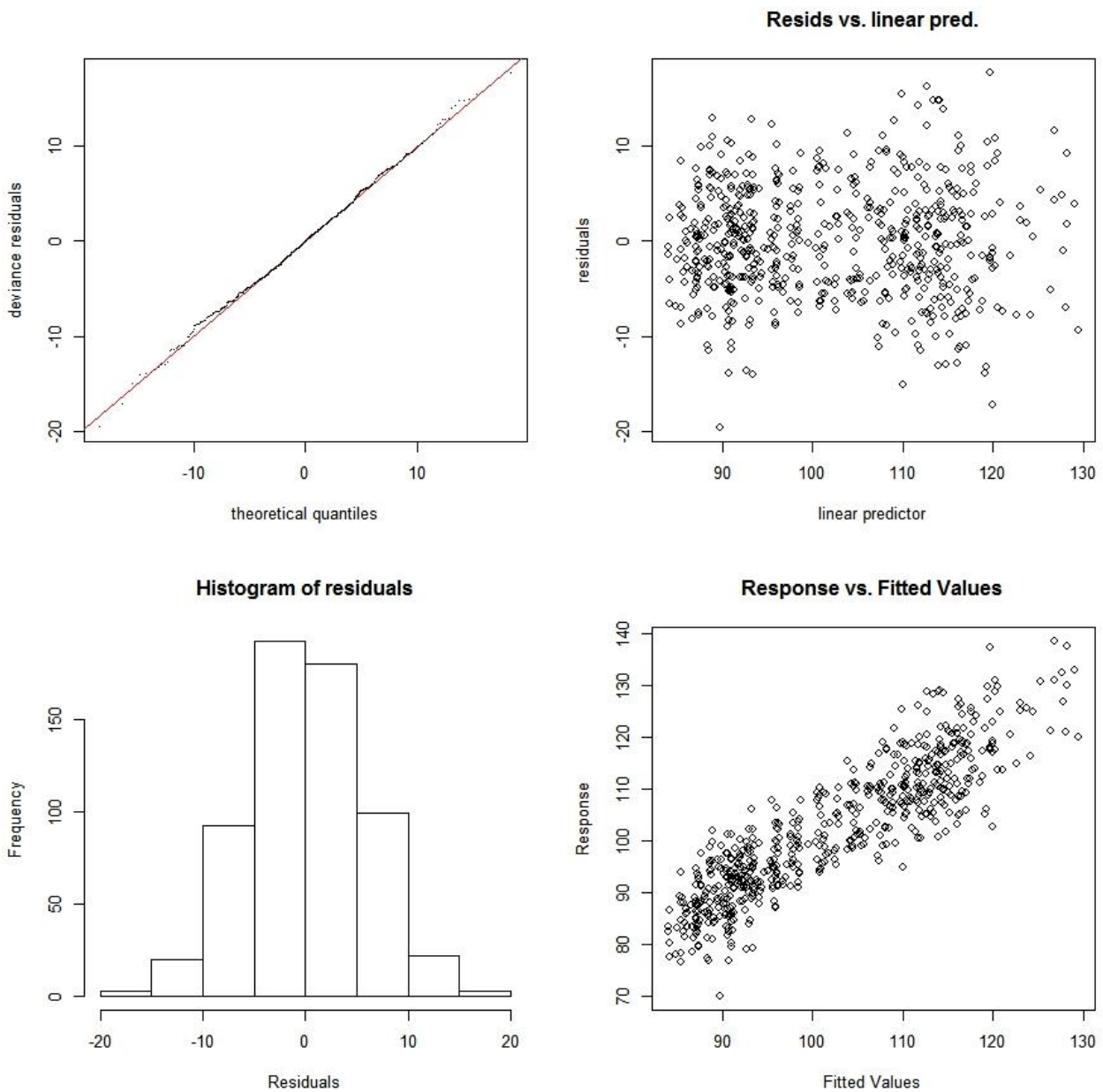
1205

1206

1207

1208

Fig. 6. GAM's results for iWUE. Generalized additive models (GAMs) results show the relationship between iWUE and environmental and biologic factors. On y-axis values indicate the x covariate effect on the tree rings- iWUE predicted by the model (continuous line) dimensionless and centered around 0, plus the estimated degree of freedom (edf). On x-axis each x variable values. Points represent partial residuals from the fitted function and the shaded areas indicate the 95% confidence interval.



1209

1210 **Fig.7 iWUE's GAMs model assessment.** Residual distribution of the whole model selected by a
 1211 stepwise procedure and against linear predictor. Response against fitted values for the whole model

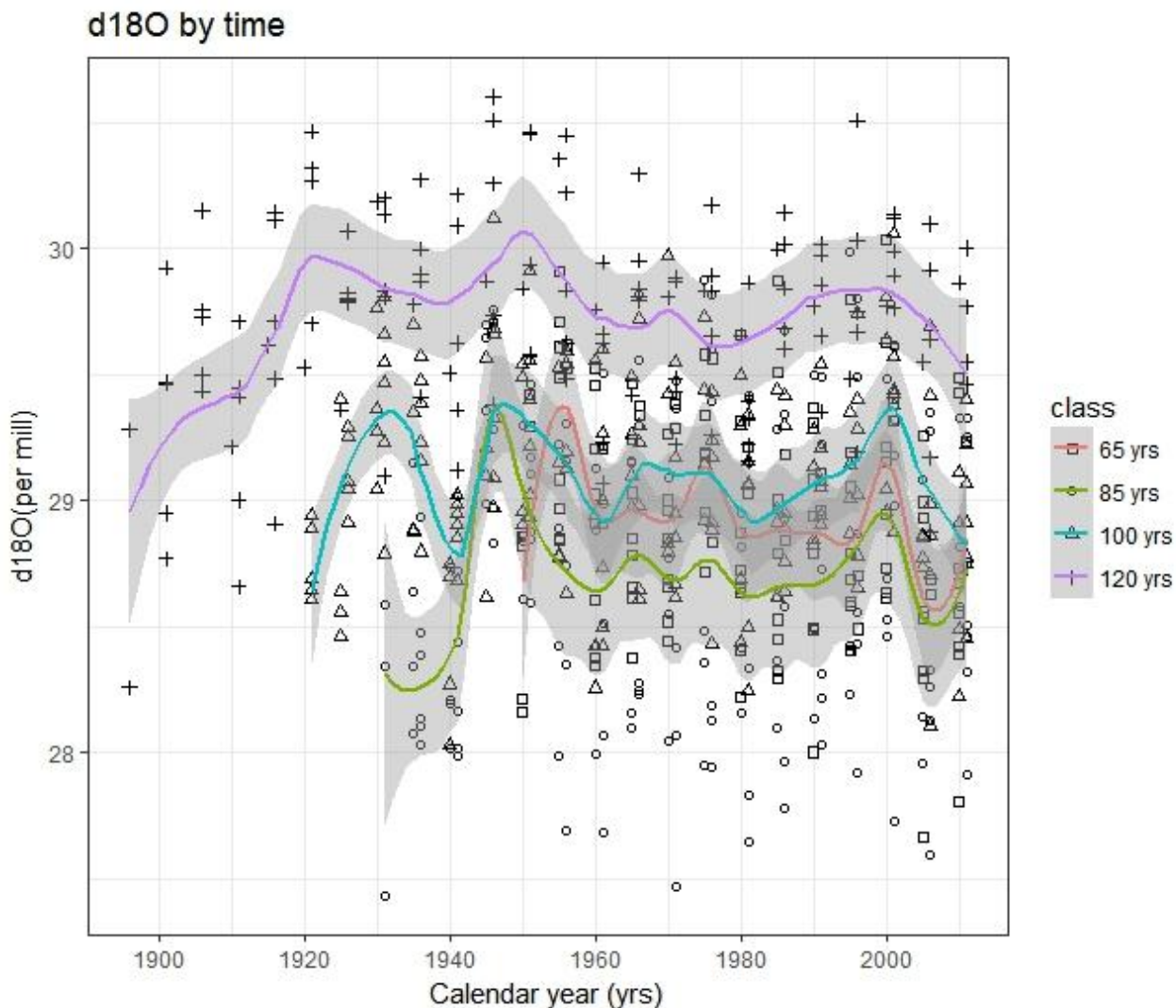
1212

1213 3.3 Oxygen isotope dynamics

1214 In contrast with C isotopes, ^{18}O values for the different age-classes show a pronounced shift
 1215 among the old class and the others but no clear trends over time on raw series (Fig.8). However, all
 1216 the classes seem to be roughly aligned with two major peaks, corresponding to the periods when the
 1217 two biggest drought events of the last century have occurred (year 1945 and in particular 2003).

1218 Considering the apparent pattern against age (Fig. 9), no clear trend is apparent, apart from a
1219 general increase at young age.

1220



1221

1222 **Fig.8 Time-related dynamics of ^{18}O in different age-classes.** ^{18}O time series, grouped by age-
1223 classes and fitted with a cubic spline. The shaded areas indicate the 95% prediction interval of
1224 the function



1225

1226 **Fig.9 Diachronic analysis of age effects on ^{18}O in different age-classes.** ^{18}O time series, grouped
 1227 by age-classes and fitted with a cubic spline. ^{18}O (‰), on y-axis, and cambial age (Yrs), on x-axis.
 1228 The shaded areas indicate the 95% prediction interval of the spline function

1229

1230 This is confirmed by the preliminary GAMs analysis, which highlighted a significant effect of time
 1231 but not of age *per se*. When applying GAMs to explain directly the time-dependent behavior of O
 1232 isotopic composition in terms of individual global change drivers, the model specification after the
 1233 backward variable selection procedure was:

1234
$$^{18}\text{O} = s(\text{CO}_2) + s(\text{T}_{\text{max}}) + s(\text{P}_{\text{sum}}) + \text{factor}(\text{elevation}) + \epsilon_i \quad (11)$$

1235 where CO_2 is the annual level of atmospheric $[\text{CO}_2]$, T_{max} is the mean of annual maximum
 1236 temperature over the 5-yr period, P_{sum} is the sum of annual precipitation, and elevation is a

1237 parametric term which considers each plot's elevation above sea level as a factor (Fig. 10). Only
 1238 CO₂, among all variables, is not significant at the 0.001 p-level, but only at the 0.05 level. It's worth
 1239 noting that the effect of elevation (Fig. 10d) appears to account to a large extent for the higher
 1240 values observed in the oldest age class in Fig. 8 and 9. The adjusted R² for the whole model is 0.458
 1241 and the most relevant variable which explains the ¹⁸O patterns appears to be the annual sum of
 1242 precipitation (F-test = 2.036). A test of model assumptions demonstrated a general lack of bias
 1243 (Fig.11).

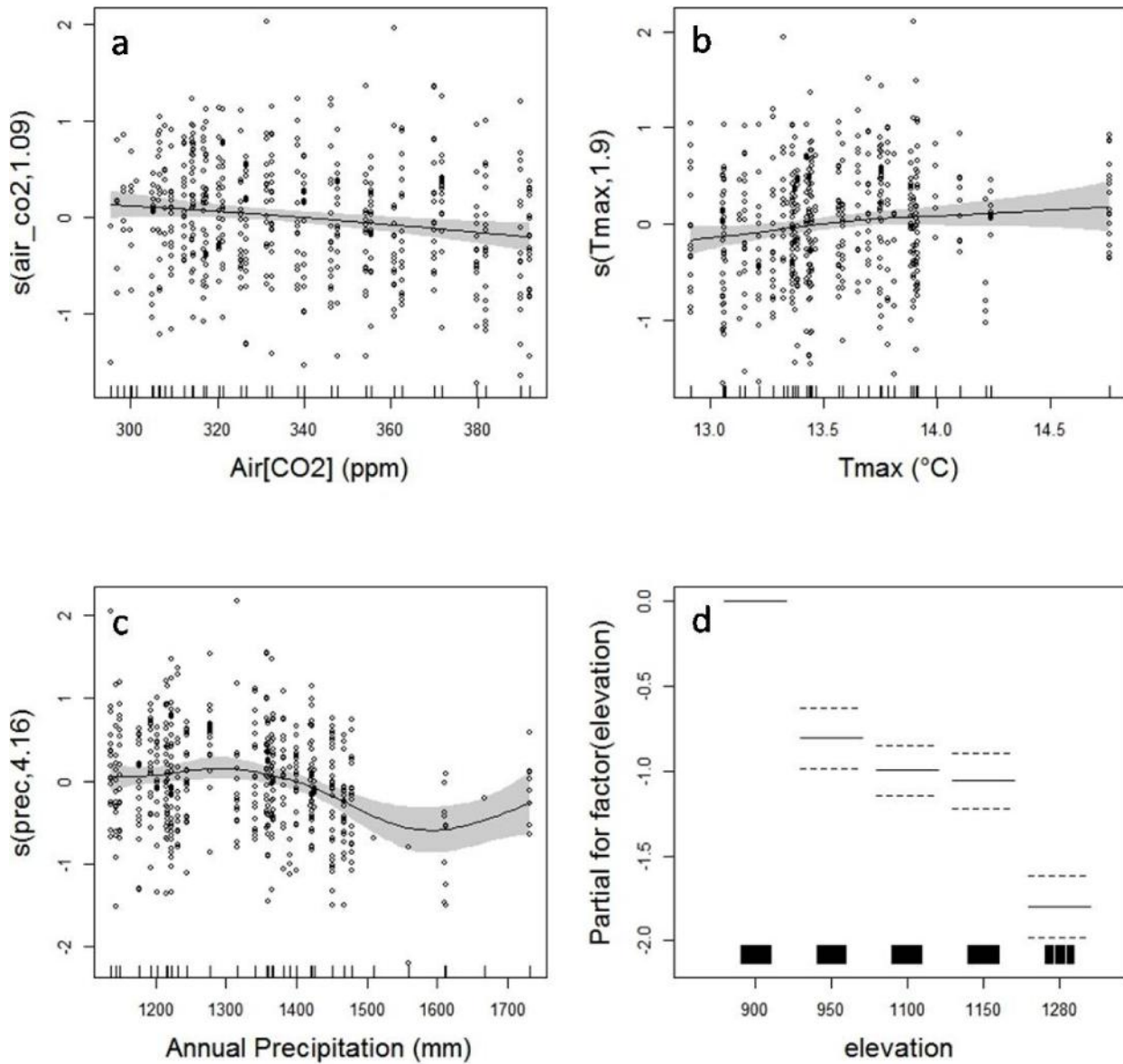
1244

Tab. 3 Generalized additive model results. Environmental and biological covariates' relationships with δ¹⁸O series (as dependent variable) in *Pseudotsuga menziesii*.

Factor	<i>e.d.f.</i>	<i>F</i>	<i>P</i>	<i>R</i> ² (<i>adj</i>)
CO ₂	1.534	0.997	0.001334	
T _{max}	1.972	1.243	0.000664	
P _{sum}	3.613	2.036	0.000137	
				0.458

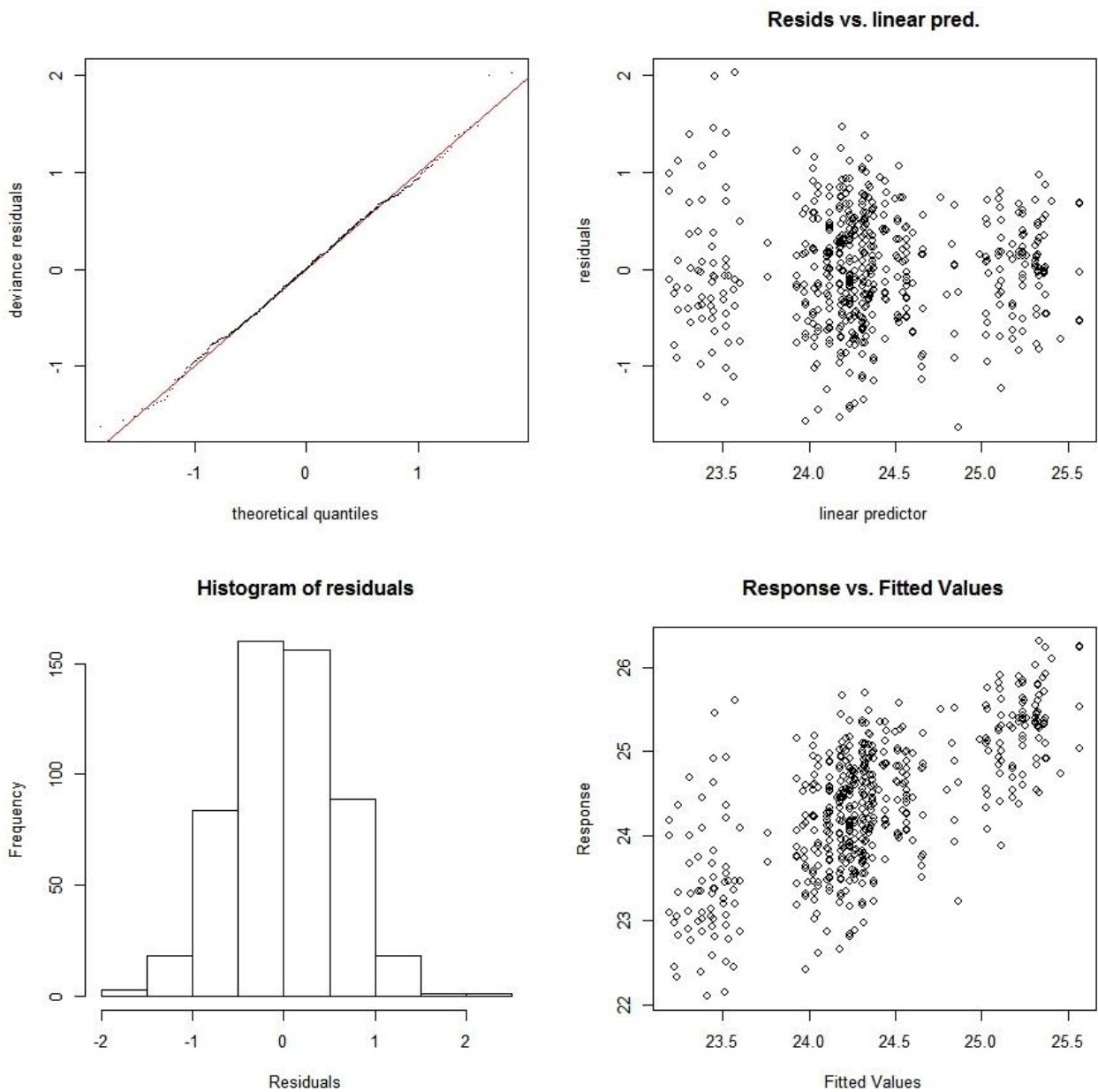
1245 *e.d.f.* are effective degree of freedom, *F* is the F-test for variance explained, *P* is the p-values and *R*²(*adj*) is the adjusted
 1246 regression coefficient of the model.

1247



1248

1249 **Fig. 10** GAM's results for ^{18}O . Generalized additive models (GAMs) results show the relationship
 1250 between ^{18}O and environmental and biologic factors. On y-axis values indicate the x covariate effect on the
 1251 tree rings- ^{18}O predicted by the model (continuous line) dimensionless and centered around 0, plus the
 1252 estimated degree of freedom (edf). On x-axis each x variable values. Points represent partial residuals from
 1253 the fitted function and the shaded areas indicate the 95% confidence interval.



1254

1255 **Fig.11 ^{18}O 's GAMs validation** Residual distribution of the whole model and against linear predictor.
 1256 Response against fitted values for the whole model.

1257

1258 **3.4 Dual isotope approach**

1259

1260 Finally, the Scheidegger conceptual model was applied in order to disentangle whether stomatal
 1261 conductance or photosynthetic response has determined the trend in iWUE over the last century,
 1262 looking at the relationship between $\delta^{18}\text{O}$ and $\delta^{13}\text{C}$ averaged over all the trees (Fig.12). The pattern
 1263 between time periods (10 year means) reveals an initial part of the century dominated by a stomatal

1264 response. For example, the 1924-33 and 1944-53 decades, which are characterized by drought crisis
1265 events and show a parallel increase in both $\delta^{13}\text{C}$ and $\delta^{18}\text{O}$, appear to correspond to the c scenario of
1266 the Schedigger model (Fig. 1), that is to a marked decrease in g_s without a similar change in A_{max} .
1267 In the second part of the century, from the 1954-63 to the 1974-83 decades, the increase in $\delta^{18}\text{O}$
1268 without a parallel change in $\delta^{13}\text{C}$ would correspond to scenario b, suggesting a strong increase in
1269 photosynthetic activity without a parallel change in stomatal conductance. This response appears to
1270 come to an end approximately in the first part of the 1980s, and afterwards it changes its direction,
1271 suggesting a pronounced reduction in assimilation rate for the 1994-2003 decade (e scenario)
1272 possibly associated to the 2003 drought crisis. The last decade unexpectedly shows a parallel
1273 decline in both isotopic compositions, corresponding to scenario g of the Scheidegger model, that is
1274 to an increase in g_s without a parallel change in A_{max} ; precipitation in the 2004-08 period was
1275 above average, although this could have been counter-balanced by the droughts experienced in the
1276 following years.

1277

1278 **4. Discussion**

1279 **4.1 Age-related effects**

1280 The first aim of this study was to explore the possible influence of a biological (i.e. age/size) effect
1281 on isotopic long-term variations. Such an effect could introduce a confounding element when trying
1282 to assess the impact of long-term changes in environmental factors affecting tree physiology, or
1283 when using stable isotopes for past climate reconstruction (Esper et al. 2010; Brien et al., 2017).
1284 Data analysis showed a strong positive age-related effect on iWUE, while no significant impact was
1285 detected in the ^{18}O signal. Previous dendroecological studies suggested that an age-related trend is
1286 only observed in the early ontogenetic phase of trees' life, defined as juvenile effect (Loader et al.
1287 2007) (Leavitt 2010). This is known to display an increase of about 1.5–2‰ in $^{13}\text{C}_p$, normally
1288 occurring in the first 40-50 years, implying that no correction for age is needed outside beyond this
1289 first interval. The pattern is attributed to enriched $^{13}\text{CO}_2$ produced by the respiration of surrounding

1290 dominant trees, and re-absorbed by the young, shaded trees. However, this hypothesis fails to
1291 explain our results due to the stand structure (even-aged), and the social position of the sampled
1292 trees (always dominant), which were never relegated to the understory layer. Moreover, the age-
1293 related effect that is apparent both from a simple synchronic comparison between age classes (Fig.
1294 3) and from the GAMs analysis (Fig. 5) far exceeds the juvenile development stage. More likely,
1295 the physiological mechanism implied in this iWUE increase with age-size could be explained if the
1296 hydraulic limitation hypothesis (HLH) is taken into consideration (Ryan et al., 1997). The
1297 hypothesis suggests a progressive reduction of stomatal conductance as a result of the increased
1298 hydraulic resistance of longer stems and branches, as well as the increased gravitational potential
1299 opposing the ascent of water in taller trees, and the homeostatic maintenance of a minimum water
1300 potential in leaves (Ryan et al., 2006). Such an increase in C isotope discrimination with tree
1301 height, beyond the juvenile phase, has been demonstrated for a number of species, including
1302 Douglas fir (Mc Dowell *et al.* 2002, Martinez-Vilalta *et al.* 2007). However, assuming that the
1303 iWUE trend related to age is influenced by a decline in stomatal conductance, it is surprising not to
1304 detect the same effect also in the oxygen isotopic signal, which is well known to be affected by g_s .
1305 A possible explanation could be the shift in the ^{18}O of soil water as roots become deeper with age.
1306 This process of gradually discrimination against H_2^{18}O , would act in the opposite direction to the
1307 pattern associated with the decrease in g_s and could counteract the g_s -dominated age effect,
1308 nullifying its trend. The alternative possibility of an age-related increase in iWUE as a result of an
1309 increase in A_{max} is not supported by any physiological evidence.

1310

1311 **4.2.Environmental and biogeochemical effects**

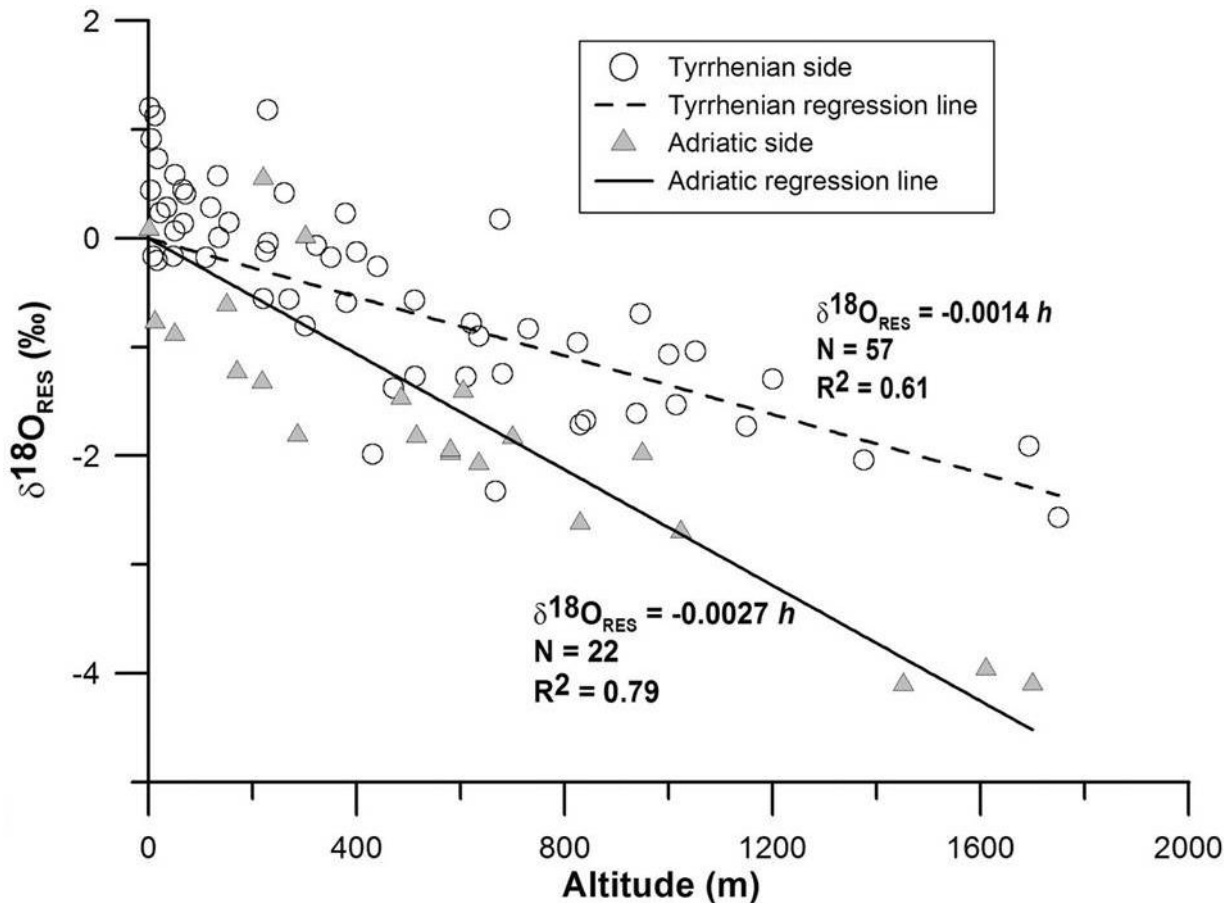
1312 The second objective of the present study was to distinguish, between the main explanatory
1313 environmental and biogeochemical variables which have changed over the last century, which ones
1314 have determined the overall increase in iWUE observed over the last century, after correcting for
1315 age-related effects. As expected, this pattern was found to be directly and linearly related to air

1316 [CO₂] (Saurer et al., 2004;Peñuelas et al., 2011;Keenan et al. 2013), due to the increase in the
1317 photosynthetic substrate available to trees. Interestingly, the rate of N deposition was also found to
1318 be directly related with iWUE, as already shown in other conifers (Guerrieri et al. 2011; Leonardi et
1319 al. 2012), even if in the present study the oxide form alone (NO_y,) was selected by the stepwise
1320 procedure applied. The long-term effect of N deposition on iWUE is understood to be dominated by
1321 its stimulation of A_{max} (Ripullone et al. 2004), which should increase as the N leaf concentration
1322 level (and thus Rubisco and photosynthetic pigments) rise. Such an effect could be caused by both
1323 direct canopy uptake (Nair et al. 2015) and increase of N in the soil, which can promote net
1324 mineralization and consequently, advance the N available to the trees (Aber et al. 2003). The
1325 amount of NO_y deposited at this site, after a strong increase from pre-industrial times until the
1326 1960-1980 period, has shown a reduction in the last 30 years. Remarkably, this trend matches
1327 closely also the observed recent stabilization in iWUE. Hence, taking into consideration also the
1328 results of the dual isotope analysis, which displays a reduction in the A_{max} after roughly the 1980s,
1329 it would appear that a nutritional constraint has determined at least in part the recent variation in
1330 iWUE in Douglas-fir. This hypothesis is consistent with previous findings from controlled FACE
1331 (Free-Air Carbon Enrichment) experiments (Norby et al. 2010) which demonstrated how N
1332 availability could be limiting for tree growth, suppressing the tree response to elevated CO₂.

1333 Finally, the water availability in the previous summer (as captured by the SPEI index) was the other
1334 significant covariate related with iWUE. Its inverse relationship with the dependent variable could
1335 be explained as a consequence of the direct linkage between g_s and water availability. As a result,
1336 this forcing of the previous year could influences the canopy status and the leaf area of the current
1337 season (Zweifel et al. 2006).

1338 Coming to consider the factors affecting ¹⁸O, the most relevant seems to be the precipitation effect
1339 (Fig.10c), possibly because of its relationship with air relative humidity and e_a/e_i; the inverse
1340 relationship observed between this covariate and ¹⁸O discrimination potentially reflects the increase
1341 of g_s in periods with greater atmospheric moisture (see Eq. 6).

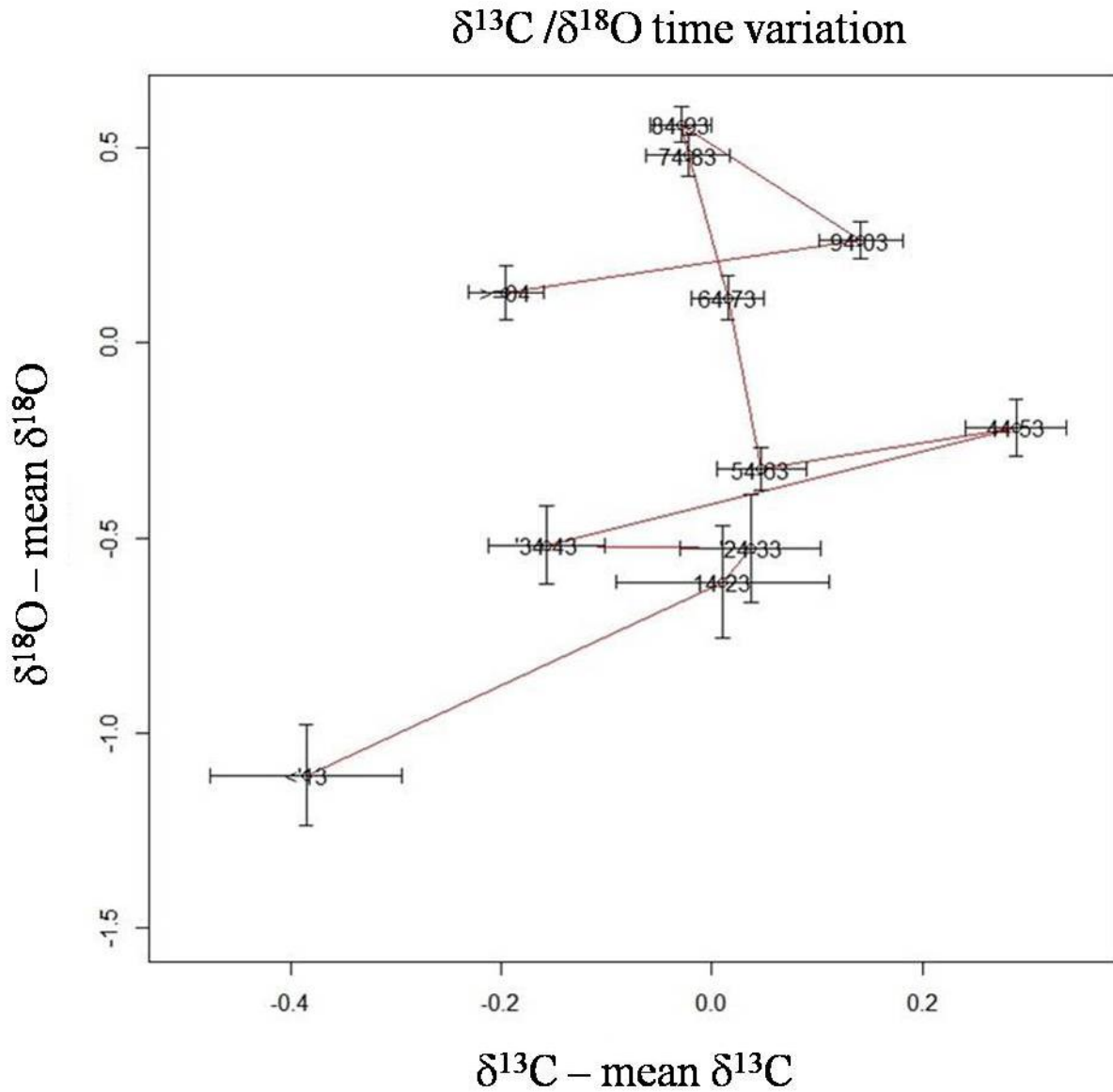
1342 Interestingly, a pronounced altitudinal gradient was also detected in the $\delta^{18}\text{O}$ signal (Fig.10d). This
 1343 could be attributed either to different levels of leaf enrichment, linked to differences in temperature
 1344 and VPD between plots (Treydte et al. 2014) or to an effect of altitude on source $^{18}\text{O}_s$. This would
 1345 be consistent with the recent observation of an altitudinal pattern in source $^{18}\text{O}_s$ on both sides of
 1346 the Apennine range (Giustini *et al.* 2016)(Fig.13).
 1347



1348
 1349 **Fig.13 Elevation effect on ^{18}O s.** Relationship between altitude (m a.s.l.), on the x-axis, and ^{18}O
 1350 precipitation residuals, on the y-axis for both the Tyrrhenian and the Adriatic side of Italy. From
 1351 Giustini *et al.* 2016

1352
 1353 It seems likely that ^{18}O measurements could be substantially affected by the source signal
 1354 influence, partially hiding the leaf enrichment signal; this source signal influence would be
 1355 accounted only to some extent by elevation; other significant variables highlighted by the GAMs
 1356 analysis, such as maximum annual temperature, could also vary locally and be responsible for
 1357 differences in $^{18}\text{O}_s$. Direct measurements of source $^{18}\text{O}_s$ could be therefore needed in order to

1358 refine the analysis. A possible solution could be to measure stem water ^{18}O as a reference baseline
 1359 for site-specific differences and to ensure model applicability and interpretation (Roden and
 1360 Siegwolf 2012).



1361
 1362 **Fig.12 Dual isotope variation over time.** Relationship between normalized ^{13}C , on the x -axis, and
 1363 ^{18}O , on the y -axis. Points are representative of 10-year means of all the trees for the corresponding
 1364 time period of the last century, as indicated by figures next to the points.

1365

1366

1367 5.Conclusions

1368 Tree ageing appears to result in Douglas fir in an almost linear increase in WUE_i, presumably due
1369 to the progressive decline in stomatal conductance with increasing height.

1370 Once this effect of age is discounted, global change was found to have induced an initial increase in
1371 iWUE during the 1950-1980 period, because of the stimulation of photosynthesis (as demonstrated
1372 by the dual-isotope analysis) by the combination of increasing atmospheric [CO₂] and N deposition;
1373 this was followed by an apparent saturation over the last decades. This is possibly because of the
1374 mismatch between [CO₂] and nutrient availability and the climate-change related increase in
1375 transpiration demand, as confirmed by the dual isotope approach application.

1376 Since the analysis of the main factors which have determined the overall increase in iWUE over the
1377 last century seems to highlight a multi-factorial control of the physiological response, the use of an
1378 additive non-linear model such as GAMs appears to be most appropriate, as it allows to describe
1379 such variability, at least partially, and to highlight the long-term influence of each covariate. On the
1380 other hand, it should be kept in mind that complex interactions between drivers could lead to
1381 misinterpretation in variable selection, due to the additive nature of the model applied.



1382

1383

1384 **6.Bibliography**

1385 ABER, JOHN D., CHRISTINE L. GOODALE, SCOTT V. OLLINGER, MARIE-LOUISE
1386 SMITH, ALISON H. MAGILL, MARY E. MARTIN, RICHARD A. HALLETT, and JOHN
1387 L. STODDARD. 2003. "Is Nitrogen Deposition Altering the Nitrogen Status of Northeastern
1388 Forests?" *BioScience* 53 (4): 375. doi:10.1641/0006-3568(2003)053[0375:INDATN]2.0.CO;2.

1389 Aho, Ken, DeWayne Derryberry, and Teri Peterson. 2014. "Model Selection for Ecologists: The
1390 Worldview of AIC and BIC." *Ecology* 95 (March): 631–36. doi:10.1890/13-1452.1.

- 1391 Ainsworth, Elizabeth A., and Stephen P. Long. 2005. "What Have We Learned from 15 Years of
1392 Free-Air CO₂ Enrichment (FACE)? A Meta-Analytic Review of the Responses of
1393 Photosynthesis, Canopy Properties and Plant Production to Rising CO₂." *New Phytologist* 165
1394 (2): 351–71. doi:10.1111/j.1469-8137.2004.01224.x.
- 1395 Babst, Flurin, M. Ross Alexander, Paul Szejner, Olivier Bouriaud, Stefan Klesse, John Roden,
1396 Philippe Ciais, et al. 2014. "A Tree-Ring Perspective on the Terrestrial Carbon Cycle."
1397 *Oecologia* 176 (2): 307–22. doi:10.1007/s00442-014-3031-6.
- 1398 Beedlow, Peter A., E. Henry Lee, David T. Tingey, Ronald S. Waschmann, and Connie A. Burdick.
1399 2013. "The Importance of Seasonal Temperature and Moisture Patterns on Growth of Douglas-
1400 Fir in Western Oregon, USA." *Agricultural and Forest Meteorology* 169. Elsevier B.V.: 174–
1401 85. doi:10.1016/j.agrformet.2012.10.010.
- 1402 Biondi, Franco. 1999. "Comparing Tree-Ring Chronologies and Repeated timber Inventories as
1403 Forest Monitoring Tools." *Ecological Applications* 9 (1): 216–27. doi:10.1890/1051-
1404 0761(1999)009[0216:CTRCAR]2.0.CO;2.
- 1405 Boettger, Tatjana, Marika Haupt, Kay Knöller, Stephan M. Weise, John S. Waterhouse, Katja T.
1406 Rinne, Neil J. Loader, et al. 2007. "Wood Cellulose Preparation Methods and Mass
1407 Spectrometric Analyses of $\delta^{13}\text{C}$, $\delta^{18}\text{O}$, and Nonexchangeable $\delta^2\text{H}$ Values in Cellulose,
1408 Sugar, and Starch: An Interlaboratory Comparison." *Analytical Chemistry* 79 (12): 4603–12.
1409 doi:10.1021/ac0700023.
- 1410 Boisvenue, Céline, and Steven W. Running. 2006. "Impacts of Climate Change on Natural Forest
1411 Productivity - Evidence since the Middle of the 20th Century." *Global Change Biology* 12 (5):
1412 862–82. doi:10.1111/j.1365-2486.2006.01134.x.
- 1413 Brienen, R J W, E Gloor, S Clerici, R Newton, L Arppe, A Boom, S Bottrell, et al. n.d. "Isotopes."
1414 *Nature Communications*. Springer US, 1–10. doi:10.1038/s41467-017-00225-z.
- 1415 Brunel, J.P., G.R. Walker, C.D. Walker, J.C. Dighton, and A. Kennett-Smith. 1991. "Using Stable
1416 Isotopes of Water to Trace Plant Water Uptake." *International Symposium on the Use of Stable*
1417 *Isotopes in Plant Nutrition, Soil Fertility and Environmental Studies*, 543–551.
1418 doi:10.2144/000114133.
- 1419 Bunn, Andrew G. 2008. "A Dendrochronology Program Library in R (dplR)." *Dendrochronologia*
1420 26 (2): 115–24. doi:10.1016/j.dendro.2008.01.002.
- 1421 Camarero, J. Julio, Antonio Gazol, Jacques C. Tardif, and France Conciatori. 2015. "Attributing
1422 Forest Responses to Global-Change Drivers: Limited Evidence of a CO₂-Fertilization Effect in
1423 Iberian Pine Growth." *Journal of Biogeography* 42 (11): 2220–33. doi:10.1111/jbi.12590.
- 1424 Carrer, Marco, and C Urbinati. 2006. "Long-Term Change in the Sensitivity of Tree ring Growth
1425 to Climate Forcing in *Larix Decidua*." *New Phytologist* 170 (iv): 861–72.
- 1426 Cook, Edward R., Keith R. Briffa, David M Meko, Donald A Graybill, and Gary Funkhouser. 1995.
1427 "The 'segment Length Curse' in Long Tree-Ring Chronology Development for Palaeoclimatic
1428 Studies." *The Holocene* 5 (2): 229–37. doi:10.1177/095968369500500211.
- 1429 Dawson, T E. 1998. "Fog in the Californian Redwood Forest: Ecosystem Inputs and Use by
1430 Plants." *Oecologia* 117: 476–85.
- 1431 Dawson, Todd E., Stefania Mambelli, Agneta H. Plamboeck, Pamela H. Templer, and Kevin P. Tu.

- 1432 2002. "Stable Isotopes in Plant Ecology." *Annual Review of Ecology and Systematics* 33 (1):
1433 507–59. doi:10.1146/annurev.ecolsys.33.020602.095451.
- 1434 Dawson, Todd E., and John S Pate. 1996. "Seasonal Water Uptake and Movement in Root Systems
1435 of Australian Phraeatophytic Plants of Dimorphic Root Morphology: A Stable Isotope
1436 Investigation." *Oecologia* 107 (1): 13–20. doi:10.1007/BF00582230.
- 1437 Di Biase, Giampaolo, Gloria Falsone, Anna Graziani, Gilmo Vianello, and Livia Vittori Antisari.
1438 2015. "Carbon Sequestration in Soils Affected By Douglas Fir Reforestation in Apennines
1439 (Northern Italy)." *Eqa-International Journal of Environmental Quality* 17: 1–11.
1440 doi:10.6092/issn.2281-4485/5208.
- 1441 Dongmann, G, and H W Nürnberg. 1974. "On the Enrichment of H²18O in the Leaves of
1442 Transpiring Plants I T L Q E" 52: 1–2.
- 1443 Esper, Jan, Edward R Cook, and Fritz H Schweingruber. 2002. "Low-Frequency Signals in Long
1444 Tree-Ring Chronologies for Reconstructing Past Temperature Variability." *Science (New York,
1445 N.Y.)* 295 (5563). American Association for the Advancement of Science: 2250–53.
1446 doi:10.1126/science.1066208.
- 1447 Esper, Jan, David C. Frank, Giovanna Battipaglia, Ulf Büntgen, Christopher Holert, Kerstin
1448 Treydte, Rolf Siegwolf, and Matthias Saurer. 2010a. "Low-Frequency Noise in ¹³C and
1449 ¹⁸O Tree Ring Data: A Case Study of Pinus Uncinata in the Spanish Pyrenees." *Global
1450 Biogeochemical Cycles* 24 (4): 1–11. doi:10.1029/2010GB003772.
- 1451 Esper, Jan, David C Frank, Giovanna Battipaglia, Ulf Büntgen, Christopher Holert, Kerstin Treydte,
1452 Rolf Siegwolf, and Matthias Saurer. 2010b. "Low Frequency Noise in D ¹³ C and D ¹⁸ O
1453 Tree Ring Data : A Case Study of Pinus Uncinata in the Spanish Pyrenees" 24 (2): 1–11.
1454 doi:10.1029/2010GB003772.
- 1455 Farquhar, G. D., L. A. Cernusak, and B. Barnes. 2006. "Heavy Water Fractionation during
1456 Transpiration." *Plant Physiology* 143 (1): 11–18. doi:10.1104/pp.106.093278.
- 1457 Farquhar, G D, J R Ehleringer, and K T Hubick. 1989. "Carbon Isotope Discrimination and
1458 Photosynthesis." *Annual Review of Plant Physiology and Plant Molecular Biology*.
1459 doi:10.1146/annurev.pp.40.060189.002443.
- 1460 Federal, Swiss, Universitat De Barcelona, J. Julio Camarero, Antonio Gazol, Juan Diego Galván,
1461 Gabriel Sangüesa-Barreda, and Emilia Gutiérrez. 2015. "Disparate Effects of Global-Change
1462 Drivers on Mountain Conifer Forests: Warming-Induced Growth Enhancement in Young Trees
1463 vs. CO₂ Fertilization in Old Trees from Wet Sites." *Global Change Biology* 21 (2): 738–49.
1464 doi:10.1111/gcb.12787.
- 1465 Fenn, Mark E, Jeremy S Fried, Haiganoush K Preisler, Andrzej Bytnerowicz, Susan Schilling,
1466 Sarah Jovan, and Olaf Kuegler. 2015. "REMEASURED FIA PLOTS REVEAL TREE-LEVEL
1467 DIAMETER GROWTH AND TREE MORTALITY IMPACTS OF NITROGEN
1468 DEPOSITION ON CALIFORNIA ' S FORESTS" 2013 (Time 2): 2013–16.
- 1469 Francey, R. J., C. E. Allison, D. M. Etheridge, C. M. Trudinger, I. G. Enting, M. Leuenberger, R. L.
1470 Langenfelds, E. Michel, and L. P. Steele. 1999. "A 1000-Year High Precision Record of ¹³C
1471 in Atmospheric CO₂." *Tellus, Series B: Chemical and Physical Meteorology* 51 (2): 170–93.
1472 doi:10.1034/j.1600-0889.1999.t01-1-00005.x.
- 1473 Frank, D. C., B. Poulter, M. Saurer, J. Esper, C. Huntingford, G. Helle, K. Treydte, et al. 2015.

- 1474 “Water-Use Efficiency and Transpiration across European Forests during the Anthropocene.”
1475 *Nature Climate Change*, no. May. doi:10.1038/nclimate2614.
- 1476 Giustini, Francesca, Mauro Brilli, and Antonio Patera. 2016. “Mapping Oxygen Stable Isotopes of
1477 Precipitation in Italy.” *Journal of Hydrology: Regional Studies* 8. Elsevier B.V.: 162–81.
1478 doi:10.1016/j.ejrh.2016.04.001.
- 1479 Gómez-Guerrero, Armando, Lucas C.R. R Silva, Miguel Barrera-Reyes, Barbara Kishchuk,
1480 Alejandro Velázquez-Martínez, Tomás Martínez-Trinidad, Francisca Ofelia Plascencia-
1481 Escalante, and William R. Horwath. 2013. “Growth Decline and Divergent Tree Ring Isotopic
1482 Composition (^{13}C and ^{18}O) Contradict Predictions of CO_2 Stimulation in High Altitudinal
1483 Forests.” *Global Change Biology* 19 (6): 1748–58. doi:10.1111/gcb.12170.
- 1484 Griffin, Daniel, and Kevin J Anchukaitis. 2014. “How Unusual Is the 2012 – 2014 California
1485 Drought ?,” 9017–23. doi:10.1002/2014GL062433.1.
- 1486 Guerrieri, R, Maurizio Mencuccini, L J Sheppard, M Saurer, M P Perks, P Levy, M a Sutton, Marco
1487 Borghetti, and J Grace. 2011. “The Legacy of Enhanced N and S Deposition as Revealed by
1488 the Combined Analysis of Delta ^{13}C , Delta ^{18}O and Delta ^{15}N in Tree Rings.” *Global
1489 Change Biology* 17 (5): 1946–62. doi:10.1111/j.1365-2486.2010.02362.x.
- 1490 Harris, I., P. D. Jones, T. J. Osborn, and D. H. Lister. 2014. “Updated High-Resolution Grids of
1491 Monthly Climatic Observations - the CRU TS3.10 Dataset.” *International Journal of
1492 Climatology* 34 (3): 623–42. doi:10.1002/joc.3711.
- 1493 Hastie, T. J., and R. J. Tibshirani. 1990. “Generalized Additive Models.” *Monographs on Statistics
1494 and Applied Probability*. doi:10.1016/j.csda.2010.05.004.
- 1495 IPCC. 2014. “Climate Change 2014 Synthesis Report Summary Chapter for Policymakers.” *Ippc*,
1496 31. doi:10.1017/CBO9781107415324.
- 1497 Keenan, Trevor F, David Y Hollinger, Gil Bohrer, Danilo Dragoni, J William Munger, Hans Peter
1498 Schmid, and Andrew D Richardson. 2013. “Increase in Forest Water-Use Efficiency as
1499 Atmospheric Carbon Dioxide Concentrations Rise.” *Nature* 499 (7458): 324–27.
1500 doi:10.1038/nature12291.
- 1501 Korner, C. 2005. “Carbon Flux and Growth in Mature Deciduous Forest Trees Exposed to Elevated
1502 CO_2 .” *Science* 309 (5739): 1360–62. doi:10.1126/science.1113977.
- 1503 Leavitt, Steven W. 2010. “Tree-Ring C-H-O Isotope Variability and Sampling.” *The Science of the
1504 Total Environment* 408 (22): 5244–53. doi:10.1016/j.scitotenv.2010.07.057.
- 1505 Lee, E. Henry, Peter A. Beedlow, Ronald S. Waschmann, David T. Tingey, Charlotte Wickham,
1506 Steve Cline, Michael Bollman, and Cailie Carlile. 2016. “Douglas-Fir Displays a Range of
1507 Growth Responses to Temperature, Water, and Swiss Needle Cast in Western Oregon, USA.”
1508 *Agricultural and Forest Meteorology* 221. Elsevier B.V.: 176–88.
1509 doi:10.1016/j.agrformet.2016.02.009.
- 1510 Leonardi, Stefano, Tiziana Gentilesca, Rossella Guerrieri, Francesco Ripullone, Federico Magnani,
1511 Maurizio Mencuccini, Twan V. Noije, and Marco Borghetti. 2012. “Assessing the Effects of
1512 Nitrogen Deposition and Climate on Carbon Isotope Discrimination and Intrinsic Water-Use
1513 Efficiency of Angiosperm and Conifer Trees under Rising CO_2 Conditions.” *Global Change
1514 Biology* 18 (9): 2925–44. doi:10.1111/j.1365-2486.2012.02757.x.

- 1515 L vesque, Mathieu, Rolf Siegwolf, Matthias Saurer, Britta Eilmann, and Andreas Rigling. 2014.
1516 "Increased Water-Use Efficiency Does Not Lead to Enhanced Tree Growth under Xeric and
1517 Mesic Conditions." *New Phytologist* 203 (1): 94–109. doi:10.1111/nph.12772.
- 1518 Linares, Juan Carlos, Jes s Julio Camarero, and Jos  Antonio Carreira. 2010. "Competition
1519 Modulates the Adaptation Capacity of Forests to Climatic Stress: Insights from Recent Growth
1520 Decline and Death in Relict Stands of the Mediterranean Fir *Abies Pinsapo*." *Journal of
1521 Ecology* 98 (3): 592–603. doi:10.1111/j.1365-2745.2010.01645.x.
- 1522 Magnani, Federico, Maurizio Mencuccini, Marco Borghetti, Paul Berbigier, Frank Berninger,
1523 Sylvain Delzon, Achim Grelle, et al. 2007. "The Human Footprint in the Carbon Cycle of
1524 Temperate and Boreal Forests." *Nature* 447 (7146): 848–50. doi:10.1038/nature05847.
- 1525 Marshall, D D, and R O Curtis. 2002. "Levels-of-Growing-Stock Cooperative Study in Douglas-
1526 Fir: Report No. 15 - Hoskins: 1963-1998." *Research Paper Pacific Northwest Research
1527 Station, USDA Forest Service*, no. PNW-RP-537: 80.
- 1528 McCarroll, Danny, and Neil J. Loader. 2004. "Stable Isotopes in Tree Rings." *Quaternary Science
1529 Reviews* 23 (7–8): 771–801. doi:10.1016/j.quascirev.2003.06.017.
- 1530 McMahon, Sean M, Geoffrey G Parker, and Dawn R Miller. 2010. "Evidence for a Recent Increase
1531 in Forest Growth." *Proceedings of the National Academy of Sciences of the United States of
1532 America* 107 (8): 3611–15. doi:10.1073/pnas.0912376107.
- 1533 Medlyn, B. E., F. -W. Badeck, D. G. G. De Pury, C. V. M. Barton, M. Broadmeadow, R.
1534 Ceulemans, P. De Angelis, et al. 1999. "Effects of Elevated [CO₂] on Photosynthesis in
1535 European Forest Species: A Meta-Analysis of Model Parameters." *Plant, Cell & Environment*
1536 22 (12): 1475–1495. doi:10.1046/j.1365-3040.1999.00523.x.
- 1537 Nair, Richard K F, Micheal P Perks, Andrew Weatherall, Elizabeth M Baggs, and Maurizio
1538 Mencuccini. 2015. "Does Canopy Nitrogen Uptake Enhance Carbon Sequestration by Trees?"
1539 *Global Change Biology*, September. doi:10.1111/gcb.13096.
- 1540 Nehrbass-Ahles, Christoph, Flurin Babst, Stefan Klesse, Magdalena N tzli, Olivier Bouriaud,
1541 Raphael Neukom, Matthias Dobbertin, and David Frank. 2014. "The Influence of Sampling
1542 Design on Tree-Ring-Based Quantification of Forest Growth." *Global Change Biology* 20 (9).
1543 doi:10.1111/gcb.12599.
- 1544 Norby, Richard J, Jeffrey M Warren, Colleen M Iversen, Belinda E Medlyn, and Ross E
1545 McMurtrie. 2010. "CO₂ Enhancement of Forest Productivity Constrained by Limited Nitrogen
1546 Availability." *Proceedings of the National Academy of Sciences of the United States of
1547 America* 107 (45): 19368–73. doi:10.1073/pnas.1006463107.
- 1548 Pe uelas, Josep, Josep G. Canadell, and Rom  Ogaya. 2011. "Increased Water-Use Efficiency
1549 during the 20th Century Did Not Translate into Enhanced Tree Growth." *Global Ecology and
1550 Biogeography* 20 (4): 597–608. doi:10.1111/j.1466-8238.2010.00608.x.
- 1551 Perakis, Steven S., and Emily R. Sinkhorn. 2011. "Biogeochemistry of a Temperate Forest Nitrogen
1552 Gradient." *Ecology* 92 (7): 1481–91. doi:10.1890/10-1642.1.
- 1553 Peters, Richard L., Peter Groenendijk, Mart Vlam, and Pieter a. Zuidema. 2015. "Detecting Long-
1554 Term Growth Trends Using Tree Rings: A Critical Evaluation of Methods." *Global Change
1555 Biology*, n/a-n/a. doi:10.1111/gcb.12826.

- 1556 Phillips, Nathan G., Thomas N. Buckley, and David T. Tissue. 2008. "Capacity of Old Trees to
1557 Respond to Environmental Change." *Journal of Integrative Plant Biology* 50 (11): 1355–64.
1558 doi:10.1111/j.1744-7909.2008.00746.x.
- 1559 Piovesan, Gianluca, Franco Biondi, Aalfredo Di Filippo, Alfredo Alessandrini, and Maurizio
1560 Maugeri. 2008. "Drought-Driven Growth Reduction in Old Beech (*Fagus Sylvatica* L.) Forests
1561 of the Central Apennines, Italy." *Global Change Biology* 14 (6): 1265–81. doi:10.1111/j.1365-
1562 2486.2008.01570.x.
- 1563 Poage, Nathan J, and John C Tappeiner, II. 2002. "Long-Term Patterns of Diameter and Basal Area
1564 Growth of Old-Growth Douglas-Fir Trees in Western Oregon." *Canadian Journal of Forest
1565 Research* 32: 1232–43. doi:10.1139/x02-045.
- 1566 Rehfeldt, Gerald E., Barry C. Jaquish, Javier Lòpez-Upton, Cuauhtémocmoc Sáenz-Romero, J.
1567 Bradley St Clair, Laura P. Leites, and Dennis G. Joyce. 2014. "Comparative Genetic
1568 Responses to Climate for the Varieties of *Pinus Ponderosa* and *Pseudotsuga Menziesii*:
1569 Realized Climate Niches." *Forest Ecology and Management* 324. Elsevier B.V.: 126–37.
1570 doi:10.1016/j.foreco.2014.02.035.
- 1571 Ripullone, Francesco, Marco Lauteri, Giacomo Grassi, Mariana Amato, and Marco Borghetti. 2004.
1572 "Variation in Nitrogen Supply Changes Water-Use Efficiency of *Pseudotsuga Menziesii* and
1573 *Populus X Euroamericana*; a Comparison of Three Approaches to Determine Water-Use
1574 Efficiency." *Tree Physiology* 24 (6): 671–79.
- 1575 Rita, Angelo, Marco Borghetti, Luigi Todaro, and Antonio Saracino. 2016. "Interpreting the
1576 Climatic Effects on Xylem Functional Traits in Two Mediterranean Oak Species: The Role of
1577 Extreme Climatic Events." *Frontiers in Plant Science* 7 (August): 1–11.
1578 doi:10.3389/fpls.2016.01126.
- 1579 Roden, John, and Rolf Siegwolf. 2012. "Is the Dual-Isotope Conceptual Model Fully Operational?"
1580 *Tree Physiology* 32 (10): 1179–82. doi:10.1093/treephys/tps099.
- 1581 Rozanski, Kazimierz, Luis Araguas-araguas, and Roberto Gonfiantini. 2016. "Relation Between
1582 Long-Term Trends of Oxygen-18 Isotope Composition of Precipitation and Climate Author (S
1583): Kazimierz Rozanski , Luis Araguás-Araguás and Roberto Gonfiantini Published by :
1584 American Association for the Advancement of Science Stable URL :." 258 (5084): 981–85.
- 1585 Ryan, Mg, D Binkley, and Jh Fownes. 1997. "Age-Related Decline in Forest Productivity: Pattern
1586 and Process." *Advances in Ecological Research*.
- 1587 Ryan, Michael G., Nathan Phillips, and Barbara J. Bond. 2006. "The Hydraulic Limitation
1588 Hypothesis Revisited." *Plant, Cell and Environment* 29 (3): 367–81. doi:10.1111/j.1365-
1589 3040.2005.01478.x.
- 1590 Ryan, Michael G., and Barbara J. Yoder. 1997. "Hydraulic Limits to Tree Height and Tree
1591 Growth." *BioScience* 47 (4): 235–42. doi:10.2307/1313077.
- 1592 Saurer, Matthias, Rolf T. W. Siegwolf, and Fritz H. Schweingruber. 2004. "Carbon Isotope
1593 Discrimination Indicates Improving Water-Use Efficiency of Trees in Northern Eurasia over
1594 the Last 100 Years." *Global Change Biology* 10 (12): 2109–20. doi:10.1111/j.1365-
1595 2486.2004.00869.x.
- 1596 Scheidegger, Y., M. Saurer, M. Bahn, and R. Siegwolf. 2000. "Linking Stable Oxygen and Carbon
1597 Isotopes with Stomatal Conductance and Photosynthetic Capacity: A Conceptual Model."

- 1598 *Oecologia* 125 (3): 350–57. doi:10.1007/s004420000466.
- 1599 Sitch, Stephan, C. Huntingford, N. Gedney, P. E. Levy, M. Lomas, S. L. Piao, R. Betts, et al. 2008.
1600 “Evaluation of the Terrestrial Carbon Cycle, Future Plant Geography and Climate-Carbon
1601 Cycle Feedbacks Using Five Dynamic Global Vegetation Models (DGVMs).” *Global Change
1602 Biology* 14 (9): 2015–39. doi:10.1111/j.1365-2486.2008.01626.x.
- 1603 Sternberg, Leonel Da Silveira Lobo O.Reilly. 2009. “Oxygen Stable Isotope Ratios of Tree-Ring
1604 Cellulose: The next Phase of Understanding.” *New Phytologist* 181 (3): 553–62.
1605 doi:10.1111/j.1469-8137.2008.02661.x.
- 1606 Treydte, Kerstin, Sonja Boda, Elisabeth Graf Pannatier, Patrick Fonti, David Frank, Bastian Ullrich,
1607 Matthias Saurer, et al. 2014. “Seasonal Transfer of Oxygen Isotopes from Precipitation and
1608 Soil to the Tree Ring : Source Water versus Needle Water Enrichment.”
- 1609 Vicente-Serrano, Sergio M., Santiago Beguería, and Juan I. López-Moreno. 2010. “A Multiscalar
1610 Drought Index Sensitive to Global Warming: The Standardized Precipitation
1611 Evapotranspiration Index.” *Journal of Climate* 23 (7): 1696–1718.
1612 doi:10.1175/2009JCLI2909.1.
- 1613 Vicente-Serrano, Sergio M., J. Julio Camarero, and Cesar Azorin-Molina. 2014. “Diverse
1614 Responses of Forest Growth to Drought Time-Scales in the Northern Hemisphere.” *Global
1615 Ecology and Biogeography* 23 (9): 1019–30. doi:10.1111/geb.12183.
- 1616 Vitas, A., and K. Žeimavi ius. 2006. “Trends of Decline of Douglas Fir in Lithuania :
1617 Dendroclimatological Approach.” *Baltic Forestry* 12 (2): 200–208.
- 1618 Walker, Lawrence R., David a. Wardle, Richard D. Bardgett, and Bruce D. Clarkson. 2010. “The
1619 Use of Chronosequences in Studies of Ecological Succession and Soil Development.” *Journal
1620 of Ecology* 98 (4): 725–36. doi:10.1111/j.1365-2745.2010.01664.x.
- 1621 Warren, Cr, Jf McGrath, and Ma Adams. 2001. “Water Availability and Carbon Isotope
1622 Discrimination in Conifers.” *Oecologia* 127 (4): 476–86. doi:10.1007/s004420000609.
- 1623 Williams, David G., R. David Evans, Jason B. West, and James R. Ehleringer. 2007. *Stable
1624 Isotopes as Indicators of Ecological Change. Terrestrial Ecology*. Vol. 1. doi:10.1016/S1936-
1625 7961(07)01024-X.
- 1626 Wood, Simon N. 2014. “Package ‘ Mgcv ’.” doi:10.1186/1471-2105-11-11.Bioconductor.
- 1627 Wood, Simon N. 2017. “Package ‘ Mgcv . ’”
- 1628 Wood, Simon N. 2006. *Generalized Additive Models: An Introduction with R*. Chapman and
1629 Hall/CRC.
- 1630 Wood, Simon N. 2008. “Fast Stable Direct Fitting and Smoothness Selection for Generalized
1631 Additive Models.” *Journal of the Royal Statistical Society. Series B: Statistical Methodology*
1632 70 (3): 495–518. doi:10.1111/j.1467-9868.2007.00646.x.
- 1633 Zhao, Maosheng, and Steven W Running. 2010. “Drought-Induced Reduction in Global Terrestrial
1634 Net Primary Production from 2000 Through 2009.” *Science* 329 (5994): 940–43.
1635 doi:10.1126/science.1192666.
- 1636 Zweifel, Roman, Lukas Zimmermann, Fabienne Zeugin, and David M. Newbery. 2006. “Intra-

1637 Annual Radial Growth and Water Relations of Trees: Implications towards a Growth
1638 Mechanism.” *Journal of Experimental Botany* 57 (6): 1445–59. doi:10.1093/jxb/erj125.

1639

1640

1641

1642 **Chapter III - Old-growth stand trees** 1643 **reaction to global change, an explorative** 1644 **study**

1645

1646 **1. Introduction**

1647 Over the last 150 years, anthropogenic emissions have dramatically raised the level of [CO₂] in the
1648 atmosphere, increased by 45%, from 278 ppm in 1750 to approximately 400 ppm in 2014 (IPCC
1649 2014). The effect of this major forcing of climate change on stem growth in adult trees is still
1650 controversial (Korner 2005), as the positive effect of CO₂ could be potentially negated by co-
1651 occurring changes in temperature and drought , as well as competition at inter-tree level (Linares et
1652 al., 2010). Another potential confounding issues is represented by the difficulty to disentangle
1653 biological effects (i.e associated to age/size-related changes taking place over the same time span)
1654 from environmental effects (i.e [CO₂], temperature, drought...) when the trees analyzed have been
1655 exposed to the external forcing for their entire lifetime (Phillips et al, 2008).

1656 The age-related growth pattern, on the other hand, could be modified by global change itself. It is
1657 generally assumed that with increasing age productivity is reduced by a complex interaction of
1658 decreasing photosynthetic capacity and increased control of stomata conductance (Ryan et al.,
1659 2006), due principally to hydraulic limitations related to age or size. If size and the related
1660 constraints, rather than age *per se*, is indeed the main driver which affects carbon gain in old trees
1661 (Mencuccini et al. 2005), this implies the possibility that old trees could react to factors which can

1662 improve photosynthetic rates or decrease water constraints responsible for stomatal control
1663 (Farquhar et al., 1989); this would suggest the possibility of using old trees and their growth as
1664 indicators of global change. On the other hand, radial growth is known to be substantially affected
1665 by developmental changes in stand density, which could make it difficult to ascertain the effects of
1666 age or global change.

1667 In the Pacific Northwest of the United States, old-growth stands of Douglas-fir (*Pseudotsuga*
1668 *menziesii* (Mirb.) Franco typically display a structure characterized by sparse large trees in the
1669 overstory, dominating smaller trees of different sizes and species in the lower and middle canopy
1670 layers, with a great amount of dead organic matter, and a patchy distribution of gaps (Spies and
1671 Franklin 1991). These old-growth forests show low but highly variable stand densities. For
1672 example, in the Oregon Coast Range, stands with a number of trees >100 cm in diameter at breast
1673 height (dbh) ranging from 18 to 29 trees/ha and a density of trees >50 cm in dbh of about 39
1674 trees/ha are commonly observed (Spies and Franklin 1991). On the other hand, natural young-
1675 growth Douglas-fir stands regenerated after large scale disturbance (logging, wild-fire, wind storm)
1676 are reported to have a density of trees >20 cm in dbh of about 363 trees/ha at the age of 50-60,
1677 while plantations typically have over 600 trees/ha at the same age (Marshall and Curtis 2002). Due
1678 to their complex stand structure and reduced densities in the upper layer, the effects of inter-tree
1679 competition could be negligible in old-growth forests, at least in the advanced developmental
1680 stages. Furthermore, if the stand is not generated by a large-scale disturbance (where earlier phases
1681 can be assimilated to even-aged stands, with locally high densities) also inter-tree competition
1682 which affects young individuals, could be less pronounced compared to artificial plantations. In
1683 fact, after an initial phase of about 30 years, when intense self-thinning has been reported to reduce
1684 the density by an average of 53%, their natural development would lead to growth in less dense
1685 conditions (Marshall et al. 1992).

1686 Three possible advantages in the analysis of the effects of global change on trees could be achieved
1687 by considering old-growth forest trees.

1688 First, the problem associated with the so-called "segment length curse" (Cook et al. 1995), i.e. the
1689 need in dendroclimatological studies to combine together different chronologies derived from living
1690 trees as well as preserved wood samples, could be minimized using tree-ring series which span the
1691 entire industrial age period; this would make it easier to retain low-frequency signal information, as
1692 typically associated with climatic changes.

1693 Second, the analysis of very old trees would make it possible to avoid the use of trees which have
1694 lived for their entire lifetime under conditions of elevated [CO₂] that have occurred over the last
1695 150 years, making it easier to assess its real influence on growth (Phillips et al., 2008). Finally,
1696 dealing with uneven-aged old-growth stands would result in the possibility to deal with a less
1697 pronounced effect on growth of competition and stand density, as discussed above, compared to
1698 even-aged forest trees.

1699 The aim of the present study is twofold: to evaluate the possibility of separating age -related growth
1700 changes from environmentally-driven long-term growth trends superimposed to them, and to
1701 understand if Douglas-fir in its native range on the Pacific coast is affected by the changing
1702 environmental pressure in a long-term prospective, looking in particular at which variable or
1703 combination of variables drives any observed change in growth.

1704

1705

1706

1707

1708

1709

1710

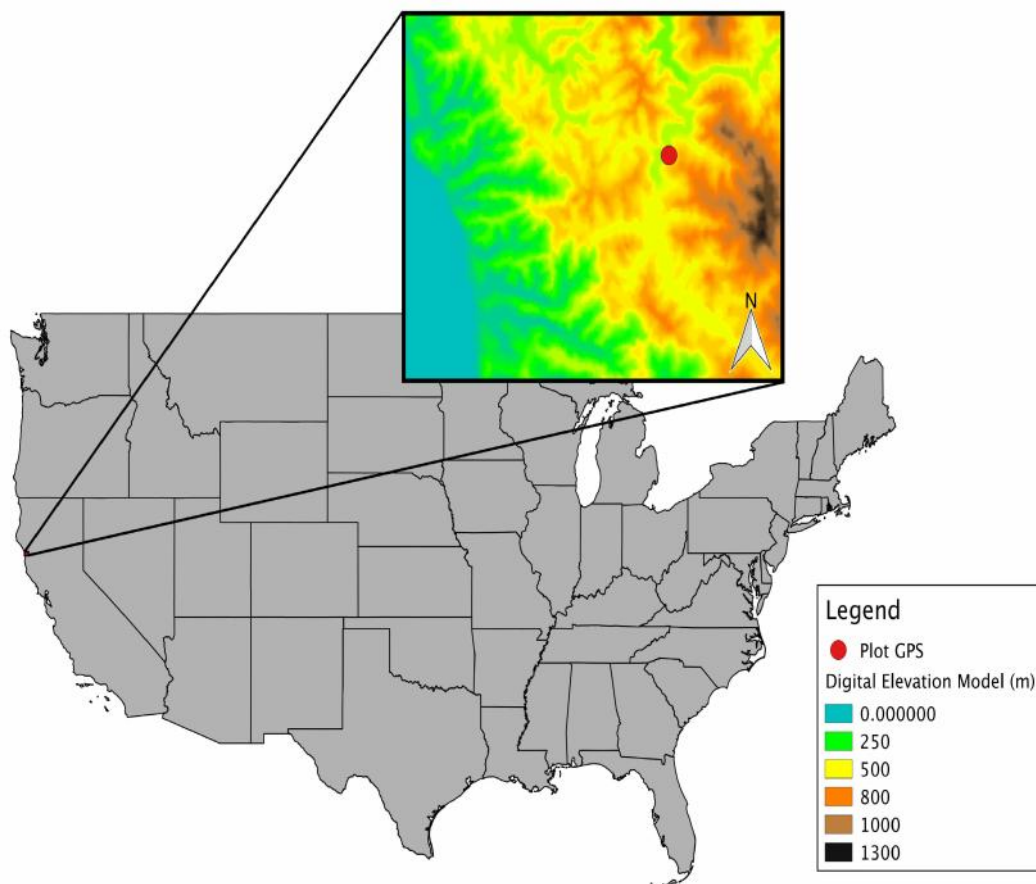
1711

1712

1713 2 Material and methods

1714 2.1 Study area

1715



1716

1717 **Fig.1 Map** shows the location of the old-growth stand sampled (red dot). Different colors are
1718 related to different elevations (m, a.s.l).

1719

1720 Tree ring cores originate from a Douglas-fir old-growth stand at about 450-500 m of elevation a.s.l,

1721 in the North California Coast Range of Mendocino County. The site is located at 39°43'47.4"N,

1722 123°38'28.2"W, in the University of California Angelo Coast Range Reserve, approximately 250

1723 km north of San Francisco and 20 km east of the Pacific coast. This region has a Mediterranean

1724 climate with summer droughts, which, especially over the last few years, have reached
1725 unprecedented levels in terms of both severity and duration (Griffin and Anchukaitis 2014). Mean
1726 annual precipitation is approximately 1350 mm, of which less than 10 mm occurs in the summer
1727 months; the summer, however, is characterized by frequent fog presence which is able to mitigate
1728 the water evaporative demand (T E Dawson 1998). The mean annual temperature at the site is
1729 12.6°C. The study area is located on a steep north-facing hill slope belonging to the Eldar Creek
1730 watershed, and is covered by a mixed forest of Douglas-fir and Mediterranean evergreen species.
1731 The species composition is represented by the Pacific Douglas-fir alliance (USDA, 2005), with
1732 Douglas-fir as the most represented group associated with Interior Live Oak (*Quercus wislizeni*),
1733 Tanoak (*Lithocarpus densiflorus*), and California Bay (*Umbellularia californica*). The forest shows
1734 a typical un-even aged structure, with vertical and horizontal spatial complexity, different
1735 development stages of living and dead individuals and gaps due probably to small-scale disturbance
1736 events. The multiple-layers canopy structure is dominated by older Douglas firs in the over-storey
1737 (with heights up to 60-70 m), with low crown closure. An intermediate layer is composed by
1738 younger Douglas-firs, while shade-tolerant broad-leaf trees form the lower canopy layer.

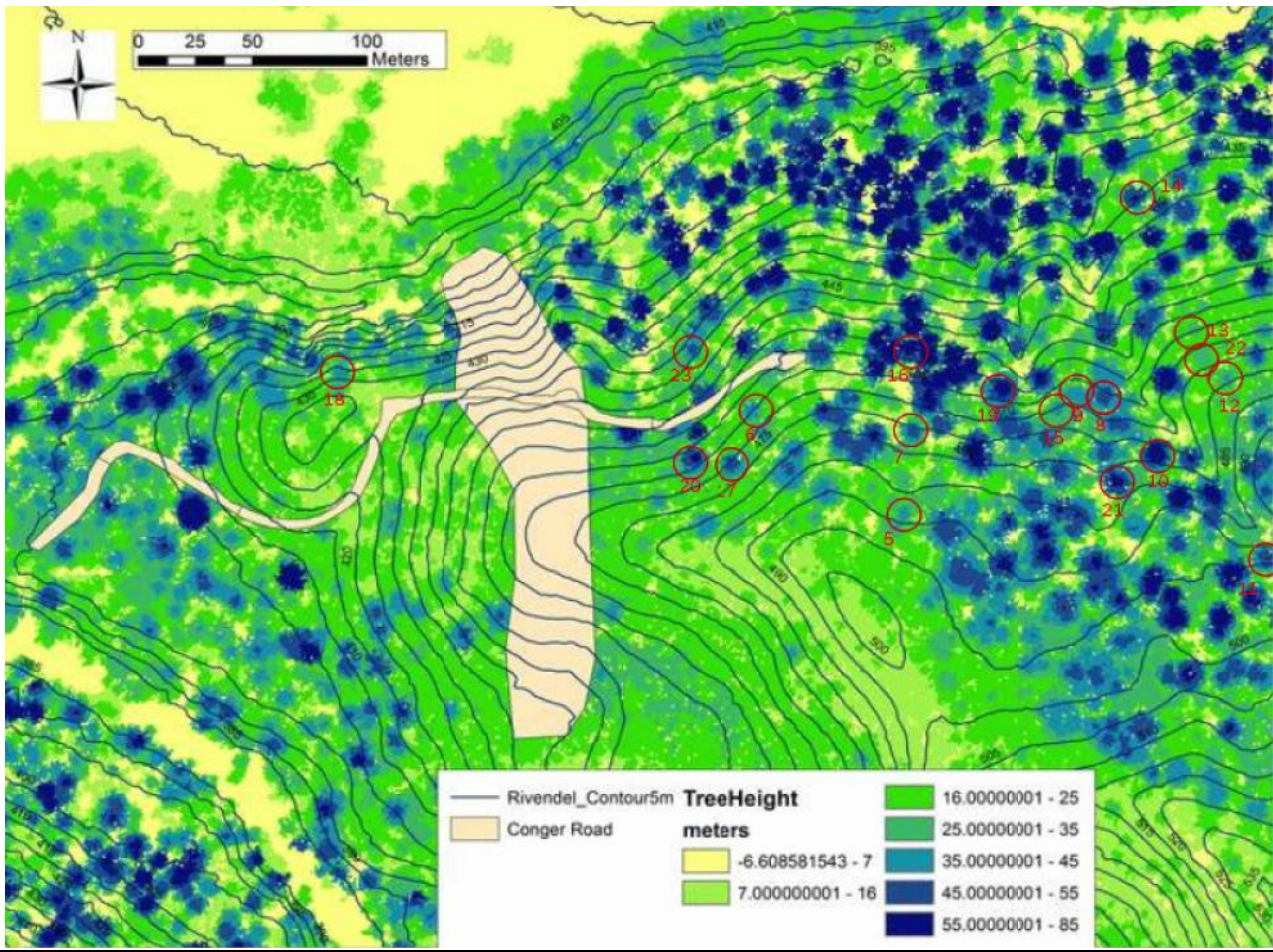
1739

1740 **2.2 Sampling strategy**

1741 The sampling strategy focused on the collection of a representative set of age-classes with the aim
1742 to reconstruct a chronosequence; assuming a strong relationship between age and height, sampled
1743 trees were therefore chosen on the basis of individual height classes, identified through a digital
1744 canopy height model derived from multiple LiDAR overflights (Fig.1), . A regression among the
1745 circumference of sampled trees and their presumptive height as determined from LiDAR maps was
1746 subsequently computed, so as to check the goodness of the tree selection approach (Fig. 2).
1747 Younger individuals were collected in medium-sized gaps, less than 50 m in diameter, originated

1748 probably from a single disturbance event and covered by a tree cohort with an even-aged structure.

1749 Older trees were sampled far from currently evident competitors.

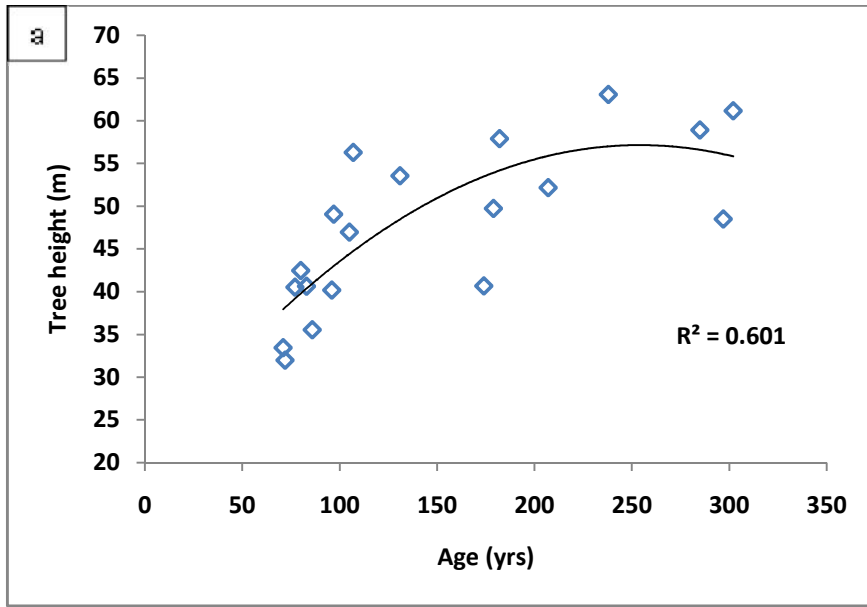


1750

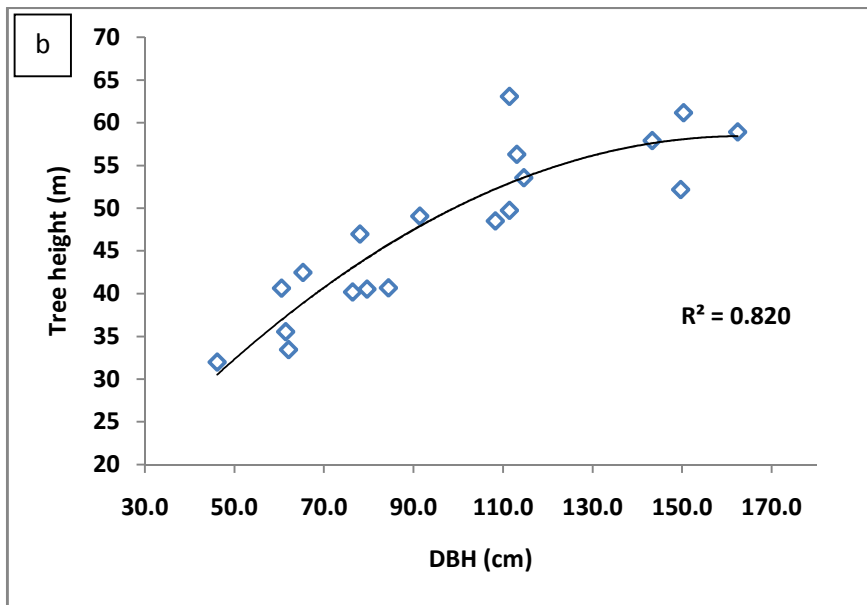
1751 **Fig. 1. Site LIDAR image.** Image derived from LIDAR flight data; the red circles correspond to the sampled
1752 trees. Different colours refer to different height classes (expressed in meters, in the legend).

1753

1754



1755



1756

1757

1758 **Fig. 2 Relationship between tree height, diameter and age.** a. Relationship between height of sampled
 1759 trees, based on LIDAR data, and (a) tree age, as reconstructed from tree ring data, or (b) diameter at
 1760 breast height (DBH), based on direct measurements. A 2-nd order polynomial curve has been fitted to
 1761 the data.

1762

1763 **2.3 Tree-ring data**

1764 In the fall of 2014, 18 dominant trees were sampled for dendro-ecological analysis. One single core
 1765 was extracted from each tree with a 5.1 mm Pressler borer (Haglöf, Sweden) at breast height from

1766 the upslope side of trees. The extracted cores were then air-dried and polished with progressively
1767 finer sandpaper (60- to 300-grit), so as to distinguish annual ring boundaries. Ring width series
1768 were measured on pictures taken with a high definition flatbed scanner (Epson V550 Photo, US),
1769 with a precision of 2400 dpi (dots per inch). Measurements were performed with COORECORDER
1770 image software analyzer (CybisElektronikand Data AB) with a 0.01 mm accuracy. Samples were
1771 visually cross-dated against a reference curve, between and within the series using a correlation
1772 coefficient, Gleichläufigkeit values and Student's t-test as indices. Since it was not possible to find
1773 a comparable reference curve in the International Tree-Ring Data Bank (TRDB), the reference
1774 curve was developed from the dataset itself, by a 'leave-one-out' approach, starting from samples
1775 which show a higher correlation between each other. Subsequently, the quality of cross-dating was
1776 checked and cross-correlation analysis was performed using CDENDRO software (Cybis
1777 Elektronik and Data AB) and the R dplR package (Bunn, 2010). Where the extracted core did not
1778 reach the pith of the tree, the length to the center was estimated using the curvature of the last
1779 complete ring, and the number of missing rings was calculated by dividing this distance by the last
1780 five-year ring average (Appelquist et al., 1958). This made it possible to reconstruct the age of each
1781 sampled tree.. Subsequently, the raw ring widths recorded were converted into basal area
1782 increments (BAI), as the latter allows to compensate for the age effect purely associated with stem
1783 geometry, especially relevant at young age, but preserving the low frequency variability (Biondi
1784 1999). Moreover, basal area increments are considered a better proxy of tree volume growth
1785 compared with radial increments. Basal area increments were calculated as:

$$1786 \quad \text{BAI} = (r_t^2 - r_{t-1}^2) \quad (1)$$

1787 where r_t is the stem radius at a given year, and r_{t-1} corresponds to the radius in the previous year.

1788 A preliminary analysis demonstrated a lack of homoscedasticity in the data, i.e. an increase in data
1789 variance with increasing BAI. All further statistical analyses were therefore performed on log-
1790 transformed BAI (Camarero et al. 2015), although at the cost of making the interpretation of results

1791 less straightforward.

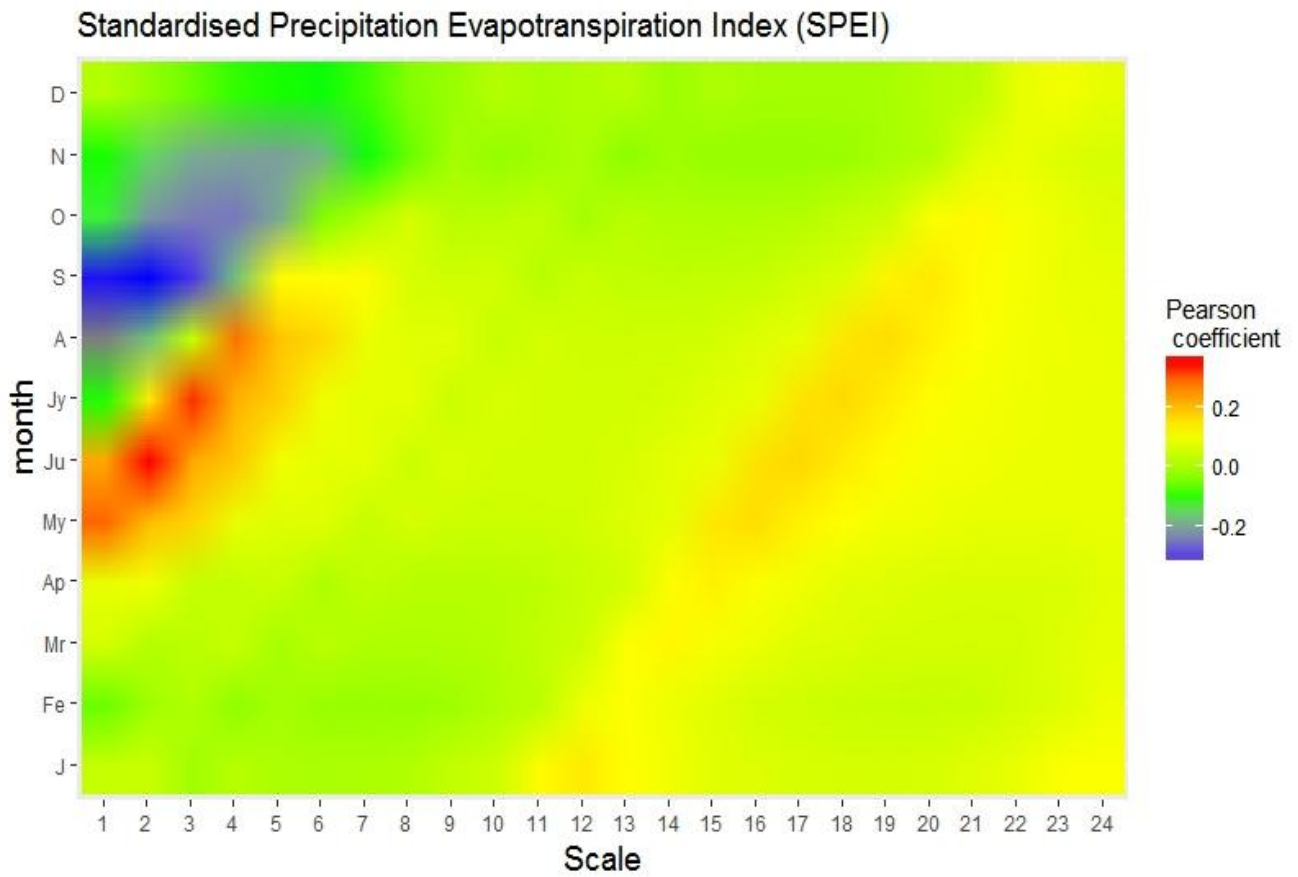
1792

1793 **2.4 Climate data**

1794 Climatic and geochemical data needed for growth change attribution were not directly measured at
1795 the study site, but derived from available datasets for the period 1901-2014.

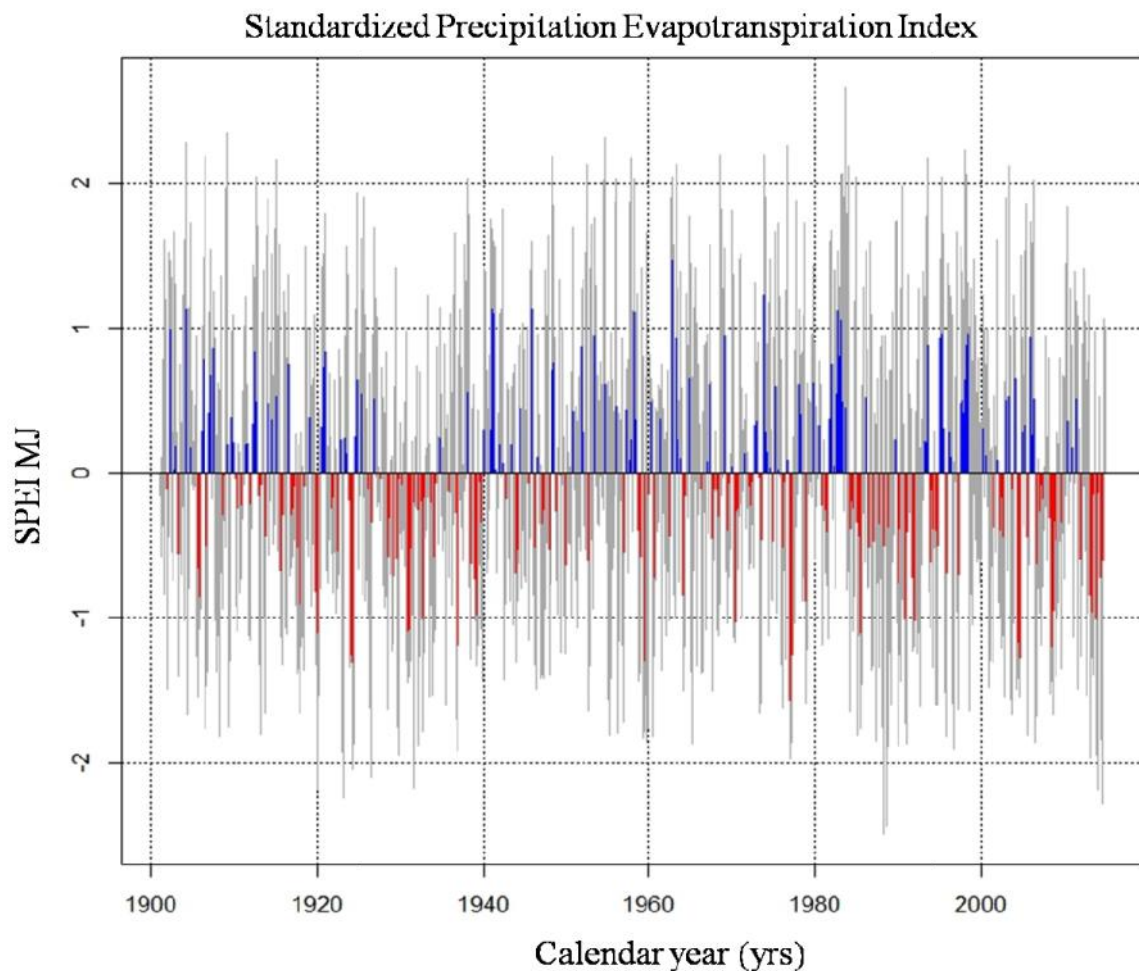
1796 Average monthly temperatures and precipitation for the period were obtained, using interpolated
1797 climatic data at gridded $0.5^\circ \times 0.5^\circ$ resolution, from the CRU (Climatic Research Unit of University
1798 of East Anglia, Norwich, UK) TS 4.1 data set (Harris et al. 2014); mean annual temperatures (T_m)
1799 and total annual sums of precipitation (P) were derived from monthly data. To evaluate the potential
1800 effect of drought stress, the Standardized Precipitation Evapotranspiration Index (SPEI) was
1801 adopted and calculated as in Vicente-Serrano et al. (2014). The 1–24 month timescale SPEI values
1802 were computed for each month (Fig.3) and a single representative value was retained for further
1803 analyses (Fig.4), based on Pearson's correlation coefficient.

1804



1805

1806 **Fig.3 SPEI correlation RWI heatmap.** Correlations (Pearson coefficient) between the Standardized
 1807 Precipitation Evapotranspiration Index (SPEI) at 1- to 24 month scales, and de-trended tree-rings index
 1808 (RWI), with on the *x*-axis temporal scale of SPEI and on the *y*-axis related months.



1809

1810 **Fig.4 SPEI MJ.** Trend of June SPEI at 2 month scales (May,June),which displays the highest correlation
 1811 with RWI, with on the x -calendar year (yrs) and on the y -axis SPEI values centered around 0. Red bar
 1812 represent water deficit, while blue bars represent water surplus.

1813

1814 **2.2 Geochemical data**

1815 Mean annual data for air CO₂ concentration were obtained from the NOAA Earth System Research
 1816 Laboratory, as recorded at the Mauna Loa observatory in Hawaii from 1959 to present, and further
 1817 integrated with the historical dataset proposed by McCarroll and Loader (2004) for the previous
 1818 period (1901-1958). Average annual values of nitrogen oxide (NO_y) and ammonium (NH_x) species
 1819 for both dry and wet atmospheric deposition were extracted from the global NCAR data set
 1820 managed by the IGAC-SPARC CCMi (Chemistry-Climate Model Initiative), (available for
 1821 download at <http://blogs.reading.ac.uk/ccmi/>). These N depositions data were generated with the
 1822 NCAR (National Center for Atmospheric Research) atmospheric transport model, covering the

1823 period between 1901 and 2014, which provides gridded (resolution of 2.0°x 2.25°, longitude x
 1824 latitude) temporal simulation of the chemical composition of the atmosphere.

1825

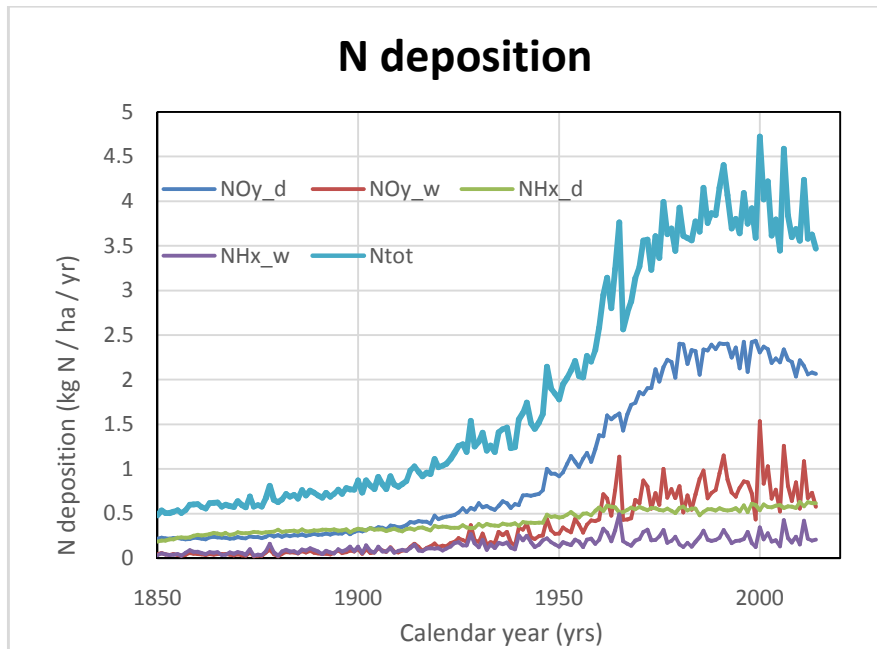


Fig 2. N deposition.
 Nitrogen deposition trends at Vallombrosa site as modeled by NCAR. Different colors represent the different species (oxide or ammonium) and different form of deposition (wet or dry) plus the total. On the x-axis calendar year (yrs), on the y-axis amount of deposition (kg N/ha/yr).

1826

1827 **2.3 GAMs**

1828 In order to take into account the possibility of non-linear responses to both biological and
 1829 environmental factors, and to prevent the loss of low-frequency variability potentially associated
 1830 with traditional de-trending methods, GAMs regression techniques (Hastie and Tibshirani 1990)
 1831 were applied to the data in the form:

1832
$$y_i = \beta_0 + f_1(x_{i1}) + \dots + f_n(x_{in}) + \epsilon_i \quad \text{where } \epsilon_i \sim N(0, \sigma^2)$$

1833 where y_i is the i-th value of the response variable, β_0 is the unknown intercept of fixed parameters,
 1834 x_1, \dots, x_n are independent variables, f_1, \dots, f_n are smooth functions and ϵ_i are residuals with normal
 1835 (Gaussian) distribution and constant variance. A cubic penalized spline was used as a smooth
 1836 function, with the amount of penalizations automatically computed by the maximum likelihood
 1837 (ML) estimation method (S. N. Wood 2006).

1838 As a first step, the approach was used to model the effects of cambial age and time (i.e. global
1839 change) on log-transformed basal area increments. As a second step, the GAM approach was
1840 applied to try and partition the effects of global change to its climatic and geochemical components.
1841 Tree age, atmospheric [CO₂], total atmospheric N deposition or its NH_x and NO_y components, mean
1842 (T_m) or maximum (T_{max}) and minimum (T_{min}) annual temperatures, annual precipitation (P) and the
1843 SPEI value of the current and previous year (SPEI_{t-1}) were considered as possible covariates.

1844 Potential covariates considered in the analysis are cambial age, atmospheric [CO₂], total N
1845 atmospheric deposition (N_{tot}, both dry and wet), its and its ammonium species (NH_x) or N oxide
1846 species componnt (NO_y), mean (T_m), maximum (T_{max}) and minimum annual temperature (T_{min}),
1847 annual precipitation (P), and the selected value of SPEI of the current year (SPEI) and the previous
1848 year (SPEI_{t-1}). The covariates selection was performed by a stepwise backward process based on p-
1849 values for candidate removal.

1850

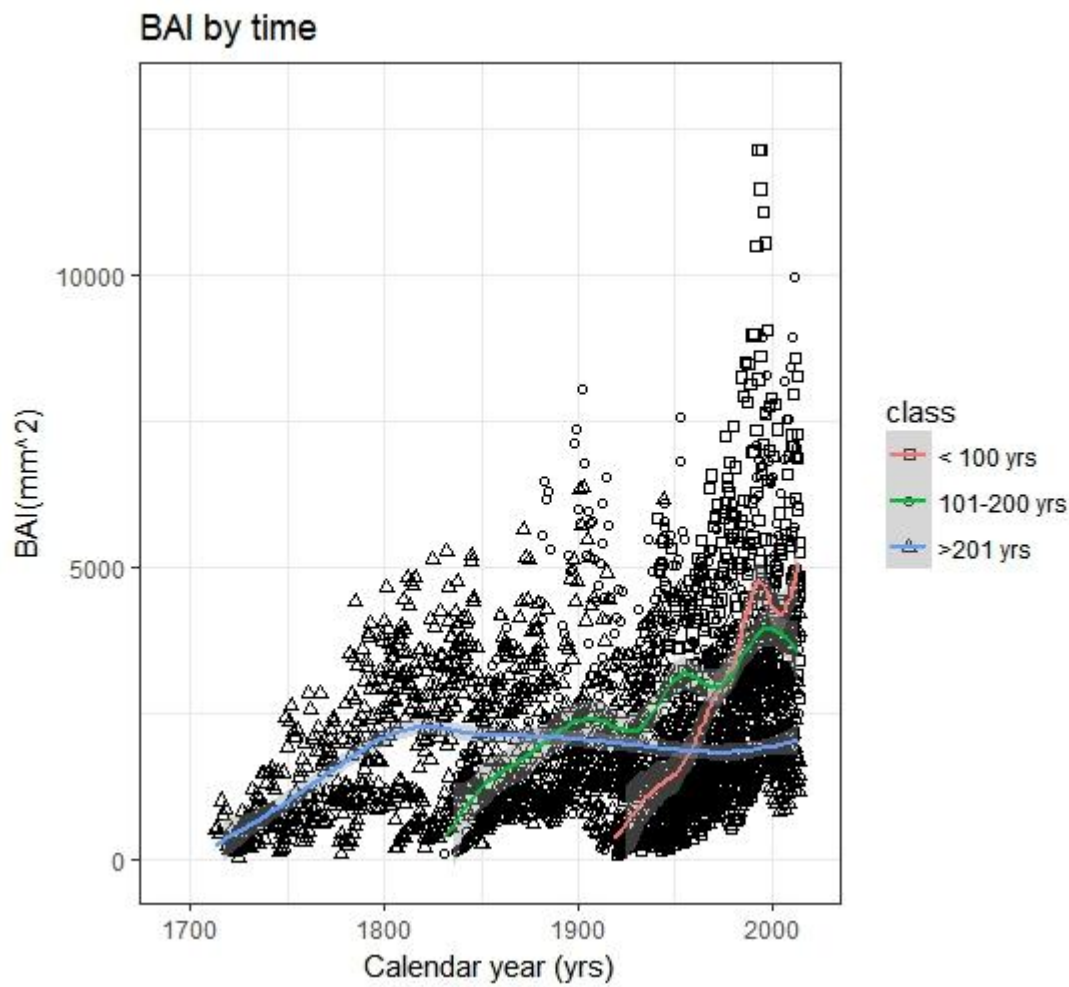
1851 **3. Results and discussion**

1852 The different age classes showed extremely different values in terms of raw basal area increments,
1853 both along calendar year and by cambial age. From a synchronic perspective (i.e. comparing values
1854 corresponding to the same calendar year in the three age classes; Fig. 3), the growth rate of old trees
1855 over the last few years appears to be much lower than for younger age classes; this contrasts,
1856 however, with the historic growth pattern of the old class, which shows a stabilization in its growth
1857 trend after an initial culmination, and only a bland increase in recent decades. The BAI trend of the
1858 youngest class shows a steep increase immediately after the 1960s, while the middle age-class
1859 shows a more gradual increase over the entire period.

1860

1861

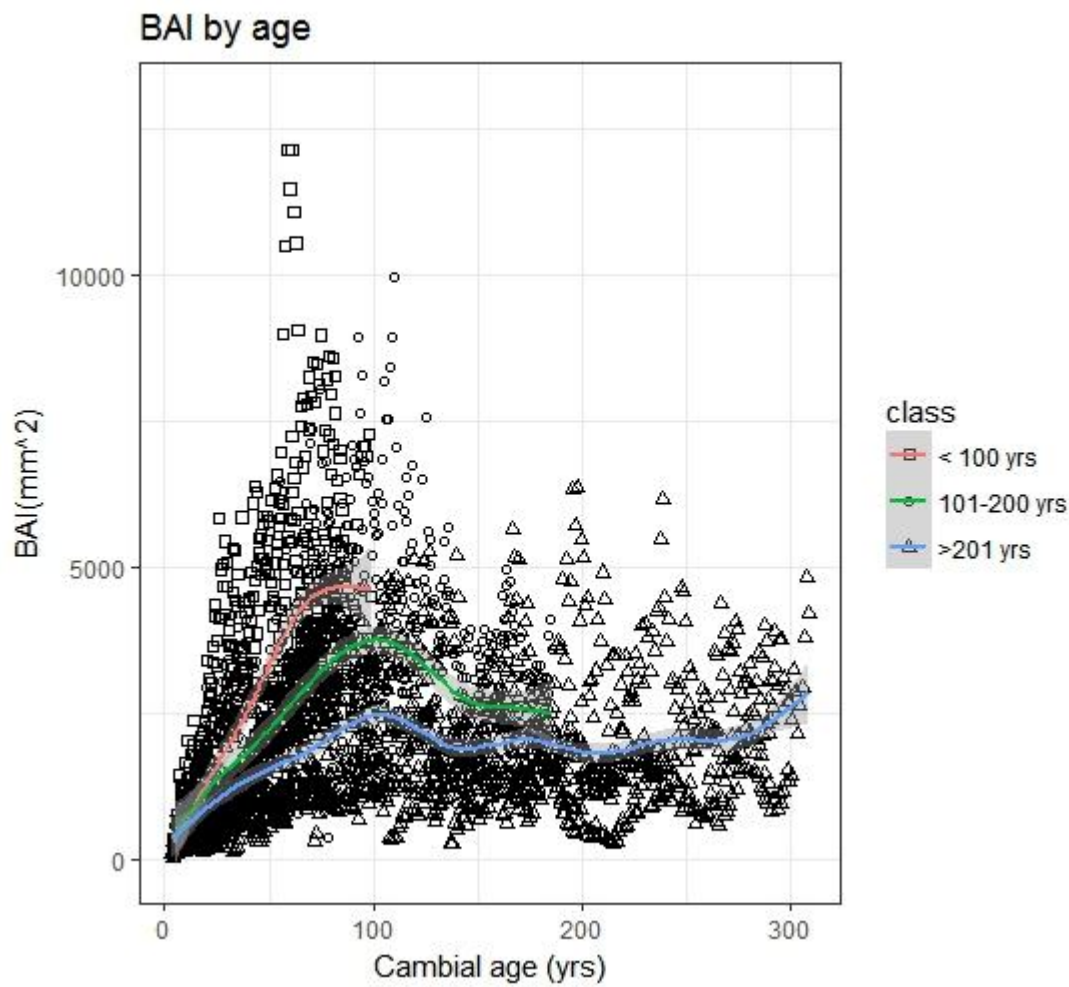
1862



1863

1864 **Fig. 3 Time-related dynamics of basal area increments in different age-classes.** Time series of
 1865 basal area increments (BAI), grouped by age-class and fitted with a cubic spline. The shaded
 1866 areas indicate the 95% prediction interval of the function.

1867 A more consistent picture emerges when taking a diachronic perspective (i.e. comparing values
 1868 aligned by cambial age; Fig. 4): in this case, the distribution of BAI for the three age-classes seems
 1869 to follow a gradient, with the younger class exhibiting significantly higher values in comparison
 1870 with the older one, and the middle-age class displaying an intermediate pattern. Apart from absolute
 1871 values, there appears to be also a shift in age-related dynamics, with an earlier culmination in the
 1872 young age class than in the middle-aged and, to an even larger extent, the oldest class. In
 1873 combination, these features suggest a progressive increase in yield class over time, possibly as a
 1874 result of a time dependent forcing (i.e global change).



1875

1876 **Fig. 4 Diachronic analysis of age effects on basal area increments in different age-classes.** Time
 1877 series of basal area increments (BAI), grouped by age-classes and fitted with a cubic spline. The shaded
 1878 areas indicate the 95% prediction interval of the spline function

1879

1880 At the same time, the possibility that the pattern could be the result of a biased sampling strategy
 1881 should be taken into account. On the one hand, the lack of a truly random selection of trees
 1882 (Nehrbass-Ahles et al. 2014) could have caused an unrepresentative sampling of the entire
 1883 population; on the other hand, we cannot rule out the possibility that the older age classes are more
 1884 represented by slow-growing trees, which have greater surviving rate (Issartel and Coffard 2011;
 1885 but see Kaufmann 1996), while younger class could be represented by a higher fraction of fast-
 1886 growing trees, leading to an apparent increase of growth rates in time (Peters et al. 2015). Another
 1887 criticism concerns the entire dataset and is represented by the strength of the common signal shared
 1888 by all series. While mean series inter-correlation (SI) is about 0.5 (Table 2), the global expressed

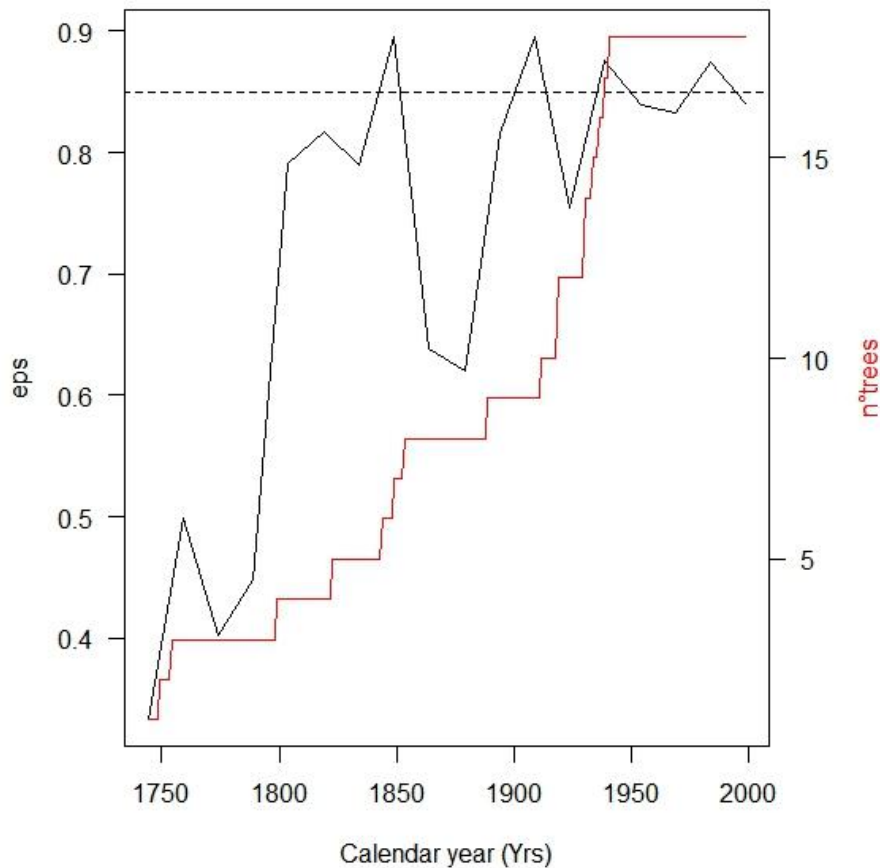
1889 population signal is 0.713, which is below the conventional threshold of 0.85 used to define the
 1890 acceptability of a tree ring chronology (Cook 1985; Mérian and Lebourgeois 2011). However the
 1891 running EPS (Fig. 5) shows that, in the more recent period where the growth/environmental analysis
 1892 was carried out (1901-2014), the EPS reaches a value close to the acceptable threshold. The limited
 1893 number of replications of this explorative study, of course, affects the strength of the signal,
 1894 suggesting that results should be considered with care.

1895

1896 **Tab.1** Descriptive statistics for raw tree ring width (TRW) and ring width index (RWI) chronologies of the
 1897 different age-classes. *Mage* in the mean age of the class, *MW* is mean ring width, *SD* is standard deviation
 1898 of ring width, *MS* is mean sensitivity, *AR1* the first order autocorrelation, *ESP* the expressed population
 1899 signal, *SI* the series inter-correlation

Age-class	<i>Mage</i>	TRW			RWI		
		<i>MW</i>	<i>SD</i>	<i>MS</i>	<i>AR1</i>	<i>ESP</i>	<i>SI</i>
100	81	3.1030	0.8265	0.1518	0.6853		
200	154	2.2798	0.8340	0.1684	0.7776		
300	267	1.4186	0.8032	0.1834	0.8524		
total	153	2.2671	0.8212	0.1679	0.7718	0.713	0.5

1900



1901

1902 **Fig. 5. Preliminary analysis of chronology sample size.** Expressed population signal (EPS,
 1903 dimensionless; black line and left axis) changes along the ring width chronology. The sample
 1904 size of the chronology, expressed as number of trees as a function of date, is also presented
 1905 (red line and right axis). The dashed line represents the threshold of 0.85, used to define the
 1906 acceptability of the chronology.

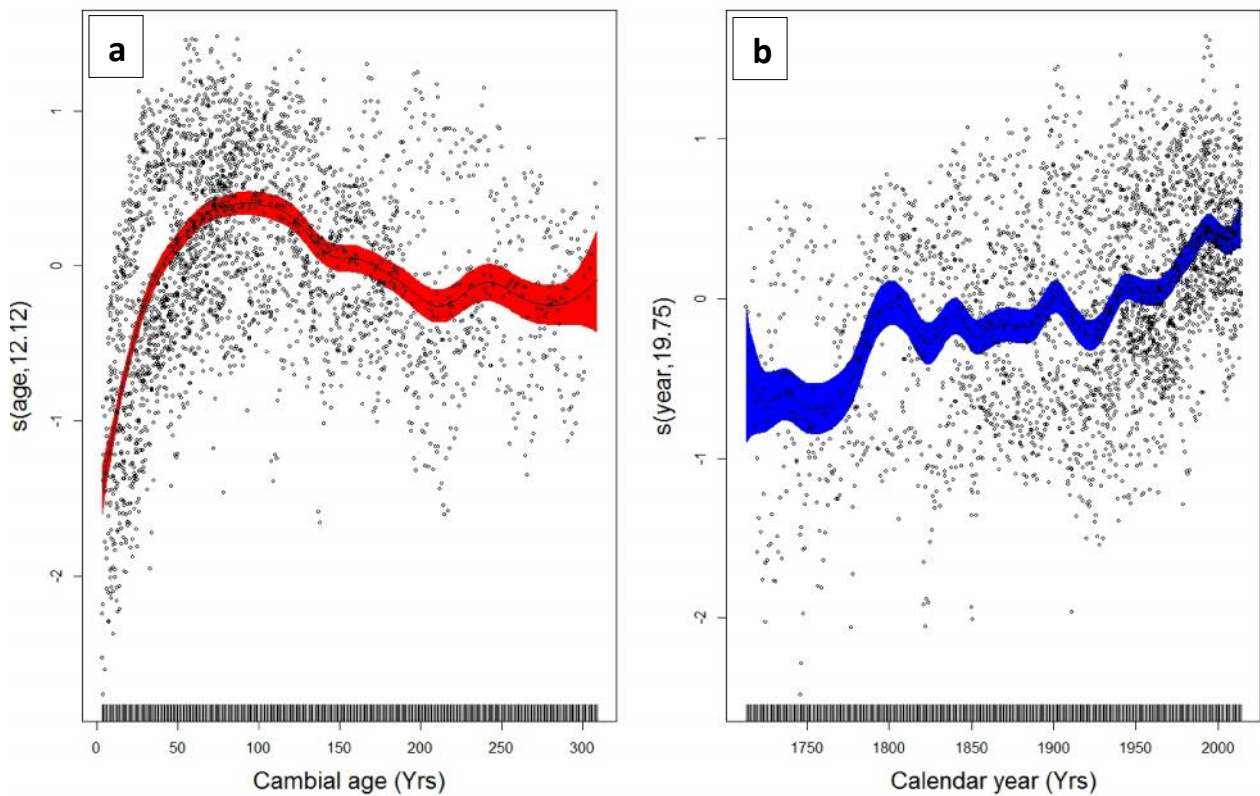
1907

1908 In order to better understand the possible change of growth rates over time, and separate it from the
 1909 co-occurring effects of age, the transformed BAI signal was first modeled by the following GAMs
 1910 model:

1911
$$\log\text{BAI} = s(\text{Age}) + s(\text{TIME}) + \epsilon_i \quad (3)$$

1912 where $s(\text{Age})$ is the cambial age effect and $s(\text{TIME})$ represents all of the environmental effects
 1913 cumulated into a single global variable, varying over time, which could be associated with a global
 1914 change effect. The age-related signal (Fig. 6a) shows a culmination in increments approximately
 1915 between an age of 80-100 years, followed by a constant decrease to an age of about 200 years, and a

1916 stabilization afterwards with only minor oscillation; a similar pattern would be expected in the age-
 1917 dependent dynamics of BAI in dominant trees (Poage and Tappeiner 2002). On other hand, the BAI
 1918 global long-term trend (Fig. 6b), after the subtraction of the age-related signal, displays a
 1919 pronounced increase in the second part of the 20th century. This trend amounts to an increase of
 1920 about 30.7% in the period between 1810 (before the beginning of the industrial revolution) and
 1921 1950 (before modern industrialization). Afterwards, a 59.5% increase was can be observed to the
 1922 present, with an accelerating trend that would appear to mirror the recent rise in atmospheric CO₂
 1923 concentration.



1924

1925 **Fig. 6 GAM analysis of the independent effects on BAI of age and time.** **a.** Trend of basal area
 1926 increments (BAI) as a function of age , after correcting for time-related effects. On x -axis age (years),
 1927 and on y -axis the function of age $f(\text{AGE})$, dimensionless and centered around 0. **b.** Global trend of
 1928 BAI as a function of time , after correcting for age-related effects. On y -axis the function of time
 1929 $s(\text{TIME})$, dimensionless and centered around 0. Points represent partial residuals from the fitted
 1930 function and the shaded areas indicate the 95% prediction interval of fitted adaptive splines. The GAM
 1931 model was applied to log-transformed BAI data, so as to correct for heteroscedasticity.

1932

1933 As a last step, in order to highlight which factors were responsible for such a growth acceleration,
 1934 climatic and geochemical variables were added to the model instead of the time variable. After a
 1935 backward stepwise selection of candidate covariates, the resulting optimal model was specified as
 1936 follow (Fig. 7):

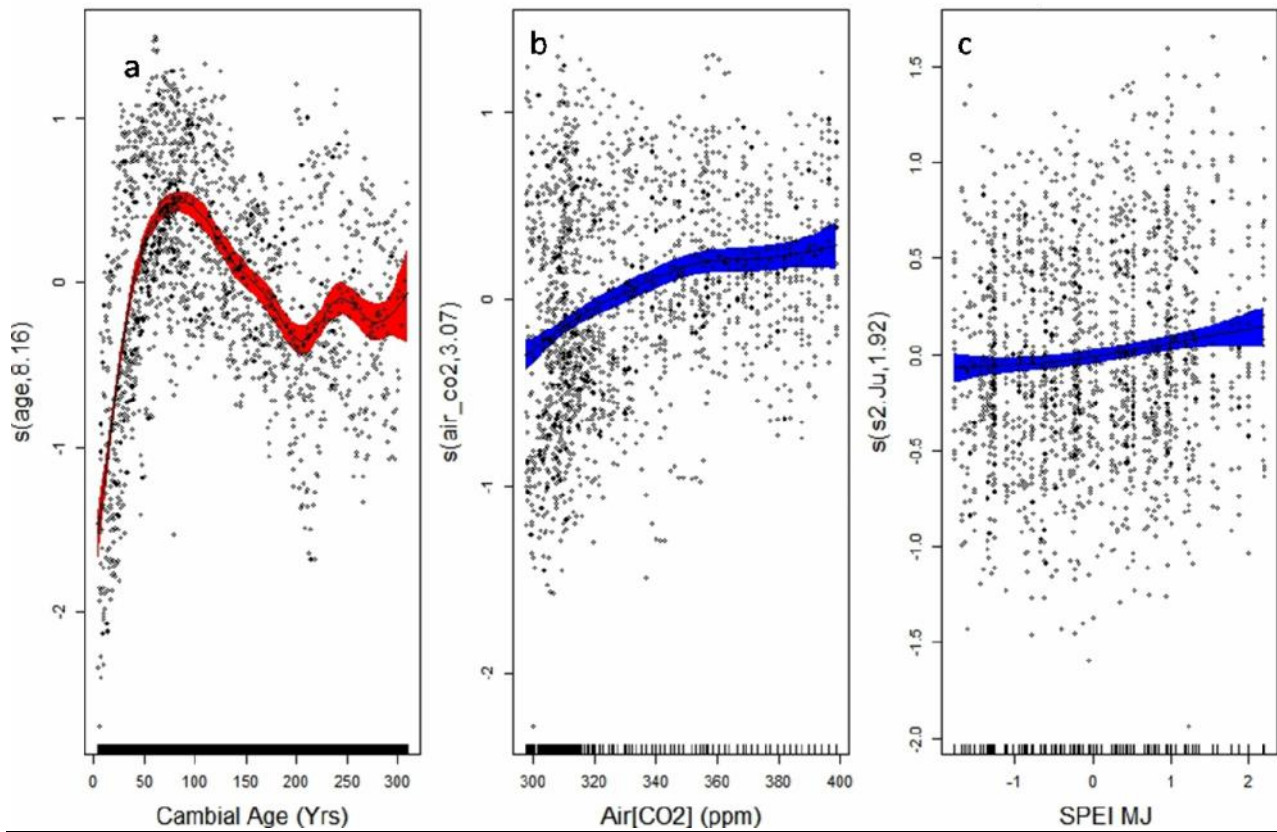
$$1937 \quad \log(\text{BAI}) = s(\text{Age}) + s(\text{CO}_2) + s(\text{SPEI MJ}) + \epsilon_i \quad (4)$$

1938 where $s(\text{Age})$ is the cambial age effect, CO_2 is the annual level of atmospheric $[\text{CO}_2]$, and SPEI MJ
 1939 represents the June SPEI values cumulated over the preceding 2-month period. All three effects
 1940 show a significant p-value at 0.001 level (Table 3) and the global adjusted R^2 for the whole model is
 1941 0.462. Atmospheric CO_2 concentrations, rather than climatic covariates, seem to be the major forcing
 1942 which has determined the long-term trend in Douglas-fir's radial growth in this old-growth forest.
 1943 Even if early summer water availability shows a significant effect, this is rather weak compared to
 1944 the geochemical variable. This could be related to the mitigating action of fog and to the changing
 1945 magnitude and inconstant time-scale of recurring drought events, although it should be considered
 1946 one of the main limiting factors in this sub-Mediterranean environment. This results makes sense if
 1947 SPEI is more related with high frequency variability and, thus, plays a secondary role compared to
 1948 the stronger increase of $[\text{CO}_2]$. In fact no clear trend are displayed by none of the climate covariates
 1949 in the last century (data not shown).

Tab. 2 | Generalized additive model results. Relationship between $\ln(\text{BAI})$ series (as dependent variable) in *Pseudotsuga menziesii* and environmental or biological factors remaining after the backward selection procedure: cambial age, atmospheric $[\text{CO}_2]$ and Standardized Precipitation Evapotranspiration Index computed over May and June (SPEI MJ). *e.d.f.* are effective degree of freedom, *F* is the F-test for variance explained, *P* is the p-value and $R^2(\text{adj})$ is the adjusted correlation coefficient of the model.

Factor	<i>e.d.f.</i>	<i>F</i>	<i>P</i>	$R^2(\text{adj})$
Age	8.131	104.347	< 2e-16	
CO2	3.987	14.201	< 2e-16	
SPEI MJ	1.258	1.807	2.47E-05	
Whole model				0.462

1950



1951

1952 **Fig. 7. GAM analysis of increment response to individual drivers.** Generalized additive models
 1953 (GAMs) results show the relationship between basal area increments (BAI) and environmental and
 1954 biological factors remaining after the backward selection procedure: cambial age, atmospheric [CO₂]
 1955 and Standardized Precipitation Evapotranspiration Index computed over May and June (SPEI MJ).
 1956 Values on the y-axis indicate the independent effect of each covariate on basal area increments, as
 1957 predicted by the model (continuous line) dimensionless and centered around 0, plus the estimated
 1958 degree of freedom (edf). Points represent partial residuals from the fitted function and the shaded areas
 1959 indicate the 95% prediction interval. The GAM model was applied to log-transformed BAI data, so as
 1960 to correct for heteroscedasticity.

1961

1962 The effects of N deposition as a covariate were found not to be significant for either of the nitrogen
 1963 forms (nor for their sum), maybe because of the low levels of pollutants which affect this site (Fig.
 1964 supplementary material). Another study (Fenn et al. 2015), covering the entire California territory
 1965 and considering 1706 permanent plots (33091 trees) found positive effects of N deposition on
 1966 conifer diameter growth, but only above a threshold value of 15 kg/ha/yr, probably because of the
 1967 damaging effects of ozone at lower N deposition rate.

1968

1969 4. Conclusions

1970

1971 From a methodological point of view, natural old-growth stands appear to have two major
1972 advantages when modelling tree growth response to environmental factors. First, they are less
1973 affected by inter-tree competition due to complex structure development or, at least, by the absence
1974 of synchronous consequences of thinning, and, second, they provide a very wide range in tree ages,
1975 so reducing the 'segment length curse' (Cook *et al.* 1995). The longer time span so covered could
1976 retain information referring to a pre-industrial world, essential when long-term environmental
1977 effects on trees growth, as well as age-related effects, are to be assessed, without the problems
1978 associated with confounding factors. At the same time, data from uneven-aged old-growth forests
1979 could be affected by a number of problems, first of all the possible link between growth rates and
1980 longevity, which would deserve further attention.

1981 Also from a methodological point of view, the study demonstrated the need to combine
1982 dendroecological studies with a chronosquence approach, so as to be able to disentangle the global
1983 change effect from the co-occurring effects of tree ageing; despite its potential limitations (mainly
1984 due to the assumption of effect additivity, with no interaction between covariates) the GAM
1985 approach appears to be the best suited for such an analysis, provided that the number of covariates
1986 is kept to a minimum, with low cross-correlation.

1987 The chronosquence approach coupled with the application of GAM models allowed us to highlight
1988 a strong increase in BAI at a constant age, which could be largely attributed to the effects of rising
1989 [CO₂]. The spring/summer water availability, even if highly significant, looks likely to affect to a
1990 smaller extent the long-term trend in radial increments in this old-growth stand. These results show
1991 how the impact of global change, in absence of other limiting factors which normally could hide or
1992 negate its effect, has already modify tree growth rates since the pre-industrial era. This could mean
1993 that forest ecosystems have really the potential to exert a mitigation action on climate change,
1994 actively increasing over time their efficiency as carbon sinks (Popkin 2017), also in old-growth

1995 forests. On the other hand, it should be stressed that a similar pattern has not always been observed
1996 across the globe (Groenendijk *et al.* 2015); future studies should ascertain if such discrepancies can
1997 be explained by methodological biases or real differences between species and biomes.

1998



1999

2000

2001 **5. Bibliography**

2002

- 2003 ABER, JOHN D., CHRISTINE L. GOODALE, SCOTT V. OLLINGER, MARIE-LOUISE
2004 SMITH, ALISON H. MAGILL, MARY E. MARTIN, RICHARD A. HALLETT, and JOHN
2005 L. STODDARD. 2003. "Is Nitrogen Deposition Altering the Nitrogen Status of Northeastern
2006 Forests?" *BioScience* 53 (4): 375. doi:10.1641/0006-3568(2003)053[0375:INDATN]2.0.CO;2.
- 2007 Aho, Ken, DeWayne Derryberry, and Teri Peterson. 2014. "Model Selection for Ecologists: The
2008 Worldview of AIC and BIC." *Ecology* 95 (March): 631–36. doi:10.1890/13-1452.1.
- 2009 Ainsworth, Elizabeth A., and Stephen P. Long. 2005. "What Have We Learned from 15 Years of
2010 Free-Air CO₂ Enrichment (FACE)? A Meta-Analytic Review of the Responses of
2011 Photosynthesis, Canopy Properties and Plant Production to Rising CO₂." *New Phytologist* 165
2012 (2): 351–71. doi:10.1111/j.1469-8137.2004.01224.x.
- 2013 Babst, Flurin, M. Ross Alexander, Paul Szejner, Olivier Bouriaud, Stefan Klesse, John Roden,
2014 Philippe Ciais, et al. 2014. "A Tree-Ring Perspective on the Terrestrial Carbon Cycle."
2015 *Oecologia* 176 (2): 307–22. doi:10.1007/s00442-014-3031-6.
- 2016 Beedlow, Peter A., E. Henry Lee, David T. Tingey, Ronald S. Waschmann, and Connie A. Burdick.
2017 2013. "The Importance of Seasonal Temperature and Moisture Patterns on Growth of Douglas-
2018 Fir in Western Oregon, USA." *Agricultural and Forest Meteorology* 169. Elsevier B.V.: 174–
2019 85. doi:10.1016/j.agrformet.2012.10.010.
- 2020 Biondi, Franco. 1999. "Comparing Tree-Ring Chronologies and Repeated timber Inventories as
2021 Forest Monitoring Tools." *Ecological Applications* 9 (1): 216–27. doi:10.1890/1051-
2022 0761(1999)009[0216:CTRCAR]2.0.CO;2.
- 2023 Boettger, Tatjana, Marika Haupt, Kay Knöller, Stephan M. Weise, John S. Waterhouse, Katja T.
2024 Rinne, Neil J. Loader, et al. 2007. "Wood Cellulose Preparation Methods and Mass
2025 Spectrometric Analyses of $\delta^{13}C$, $\delta^{18}O$, and Nonexchangeable δ^2H Values in Cellulose,
2026 Sugar, and Starch: An Interlaboratory Comparison." *Analytical Chemistry* 79 (12): 4603–12.
2027 doi:10.1021/ac0700023.
- 2028 Boisvenue, Céline, and Steven W. Running. 2006. "Impacts of Climate Change on Natural Forest
2029 Productivity - Evidence since the Middle of the 20th Century." *Global Change Biology* 12 (5):
2030 862–82. doi:10.1111/j.1365-2486.2006.01134.x.
- 2031 Brienen, R J W, E Gloor, S Clerici, R Newton, L Arppe, A Boom, S Bottrell, et al. n.d. "Isotopes."
2032 *Nature Communications*. Springer US, 1–10. doi:10.1038/s41467-017-00225-z.
- 2033 Brunel, J.P., G.R. Walker, C.D. Walker, J.C. Dighton, and A. Kennett-Smith. 1991. "Using Stable
2034 Isotopes of Water to Trace Plant Water Uptake." *International Symposium on the Use of Stable*
2035 *Isotopes in Plant Nutrition, Soil Fertility and Environmental Studies*, 543–551.
2036 doi:10.2144/000114133.
- 2037 Bunn, Andrew G. 2008. "A Dendrochronology Program Library in R (dplR)." *Dendrochronologia*
2038 26 (2): 115–24. doi:10.1016/j.dendro.2008.01.002.
- 2039 Bunn AG (2010). "Statistical and visual crossdating in R using the dplR library."
2040 *Dendrochronologia*, 28(4), pp. 251–258. ISSN 1125-7865, doi: 10.1016/j.dendro.2009.12.001

- 2041 Camarero, J. Julio, Antonio Gazol, Jacques C. Tardif, and France Conciatori. 2015. “Attributing
2042 Forest Responses to Global-Change Drivers: Limited Evidence of a CO₂-Fertilization Effect in
2043 Iberian Pine Growth.” *Journal of Biogeography* 42 (11): 2220–33. doi:10.1111/jbi.12590.
- 2044 Carrer, Marco, and C Urbinati. 2006. “Long-Term Change in the Sensitivity of Tree Ring Growth
2045 to Climate Forcing in *Larix Decidua*.” *New Phytologist* 170 (iv): 861–72.
- 2046 Cook, Edward R., Keith R. Briffa, David M Meko, Donald A Graybill, and Gary Funkhouser. 1995.
2047 “The ‘segment Length Curse’ in Long Tree-Ring Chronology Development for Palaeoclimatic
2048 Studies.” *The Holocene* 5 (2): 229–37. doi:10.1177/095968369500500211.
- 2049 Dawson, T E. 1998. “Fog in the Californian Redwood Forest: Ecosystem Inputs and Use by
2050 Plants.” *Oecologia* 117: 476–85.
- 2051 Dawson, Todd E., Stefania Mambelli, Agneta H. Plamboeck, Pamela H. Templer, and Kevin P. Tu.
2052 2002. “Stable Isotopes in Plant Ecology.” *Annual Review of Ecology and Systematics* 33 (1):
2053 507–59. doi:10.1146/annurev.ecolsys.33.020602.095451.
- 2054 Dawson, Todd E., and John S Pate. 1996. “Seasonal Water Uptake and Movement in Root Systems
2055 of Australian Phraeatophytic Plants of Dimorphic Root Morphology: A Stable Isotope
2056 Investigation.” *Oecologia* 107 (1): 13–20. doi:10.1007/BF00582230.
- 2057 Di Biase, Giampaolo, Gloria Falsone, Anna Graziani, Gilmo Vianello, and Livia Vittori Antisari.
2058 2015. “Carbon Sequestration in Soils Affected By Douglas Fir Reforestation in Apennines
2059 (Northern Italy).” *Eqa-International Journal of Environmental Quality* 17: 1–11.
2060 doi:10.6092/issn.2281-4485/5208.
- 2061 Dongmann, G, and H W Nürnberg. 1974. “On the Enrichment of H₂18O in the Leaves of
2062 Transpiring Plants I T L Q E” 52: 1–2.
- 2063 Esper, Jan, Edward R Cook, and Fritz H Schweingruber. 2002. “Low-Frequency Signals in Long
2064 Tree-Ring Chronologies for Reconstructing Past Temperature Variability.” *Science (New York,
2065 N.Y.)* 295 (5563). American Association for the Advancement of Science: 2250–53.
2066 doi:10.1126/science.1066208.
- 2067 Esper, Jan, David C. Frank, Giovanna Battipaglia, Ulf Büntgen, Christopher Holert, Kerstin
2068 Treydte, Rolf Siegwolf, and Matthias Saurer. 2010a. “Low-Frequency Noise in ¹³C and
2069 ¹⁸O Tree Ring Data: A Case Study of Pinus Uncinata in the Spanish Pyrenees.” *Global
2070 Biogeochemical Cycles* 24 (4): 1–11. doi:10.1029/2010GB003772.
- 2071 Esper, Jan, David C Frank, Giovanna Battipaglia, Ulf Büntgen, Christopher Holert, Kerstin Treydte,
2072 Rolf Siegwolf, and Matthias Saurer. 2010b. “Low Frequency Noise in D ¹³ C and D ¹⁸ O
2073 Tree Ring Data : A Case Study of Pinus Uncinata in the Spanish Pyrenees” 24 (2): 1–11.
2074 doi:10.1029/2010GB003772.
- 2075 Farquhar, G. D., L. A. Cernusak, and B. Barnes. 2006. “Heavy Water Fractionation during
2076 Transpiration.” *Plant Physiology* 143 (1): 11–18. doi:10.1104/pp.106.093278.
- 2077 Farquhar, G D, J R Ehleringer, and K T Hubick. 1989. “Carbon Isotope Discrimination and
2078 Photosynthesis.” *Annual Review of Plant Physiology and Plant Molecular Biology*.
2079 doi:10.1146/annurev.pp.40.060189.002443.
- 2080 Federal, Swiss, Universitat De Barcelona, J. Julio Camarero, Antonio Gazol, Juan Diego Galván,
2081 Gabriel Sangüesa-Barreda, and Emilia Gutiérrez. 2015. “Disparate Effects of Global-Change

- 2082 Drivers on Mountain Conifer Forests: Warming-Induced Growth Enhancement in Young Trees
 2083 vs. CO₂ Fertilization in Old Trees from Wet Sites.” *Global Change Biology* 21 (2): 738–49.
 2084 doi:10.1111/gcb.12787.
- 2085 Fenn, Mark E, Jeremy S Fried, Haiganoush K Preisler, Andrzej Bytnerowicz, Susan Schilling,
 2086 Sarah Jovan, and Olaf Kuegler. 2015. “REMEASURED FIA PLOTS REVEAL TREE-LEVEL
 2087 DIAMETER GROWTH AND TREE MORTALITY IMPACTS OF NITROGEN
 2088 DEPOSITION ON CALIFORNIA ’ S FORESTS” 2013 (Time 2): 2013–16.
- 2089 Francey, R. J., C. E. Allison, D. M. Etheridge, C. M. Trudinger, I. G. Enting, M. Leuenberger, R. L.
 2090 Langenfelds, E. Michel, and L. P. Steele. 1999. “A 1000-Year High Precision Record of ¹³C
 2091 in Atmospheric CO₂.” *Tellus, Series B: Chemical and Physical Meteorology* 51 (2): 170–93.
 2092 doi:10.1034/j.1600-0889.1999.t01-1-00005.x.
- 2093 Frank, D. C., B. Poulter, M. Saurer, J. Esper, C. Huntingford, G. Helle, K. Treydte, et al. 2015.
 2094 “Water-Use Efficiency and Transpiration across European Forests during the Anthropocene.”
 2095 *Nature Climate Change*, no. May. doi:10.1038/nclimate2614.
- 2096 Giustini, Francesca, Mauro Brilli, and Antonio Patera. 2016. “Mapping Oxygen Stable Isotopes of
 2097 Precipitation in Italy.” *Journal of Hydrology: Regional Studies* 8. Elsevier B.V.: 162–81.
 2098 doi:10.1016/j.ejrh.2016.04.001.
- 2099 Gómez-Guerrero, Armando, Lucas C.R. R Silva, Miguel Barrera-Reyes, Barbara Kishchuk,
 2100 Alejandro Velázquez-Martínez, Tomás Martínez-Trinidad, Francisca Ofelia Plascencia-
 2101 Escalante, and William R. Horwath. 2013. “Growth Decline and Divergent Tree Ring Isotopic
 2102 Composition (¹³C and ¹⁸O) Contradict Predictions of CO₂ Stimulation in High Altitudinal
 2103 Forests.” *Global Change Biology* 19 (6): 1748–58. doi:10.1111/gcb.12170.
- 2104 Griffin, Daniel, and Kevin J Anchukaitis. 2014. “How Unusual Is the 2012 – 2014 California
 2105 Drought ?,” 9017–23. doi:10.1002/2014GL062433.1.
- 2106 Guerrieri, R, Maurizio Mencuccini, L J Sheppard, M Saurer, M P Perks, P Levy, M a Sutton, Marco
 2107 Borghetti, and J Grace. 2011. “The Legacy of Enhanced N and S Deposition as Revealed by
 2108 the Combined Analysis of Delta ¹³C, Delta ¹⁸O and Delta ¹⁵N in Tree Rings.” *Global
 2109 Change Biology* 17 (5): 1946–62. doi:10.1111/j.1365-2486.2010.02362.x.
- 2110 Harris, I., P. D. Jones, T. J. Osborn, and D. H. Lister. 2014. “Updated High-Resolution Grids of
 2111 Monthly Climatic Observations - the CRU TS3.10 Dataset.” *International Journal of
 2112 Climatology* 34 (3): 623–42. doi:10.1002/joc.3711.
- 2113 Hastie, T. J., and R. J. Tibshirani. 1990. “Generalized Additive Models.” *Monographs on Statistics
 2114 and Applied Probability*. doi:10.1016/j.csda.2010.05.004.
- 2115 IPCC. 2014. “Climate Change 2014 Synthesis Report Summary Chapter for Policymakers.” *Ippc*,
 2116 31. doi:10.1017/CBO9781107415324.
- 2117 Kaufmann, M.R. 1996. To live fast or not: growth, vigor and longevity of old-growth ponderosa
 2118 pine and lodgepole pine trees. *Tree Physiology* 16:139-144.
 2119
- 2120 Keenan, Trevor F, David Y Hollinger, Gil Bohrer, Danilo Dragoni, J William Munger, Hans Peter
 2121 Schmid, and Andrew D Richardson. 2013. “Increase in Forest Water-Use Efficiency as
 2122 Atmospheric Carbon Dioxide Concentrations Rise.” *Nature* 499 (7458): 324–27.
 2123 doi:10.1038/nature12291.

- 2124 Korner, C. 2005. "Carbon Flux and Growth in Mature Deciduous Forest Trees Exposed to Elevated
2125 CO₂." *Science* 309 (5739): 1360–62. doi:10.1126/science.1113977.
- 2126 Leavitt, Steven W. 2010. "Tree-Ring C-H-O Isotope Variability and Sampling." *The Science of the
2127 Total Environment* 408 (22): 5244–53. doi:10.1016/j.scitotenv.2010.07.057.
- 2128 Lee, E. Henry, Peter A. Beedlow, Ronald S. Waschmann, David T. Tingey, Charlotte Wickham,
2129 Steve Cline, Michael Bollman, and Cailie Carlile. 2016. "Douglas-Fir Displays a Range of
2130 Growth Responses to Temperature, Water, and Swiss Needle Cast in Western Oregon, USA."
2131 *Agricultural and Forest Meteorology* 221. Elsevier B.V.: 176–88.
2132 doi:10.1016/j.agrformet.2016.02.009.
- 2133 Leonardi, Stefano, Tiziana Gentilesca, Rossella Guerrieri, Francesco Ripullone, Federico Magnani,
2134 Maurizio Mencuccini, Twan V. Noije, and Marco Borghetti. 2012. "Assessing the Effects of
2135 Nitrogen Deposition and Climate on Carbon Isotope Discrimination and Intrinsic Water-Use
2136 Efficiency of Angiosperm and Conifer Trees under Rising CO₂ Conditions." *Global Change
2137 Biology* 18 (9): 2925–44. doi:10.1111/j.1365-2486.2012.02757.x.
- 2138 Lévesque, Mathieu, Rolf Siegwolf, Matthias Saurer, Britta Eilmann, and Andreas Rigling. 2014.
2139 "Increased Water-Use Efficiency Does Not Lead to Enhanced Tree Growth under Xeric and
2140 Mesic Conditions." *New Phytologist* 203 (1): 94–109. doi:10.1111/nph.12772.
- 2141 Linares, Juan Carlos, Jesús Julio Camarero, and José Antonio Carreira. 2010. "Competition
2142 Modulates the Adaptation Capacity of Forests to Climatic Stress: Insights from Recent Growth
2143 Decline and Death in Relict Stands of the Mediterranean Fir *Abies pinsapo*." *Journal of
2144 Ecology* 98 (3): 592–603. doi:10.1111/j.1365-2745.2010.01645.x.
- 2145 Magnani, Federico, Maurizio Mencuccini, Marco Borghetti, Paul Berbigier, Frank Berninger,
2146 Sylvain Delzon, Achim Grelle, et al. 2007. "The Human Footprint in the Carbon Cycle of
2147 Temperate and Boreal Forests." *Nature* 447 (7146): 848–50. doi:10.1038/nature05847.
- 2148 Marshall, D D, and R O Curtis. 2002. "Levels-of-Growing-Stock Cooperative Study in Douglas-
2149 Fir: Report No. 15 - Hoskins: 1963-1998." *Research Paper Pacific Northwest Research
2150 Station, USDA Forest Service*, no. PNW-RP-537: 80.
- 2151 McCarroll, Danny, and Neil J. Loader. 2004. "Stable Isotopes in Tree Rings." *Quaternary Science
2152 Reviews* 23 (7–8): 771–801. doi:10.1016/j.quascirev.2003.06.017.
- 2153 McMahon, Sean M, Geoffrey G Parker, and Dawn R Miller. 2010. "Evidence for a Recent Increase
2154 in Forest Growth." *Proceedings of the National Academy of Sciences of the United States of
2155 America* 107 (8): 3611–15. doi:10.1073/pnas.0912376107.
- 2156 Medlyn, B. E., F. -W. Badeck, D. G. G. De Pury, C. V. M. Barton, M. Broadmeadow, R.
2157 Ceulemans, P. De Angelis, et al. 1999. "Effects of Elevated [CO₂] on Photosynthesis in
2158 European Forest Species: A Meta-Analysis of Model Parameters." *Plant, Cell & Environment*
2159 22 (12): 1475–1495. doi:10.1046/j.1365-3040.1999.00523.x.
- 2160 Nair, Richard K F, Micheal P Perks, Andrew Weatherall, Elizabeth M Baggs, and Maurizio
2161 Mencuccini. 2015. "Does Canopy Nitrogen Uptake Enhance Carbon Sequestration by Trees?"
2162 *Global Change Biology*, September. doi:10.1111/gcb.13096.
- 2163 Nehrbass-Ahles, Christoph, Flurin Babst, Stefan Klesse, Magdalena Nötzli, Olivier Bouriaud,
2164 Raphael Neukom, Matthias Dobbertin, and David Frank. 2014. "The Influence of Sampling
2165 Design on Tree-Ring-Based Quantification of Forest Growth." *Global Change Biology* 20 (9).

- 2166 doi:10.1111/gcb.12599.
- 2167 Norby, Richard J, Jeffrey M Warren, Colleen M Iversen, Belinda E Medlyn, and Ross E
2168 McMurtrie. 2010. "CO₂ Enhancement of Forest Productivity Constrained by Limited Nitrogen
2169 Availability." *Proceedings of the National Academy of Sciences of the United States of*
2170 *America* 107 (45): 19368–73. doi:10.1073/pnas.1006463107.
- 2171 Peñuelas, Josep, Josep G. Canadell, and Romà Ogaya. 2011. "Increased Water-Use Efficiency
2172 during the 20th Century Did Not Translate into Enhanced Tree Growth." *Global Ecology and*
2173 *Biogeography* 20 (4): 597–608. doi:10.1111/j.1466-8238.2010.00608.x.
- 2174 Perakis, Steven S., and Emily R. Sinkhorn. 2011. "Biogeochemistry of a Temperate Forest Nitrogen
2175 Gradient." *Ecology* 92 (7): 1481–91. doi:10.1890/10-1642.1.
- 2176 Peters, Richard L., Peter Groenendijk, Mart Vlam, and Pieter a. Zuidema. 2015. "Detecting Long-
2177 Term Growth Trends Using Tree Rings: A Critical Evaluation of Methods." *Global Change*
2178 *Biology*, n/a-n/a. doi:10.1111/gcb.12826.
- 2179 Phillips, Nathan G., Thomas N. Buckley, and David T. Tissue. 2008. "Capacity of Old Trees to
2180 Respond to Environmental Change." *Journal of Integrative Plant Biology* 50 (11): 1355–64.
2181 doi:10.1111/j.1744-7909.2008.00746.x.
- 2182 Piovesan, Gianluca, Franco Biondi, Aalfredo Di Filippo, Alfredo Alessandrini, and Maurizio
2183 Maugeri. 2008. "Drought-Driven Growth Reduction in Old Beech (*Fagus Sylvatica* L.) Forests
2184 of the Central Apennines, Italy." *Global Change Biology* 14 (6): 1265–81. doi:10.1111/j.1365-
2185 2486.2008.01570.x.
- 2186 Poage, Nathan J, and John C Tappeiner, II. 2002. "Long-Term Patterns of Diameter and Basal Area
2187 Growth of Old-Growth Douglas-Fir Trees in Western Oregon." *Canadian Journal of Forest*
2188 *Research* 32: 1232–43. doi:10.1139/x02-045.
- 2189 Rehfeldt, Gerald E., Barry C. Jaquish, Javier Lòpez-Upton, Cuauhtémocmoc Sáenz-Romero, J.
2190 Bradley St Clair, Laura P. Leites, and Dennis G. Joyce. 2014. "Comparative Genetic
2191 Responses to Climate for the Varieties of *Pinus Ponderosa* and *Pseudotsuga Menziesii*:
2192 Realized Climate Niches." *Forest Ecology and Management* 324. Elsevier B.V.: 126–37.
2193 doi:10.1016/j.foreco.2014.02.035.
- 2194 Ripullone, Francesco, Marco Lauteri, Giacomo Grassi, Mariana Amato, and Marco Borghetti. 2004.
2195 "Variation in Nitrogen Supply Changes Water-Use Efficiency of *Pseudotsuga Menziesii* and
2196 *Populus X Euroamericana*; a Comparison of Three Approaches to Determine Water-Use
2197 Efficiency." *Tree Physiology* 24 (6): 671–79.
- 2198 Rita, Angelo, Marco Borghetti, Luigi Todaro, and Antonio Saracino. 2016. "Interpreting the
2199 Climatic Effects on Xylem Functional Traits in Two Mediterranean Oak Species: The Role of
2200 Extreme Climatic Events." *Frontiers in Plant Science* 7 (August): 1–11.
2201 doi:10.3389/fpls.2016.01126.
- 2202 Roden, John, and Rolf Siegwolf. 2012. "Is the Dual-Isotope Conceptual Model Fully Operational?"
2203 *Tree Physiology* 32 (10): 1179–82. doi:10.1093/treephys/tps099.
- 2204 Rozanski, Kazimierz, Luis Araguas-araguas, and Roberto Gonfiantini. 2016. "Relation Between
2205 Long-Term Trends of Oxygen-18 Isotope Composition of Precipitation and Climate Author (S
2206): Kazimierz Rozanski , Luis Araguás-Araguás and Roberto Gonfiantini Published by :
2207 American Association for the Advancement of Science Stable URL :." 258 (5084): 981–85.

- 2208 Ryan, Mg, D Binkley, and Jh Fownes. 1997. "Age-Related Decline in Forest Productivity: Pattern
2209 and Process." *Advances in Ecological Research*.
- 2210 Ryan, Michael G., Nathan Phillips, and Barbara J. Bond. 2006. "The Hydraulic Limitation
2211 Hypothesis Revisited." *Plant, Cell and Environment* 29 (3): 367–81. doi:10.1111/j.1365-
2212 3040.2005.01478.x.
- 2213 Ryan, Michael G., and Barbara J. Yoder. 1997. "Hydraulic Limits to Tree Height and Tree
2214 Growth." *BioScience* 47 (4): 235–42. doi:10.2307/1313077.
- 2215 Saurer, Matthias, Rolf T. W. Siegwolf, and Fritz H. Schweingruber. 2004. "Carbon Isotope
2216 Discrimination Indicates Improving Water-Use Efficiency of Trees in Northern Eurasia over
2217 the Last 100 Years." *Global Change Biology* 10 (12): 2109–20. doi:10.1111/j.1365-
2218 2486.2004.00869.x.
- 2219 Scheidegger, Y., M. Saurer, M. Bahn, and R. Siegwolf. 2000. "Linking Stable Oxygen and Carbon
2220 Isotopes with Stomatal Conductance and Photosynthetic Capacity: A Conceptual Model."
2221 *Oecologia* 125 (3): 350–57. doi:10.1007/s004420000466.
- 2222 Sitch, Stephan, C. Huntingford, N. Gedney, P. E. Levy, M. Lomas, S. L. Piao, R. Betts, et al. 2008.
2223 "Evaluation of the Terrestrial Carbon Cycle, Future Plant Geography and Climate-Carbon
2224 Cycle Feedbacks Using Five Dynamic Global Vegetation Models (DGVMs)." *Global Change
2225 Biology* 14 (9): 2015–39. doi:10.1111/j.1365-2486.2008.01626.x.
- 2226 Sternberg, Leonel Da Silveira Lobo O.Reilly. 2009. "Oxygen Stable Isotope Ratios of Tree-Ring
2227 Cellulose: The next Phase of Understanding." *New Phytologist* 181 (3): 553–62.
2228 doi:10.1111/j.1469-8137.2008.02661.x.
- 2229 Treydte, Kerstin, Sonja Boda, Elisabeth Graf Pannatier, Patrick Fonti, David Frank, Bastian Ullrich,
2230 Matthias Saurer, et al. 2014. "Seasonal Transfer of Oxygen Isotopes from Precipitation and
2231 Soil to the Tree Ring : Source Water versus Needle Water Enrichment."
- 2232 Vicente-Serrano, Sergio M., Santiago Beguería, and Juan I. López-Moreno. 2010. "A Multiscalar
2233 Drought Index Sensitive to Global Warming: The Standardized Precipitation
2234 Evapotranspiration Index." *Journal of Climate* 23 (7): 1696–1718.
2235 doi:10.1175/2009JCLI2909.1.
- 2236 Vicente-Serrano, Sergio M., J. Julio Camarero, and Cesar Azorin-Molina. 2014. "Diverse
2237 Responses of Forest Growth to Drought Time-Scales in the Northern Hemisphere." *Global
2238 Ecology and Biogeography* 23 (9): 1019–30. doi:10.1111/geb.12183.
- 2239 Vitas, A., and K. Žeimavi ius. 2006. "Trends of Decline of Douglas Fir in Lithuania :
2240 Dendroclimatological Approach." *Baltic Forestry* 12 (2): 200–208.
- 2241 Walker, Lawrence R., David a. Wardle, Richard D. Bardgett, and Bruce D. Clarkson. 2010. "The
2242 Use of Chronosequences in Studies of Ecological Succession and Soil Development." *Journal
2243 of Ecology* 98 (4): 725–36. doi:10.1111/j.1365-2745.2010.01664.x.
- 2244 Warren, Cr, Jf McGrath, and Ma Adams. 2001. "Water Availability and Carbon Isotope
2245 Discrimination in Conifers." *Oecologia* 127 (4): 476–86. doi:10.1007/s004420000609.
- 2246 Williams, David G., R. David Evans, Jason B. West, and James R. Ehleringer. 2007. *Stable
2247 Isotopes as Indicators of Ecological Change. Terrestrial Ecology*. Vol. 1. doi:10.1016/S1936-
2248 7961(07)01024-X.

- 2249 Wood, Simon N. 2014. "Package 'Mgcv'." doi:10.1186/1471-2105-11-11. Bioconductor.
- 2250 Wood, Simon N. 2017. "Package 'Mgcv'."
- 2251 Wood, Simon N. 2006. *Generalized Additive Models: An Introduction with R*. Chapman and
2252 Hall/CRC.
- 2253 Wood, Simon N. 2008. "Fast Stable Direct Fitting and Smoothness Selection for Generalized
2254 Additive Models." *Journal of the Royal Statistical Society. Series B: Statistical Methodology*
2255 70 (3): 495–518. doi:10.1111/j.1467-9868.2007.00646.x.
- 2256 Zhao, Maosheng, and Steven W Running. 2010. "Drought-Induced Reduction in Global Terrestrial
2257 Net Primary Production from 2000 Through 2009." *Science* 329 (5994): 940–43.
2258 doi:10.1126/science.1192666.
- 2259 Zweifel, Roman, Lukas Zimmermann, Fabienne Zeugin, and David M. Newbery. 2006. "Intra-
2260 Annual Radial Growth and Water Relations of Trees: Implications towards a Growth
2261 Mechanism." *Journal of Experimental Botany* 57 (6): 1445–59. doi:10.1093/jxb/erj125.

2262

2263 Conclusions

2264

2265 Given the widely observed impact of the so-called global change on forest productivity, and the
2266 associated eco-physiological trend, a proper understanding of the dynamic response to the
2267 individual main drivers involved appears to be crucial, both to project the future role of forest as a
2268 sink or source of carbon, and to try and adapt forest management choices to a changing world.

2269 In this perspective, using tree ring width and isotopic signature analysis, we tried to disentangle
2270 which forcing factors have determined the long-term trend in growth observed in two Douglas fir
2271 (*Pseudotsuga menziesii* (Mirb.) Franco) age sequences: an even-aged chronosequence in
2272 Vallombrosa, Italy and a natural old-growth age sequence in Angelo Coast Range Reserve,
2273 California.

2274 In chapter one we focused on last century's growth variations in Vallombrosa, analyzed after
2275 decoupling it from age-size related effects. The resulting trend displays a multi-decadal oscillation
2276 and a recent decrement of basal area increments (BAI) of the order of 22.9%. Through the
2277 application of generalized additive models (GAMs) we were able to assess, among a number of

2278 potentially relevant environmental factors, which ones determined this trend. The model applied
2279 describes 37% of log(BAI) variability and the combination of covariates that were found to be
2280 significant includes N deposition (in the oxidized form) and summer water availability for both the
2281 growing season of ring formation and the previous year, all positively related with growth at a P
2282 level <0.001. On the other hand atmospheric CO₂ concentration, despite the significant effect on
2283 BAI variations, displays a non-monotonic shape of the relationship which could be most likely
2284 determined by a possible problem with the model (either concavity or failure to consider all
2285 important independent variables), rather than by a meaningful biological process alone, such as a
2286 progressive down- regulation in photosynthetic response, or a shift in resources allocation. However
2287 it is possible to state that the BAI declining trend in recent times should be attributed, at least
2288 partially, to an effect of decreasing N deposition and an increase in summer water deficit.

2289 In the second chapter, considering the same chronosequence, isotopic analyses were employed to
2290 investigate the underlying variations in tree physiological response. More specifically, the ¹³C and
2291 ¹⁸O were analyzed, also in a dual isotope perspective, so as to clarify which drivers have affected
2292 the observed trend in intrinsic water use efficiency (iWUE), whether an increase in photosynthetic
2293 rates or a reduction in stomatal conductance, or both. Once decoupled from age-related effects, the
2294 pattern over time in water use efficiency shows an increase of the order of 17.3 % in the period
2295 included between 1960-1980, followed by a less pronounced increase in the following years; at the
2296 same time the age effect *per se* displayed a pronounced rise, suggesting a possible progressive
2297 increase in stomatal control, in agreement with the hydraulic limitation hypothesis (HLH). The
2298 GAMs analysis of iWUE dynamics was found to explain 80% of its overall variability; for what
2299 concerns the single covariates effects, CO₂ was found to be positively related with iWUE, as well as
2300 NO_y deposition, as already generally observed in other studies; In addition also the water
2301 availability of the previous summer has a fully significant effect. Considering ¹⁸O dynamics, on
2302 the contrary, only 46% of overall signal variability was explained by environmental variables. An
2303 inverse relationship with precipitation and a positive one with annual maximum temperature

2304 (possibly because of its link with VPD) were detected, confirming to a certain extent the goodness
2305 of the signal recorded in tree-rings, although the possibility cannot be ruled out that a decreasing
2306 trend in the isotopic signature of the source water composition could have conditioned the analysis
2307 results. No effects of age variation were detected. The simultaneous consideration of both isotopes
2308 together in the dual-isotope approach, finally, allowed us to demonstrate that A_{\max} and not g_s
2309 appears to have driven the trend in $iWUE$ over the second part of the last century. This seems to
2310 agree with the hypothesis that the observed pattern in $iWUE$ could have been determined by an
2311 initial stimulation of assimilation driven by N deposition in combination with the CO_2 increase,
2312 successively reversed over the last decades by the reduction in N deposition, coupled with a
2313 possible influence of drought and competition.

2314 The last chapter should be considered as an explorative study, as the chronosequence is constituted
2315 by only a few trees ($n=18$); having said that, the analysis presented has the main advantage of
2316 comprising a wide range of ages, spanning all the way back to pre-industrial times, and to be
2317 located in a natural old growth forest, less prone to inter-tree competition. The results show a strong
2318 increase in BAI since the pre-industrial period, with a 59.5% increase for the last 60 years alone,
2319 especially as a result of the atmospheric CO_2 concentration effect. Moreover, the shape of age-
2320 related growth trends observed in the different age classes when taking a diachronic perspective,
2321 suggest a gradual anticipation in the culmination of increments, as would be expected as a result of
2322 increasing site fertility over time. This look like an additional confirmation of the substantial global
2323 change impact on Douglas fir growth in this old-growth stand.

2324 At last, summarizing the main finding of this study:

2325 1. The age-related pattern in $iWUE$ suggests that the observed ontogenetic dynamics in BAI could
2326 be the result of an increase in g_s control as trees grow taller; this is likely the case in the
2327 Vallombrosa chronosequence, where the increment in tree height is not yet stabilized even in oldest
2328 age class (data not shown), and possibly also in the Angelo forest. On the other hand, this runs

2329 against the absence of such an age effect in the ^{18}O signal, even if the known relevance of source
2330 water isotopic signature and the general lack of detailed information its variability lessens the
2331 potential suitability of this proxy in a long term view. Nevertheless, the effect of age on isotopic C
2332 composition should be interpreted with great care when using iWUE to infer global change effects,
2333 as there could be the risk to overestimating the relevance of stomatal regulation.

2334 2. The analysis at both sites demonstrates the importance of water availability in the summer period
2335 as a limiting factor for the growth of this species in Mediterranean environments, affecting both
2336 increments and eco-physiological traits. The increase in atmospheric CO_2 , which shows a positive
2337 contribution to the BAI trend at the Angelo site, does not display the same relationship in
2338 Vallombrosa. On the other hand, this covariate was found to strongly affect iWUE at the Italian site,
2339 by increasing leaf photosynthetic capacity as demonstrated by the dual isotope approach. Also the
2340 effect of atmospheric nitrogen deposition shows marked differences among sites. While at Angelo
2341 site no effect was observed (possibly as a result of the substantially lower level in N deposition), in
2342 Vallombrosa this covariate shows the same positive effect on both dependent variables (BAI and
2343 iWUE), probably because both are sensitive to A_{max} and leaf N contents. This consistency between
2344 the two analyses increases the reliability of our conclusions that N deposition - at this site at least -
2345 should be viewed as an influential factor affecting stem growth through its effects on photosynthetic
2346 capacity, highlighting the importance of considering N deposition when global change effects on
2347 forest growth and function are to be assessed.

2348